FINITE ELEMENT ANALYSES OF PILE LOAD TESTS PERFORMED IN THE YORKTOWN FORMATION NEWPORT NEWS, VIRGINIA

by

John Christos Daoulas

Thesis submitted to the Faculty of the
Virginia Polytechnic Institute and State University
in partial fulfillment of the requirements for the degree of

MASTER OF SCIENCE

in

Civil Engineering

APPROVED:

G. W. Clough, Chairman

T. Kupp[illegible]amy

J.M. Duncan

April 1988

Blacksburg, Virginia

FINITE ELEMENT ANALYSES OF PILE LOAD TESTS PERFORMED IN THE YORKTOWN FORMATION NEWPORT NEWS, VIRGINIA

by

John Christos Daoulas

Committee Chairman: G.W. Clough
Civil Engineering

(ABSTRACT)

The finite element method is used in determining the load-capacity and behavior of a single concrete pile modeled after full scale instrumented test piles which were employed in the Tidewater area of Virginia. Specifically, this report describes the subsurface conditions and full scale pile tests that were performed during the design phase of the foundation for the Land Level Shipbuilding Facility in Newport News, Virginia. It also addresses the testing conducted by the author to determine the material properties required for finite element analyses, including: soil sampling and in-situ tests within the Yorktown formation; standard soil laboratory tests for index properties and strength-deformation characteristics of the soil along the pile perimeter and tip, plus interface tests

to evaluate soil strength-deformation characteristics along the soil-pile interface. The data derived from the finite element method of analysis is then compared with the load-displacement and load-transfer data obtained from the full scale instrumented pile load tests. The comparative analysis shows favorable results leading to the conclusion that the finite element method shows promise for use in the design of deep foundations systems in the Tidewater area of Virginia.

ACKNOWLEDGEMENTS

The author wishes to express his appreciation to Dr. G.W. Clough, Professional Civil Engineer and Department Head, and to Dr. T. Kuppusamy, Associate Professor of Civil Engineering. Their guidance and assistance during the course of this study were invaluable. Similarly, special thanks are extended to Dr. R.E. Martin, Principal, Schnabel Engineering Associates, P.C., of Richmond, Virginia for his cooperation and assistance. In this connection, grateful acknowledgement is hereby made to Schnabel Engineering for their sponsorship of the test boring and Menard pressuremeter tests conducted specifically for this study program. In addition, I would like to thank the following persons that were involved in the typing, drafting and assembly of this manuscript: Diane Walden Ritchie, Mary Ann Jaramillo and Victoria Mitchell. Finally, I wish to extend my sincere appreciation to my parents for their encouragement and to my wife, Cheryl Lynn, for her patience and support during all phases of this study effort.

TABLE OF CONTENTS

Chapter 1

INTRODUCTION

1.0 Background

Deep pile foundation systems are commonly utilized for the support of structures in the Tidewater area of southeastern Virginia. Typically, prestressed precast concrete piles are employed due to the nature of the subsurface conditions and their low cost compared to other suitable types of foundation systems. The Tidewater area encompasses the cities of Norfolk, Virginia Beach, Portsmouth, Newport News and Hampton.

There are two distinctive geological formations associated with the Tidewater area: the Norfolk and Yorktown. The Norfolk formation varies in depth from 0 to 75 feet below the ground surface and generally consists of normally consolidated silt and clay soils of Pleistocene geological age. Underlying this formation is the Yorktown which measures up to 300 feet in thickness. The Yorktown is comprised of preconsolidated sand, silt and clay soils with varying concentration of shell fragments of Miocene geological age. Bedrock depths range from approximately 2,000 to 3,000 feet below the ground surface.

Pile capacities are normally determined by static

and dynamic formulas. These methods, however, usually provide conservative estimates of their actual load capacity due to the nature and variation of the soil strata that comprise the Yorktown Formation. The results of in-situ tests, such as Standard Penetration and Menard Pressuremeter, are adversely effected by the presence of cemented shell fragments, development of excess pore water pressure, and soil disturbance typically found to occur within this Formation. Pile driving data used in dynamic analysis has also been found to be effected by these conditions. Consequently, in the past ten years, correlation factors have been modified based on data from full scale pile load tests to improve the design of deep foundation systems based on static analyses.

This was done for the foundation system that supports the Land Level Shipbuilding Facility at Newport News, Virginia. During the design phase of the foundation, various subsurface investigations and pile load tests were conducted. These included the use of instrumented piles to determine the mechanism and magnitude of support derived from the Yorktown formation. The resultant data was then used to develop new values for correlating the unit shaft and base resistance of piles with Standard Penetration Test data (14).

Although test data for piles embedded within the Yorktown formation are useful, it generally cannot isolate

the effects of the following: in-situ stresses; soil disturbance and induced stresses caused by pile driving; variations in soil strength and soil-pile interface properties; consolidation and negative skin friction plus cyclic loading. The finite element method of analysis, however, appears capable of incorporating many of these factors. This method could therefore result in an improved understanding of the load-deformation response of piles.

1.1 Purpose

The purpose of this study is to assess the effectiveness of the finite element method for determining the capacity and behavior of piles of deep foundation systems in the Tidewater area of Virginia. In order to accomplish the above objective, field and laboratory test programs were undertaken to determine the engineering parameters required for the finite element analysis. This endeavor further permits an assessment to be made regarding the feasibility of using the finite element method in lieu of full scale pile tests for future design.

1.2 Scope of Study

The finite element method is used to ascertain the behavior of a single concrete pile under various load

conditions to include ultimate load capacity; the pile is modeled after instrumented piles utilized at the Land Level Shipbuilding Facility. The stress-deformation characteristics of the soil and soil-pile interface properties are determined. The methods and tests for developing the data required by the finite element method include: soil sampling; Standard Penetration Tests; standard laboratory tests for the determination of index properties and stress-deformation characteristics; and soil-structure interface testing to determine stress-deformation characteristics of the soil along the soil-pile interface. In addition, Menard pressuremeter tests are performed to enhance the data base. The features of the Shipbuilding Facility are discussed briefly followed by a detailed description of the subsurface conditions and the manner in which they were identified. An in-depth analysis is made of the full scale pile load tests to include delineating the procedures and tabulating the results. Test incidents which affected results are also highlighted since they have to be considered in the comparative analysis with results derived from the finite element method.

Although considerable subsurface soil data resulted from the investigations conducted by Schnabel Engineering, additional soil sampling and in-situ testing at the site was performed to support the laboratory test

program established for this study. The scope, types and results of this effort are treated in detail. Field investigations included the following: split-spoon sampling, Standard Penetration Tests; and Menard pressuremeter tests. The apparatus and procedures are addressed for each of these activities.

Standard soil laboratory tests were conducted to establish the basic properties and classification of the soils of the Yorktown formation. In addition, triaxial tests were performed to develop data required in connection with the finite element method. In this regard, the manner of determining the hyperbolic soil model parameters for soils along the pile perimeter are set forth in a step-by-step procedure and the results summarized. Similarly, laboratory tests were conducted to determine the stress-deformation characteristics along the pile-soil interface. This was accomplished by fabricating concrete blocks to represent the pile surface and using a direct shear apparatus that was appropriately modified for this phase of the test program. The test procedures, sample preparation and features of the apparatus are described in addition to the results.

The foregoing elements provided the requisite inputs for use of the finite element method of analysis. Although no attempt is made to describe the operative theory of this method, the steps that have been devised for

determining the ultimate bearing capacity of piles, their load-deformation behavior and load-transfer characteristics are addressed. The results achieved therefrom are then analyzed in relation to those from the full-scale pile test program.

The data generated from this study are reflected in several graphs and tables incorporated within the report and in the appendices. In the final section, the report is summarized and pertinent findings and conclusions are addressed.

Chapter 2

SUBSURFACE CONDITIONS AND PILE LOAD TESTS

2.0 Data Sources

Various reports prepared by Schnabel Engineering Associates, P.C. were used for the topics that are covered in the succeeding paragraphs. The specific topics include: foundation features; the description of soils associated with the strata of the Norfolk and Yorktown formations; and pile test descriptions, procedures and results.

2.1 Foundation Features

In 1984, the Tenneco Company began construction of a multi-million dollar Land Level Shipbuilding Facility at the Newport News Shipbuilding and Dry Dock Company located in Newport News, Virginia. The structure has plan dimensions of approximately 600 by 1100 feet and was designed to facilitate the construction of Navy ships and submarines. The foundation design includes approximately 10,000 closely spaced, prestressed, precast square concrete piles with a design capacity of 100 tons each. Parsons, Brinckerhoff, Quade and Douglas, Inc. were the designers of the structure to include the foundation system. Schnabel Engineering Associates, P.C., a Geotechnical engineering

consulting firm, located in Richmond, Virginia conducted the subsurface investigation and testing program for the project. Schnabel's activities included the conduct of load tests with both instrumented and non-instrumented piles in conjunction with their design effort regarding pile type, length, spacing, and installation criteria.

2.2 Subsurface Conditions

Schnabel Engineering conducted several hollow stem auger borings throughout the site at depths ranging between 50 to 130 feet below the ground surface. Standard Penetration Tests were incorporated in the test boring program and were performed in accordance with the ASTM D-1586: Standard Method of Penetration Test and Split-Barrel Sampling of Soils. Figure 2.1 illustrates the resultant subsurface profile along the central portion of the site.

Stratum A represents fill material consisting of loose to compact silty and clayey sand and soft to stiff consistency clayey silt and silty clay extending from the ground surface to depths of 2 to 29 feet. Underlying this stratum at depths ranging from 4 to 40 feet are Pleistocene geological age alluvial deposits of the Norfolk formation. Stratum B1 is comprised of beach and dune deposits consisting of loose to compact sands with varying amounts

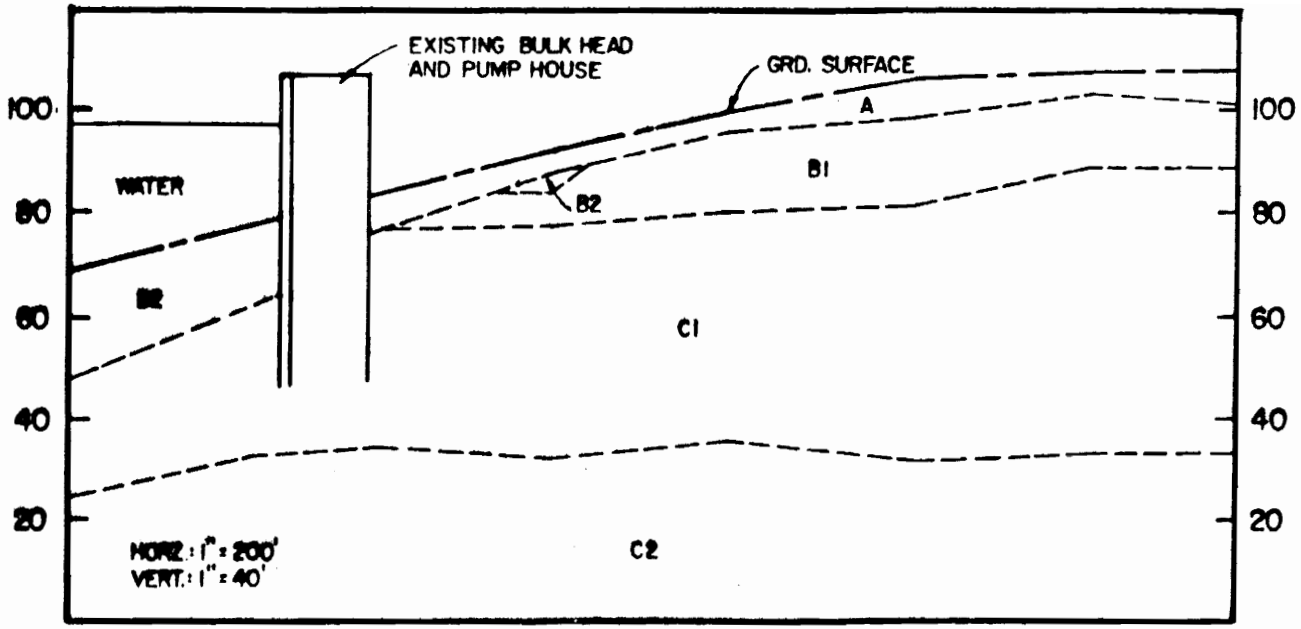

SECTION A-A

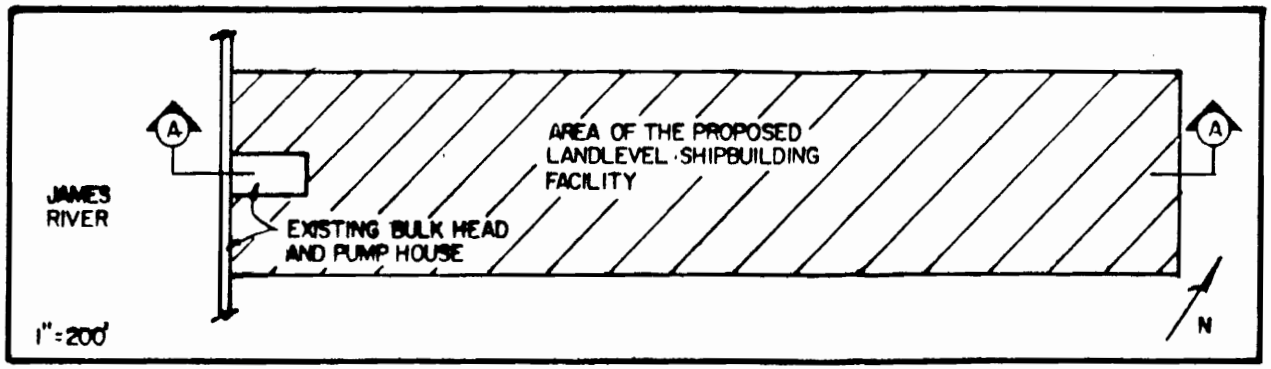

PLAN

FIGURE 2.1 SUBSURFACE PROFILE

of silt, clayey silt, silty clay and shell fragments. Stratum B2 contains lagoonal deposits consisting of very soft to medium consistency clayey silt and clay with varying amounts of sand and shell fragments. Underlying the Norfolk formation are Miocene geological age alluvial deposits referred to as the Yorktown formation. The Stratum C1 soils of the upper portion of this formation consist of loose to compact clayey silty and silty clayey sand with interbedded layers of soft to stiff consistency sandy silty clay and clayey silt. Typically, granular soils of Stratum C1 contain fines of greater than 35 percent but less than 65 percent by weight. The more plastic soils of Stratum C1 have been found typically to have liquidity indices ranging between 1.0 to 1.4 indicating that the soils are slightly sensitive (14). The lower portion of the Yorktown formation, Stratum C2, consists of soils of a loose to compact sand with less than 35 percent fines by weight.

Groundwater levels were encountered during drilling at depths between 2 to 9 feet below the ground surface. Variation in the groundwater elevation across the site reflects changes in ground surface elevation, subdrainage systems within the vicinity of the site and tidal changes of the James River which bounds the site to the south. Long term groundwater readings were not available.

2.3 Description of Pile Tests

Six test piles, identified as TP-1 through TP-6, were installed at the site. All six were 14 inch square prestressed, precast concrete piles. Test piles TP-1, TP-2, TP-5 and TP-6 were 90 feet in length and were not instrumented. Piles TP-3 and TP-4 were 70 feet in length and were instrumented with vibrating wire strain guages embedded at intervals of 10 feet along their central axis. Instrumentation was accomplished at the time the piles were cast.

Piles TP-1, TP-2 and TP-3 were embedded approximately 42 feet within Stratum C1 to depths of 55, 60 and 61 feet respectively below the ground surface. Piles TP-4, TP-5 and TP-6 were embedded approximately 44 feet within Strata C1 and C2 at depths of 58, 71 and 48 feet respectively below the ground surface. All six test piles were driven continuously to the required tip elevation using a Vulcan 010 single acting air driven pile hammer with an energy rating of 32,000 ft.-lbs. The location of each of the six test piles are shown in Figure 2.2.

Piles TP-3, TP-4 and TP-5 were selected for load tests which were performed in accordance with ASTM D-1143-81: Piles Under Axial Compressive Loads. During preparation for load testing of pile TP-4, settlement of the load frame reaction cribbing resulted in preloading.

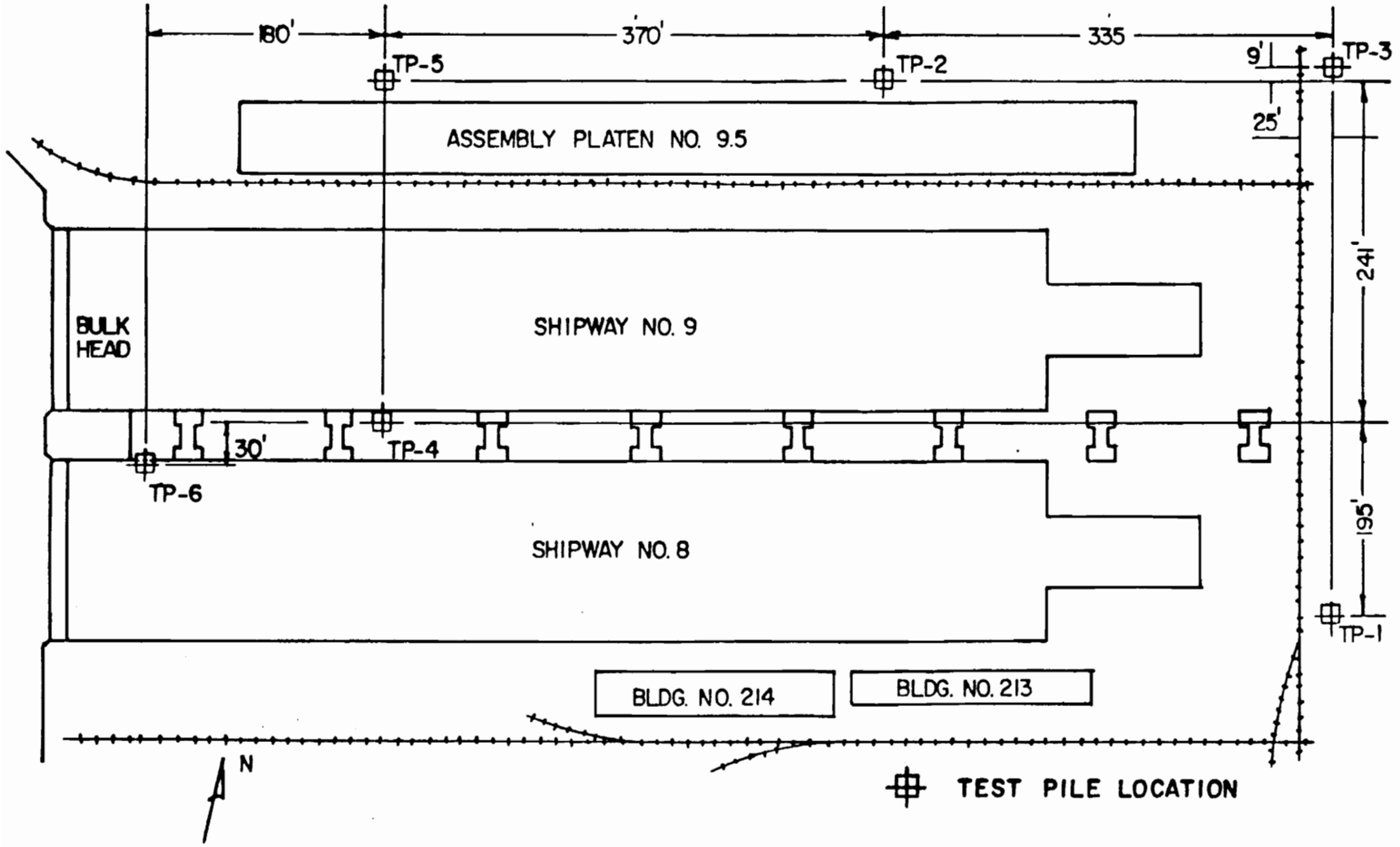

FIGURE 2.2 TEST PILE LOCATION PLAN, LANDLEVEL SHIPBUILDING FACILITY

In addition, during the test the electronic load cell malfunctioned resulting in erroneous readings. Hence, the load test was terminated at this juncture and the pile was driven an additional 4.0 feet. After a period of 72 hours, to allow for excess pore pressure dissipation and thixotropic strength gain resulting from redriving, testing of pile TP-4 was performed in accordance with ASTM D1143-81.

2.4 Test Procedures

Loads were applied by jacking against a load frame. An electronic load cell positioned between the jack head and reaction beam of the load frame was used to monitor applied loads. Three dial guages mounted independently of the load frame were used to measure vertical movement of the test pile. These were checked using an independent wire, mirror and rule system.

The procedures utilized for load testing of piles TP-3 and TP-5 were as follows. The test pile was initially loaded to twice the 100 ton design load in 25 ton increments. Each load increment was maintained until the rate of settlement was less than 0.01 inches in one hour or for a period no longer than two hours. The 200 ton load was held for a period of 15 hours and then unloaded in 50 ton increments to zero load. After a period of less than

one hour, the pile was reloaded to 200 tons in 50 ton increments with each load held for 20 minutes. Loading continued beyond 200 tons in 10 ton increments with a 20 minute hold until the pile failed to maintain the load or to the maximum 300 ton capacity of the load frame reaction system. The load application procedures described above were also used for pile TP-4 except the pile was not subjected to the unload-reload cycle. The load-settlement curves for the applied load cycles are presented in Figure 2.3 for piles TP-3, TP-4 and TP-5. The strain guages embedded within piles TP-3 and TP-4 were monitored throughout the pile load test. The resultant distribution of the force within the pile as a function of depth and applied load is presented in Figures 2.4 and 2.5.

2.5 Pile Test Results

Settlement of pile TP-5 was significantly less than that exhibited by piles TP-3 and TP-4 under similar loads. At the design load of 100 tons, total settlement of 0.18, 0.16 and 0.06 inches were recorded for piles TP-3, TP-4 and TP-5 respectively. Using the Norlund method and the load-displacement data, ultimate capacity values were determined as follows: TP-3 (250 tons); TP-4 (220 tons) and TP-5 (320 tons). Ultimate capacity is defined as the point along the load-displacement curve at which gross

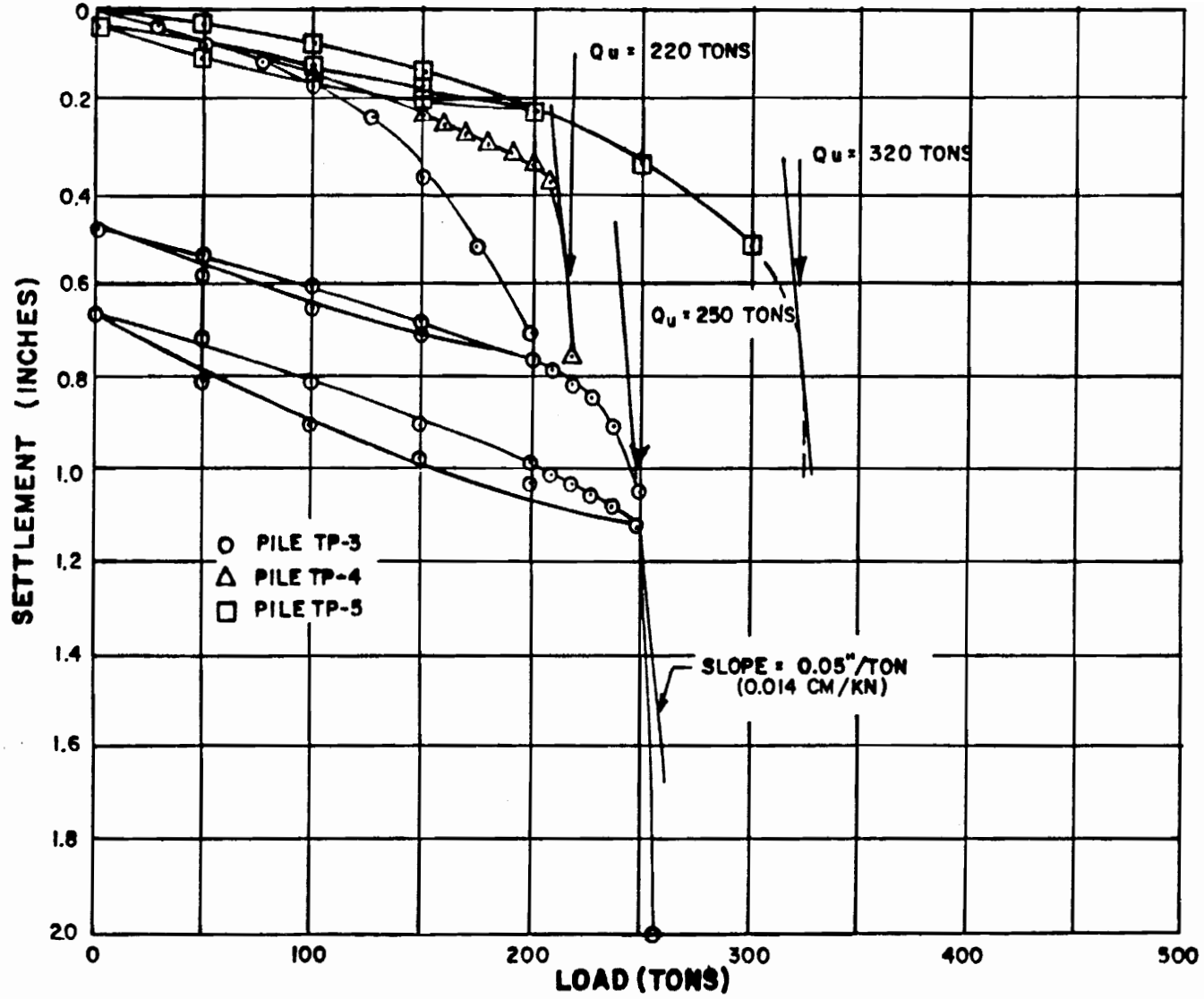

FIGURE 2.3 LOAD-SETTLEMENT CURVES FOR TEST PILES TP-3, TP-4, AND TP-5.

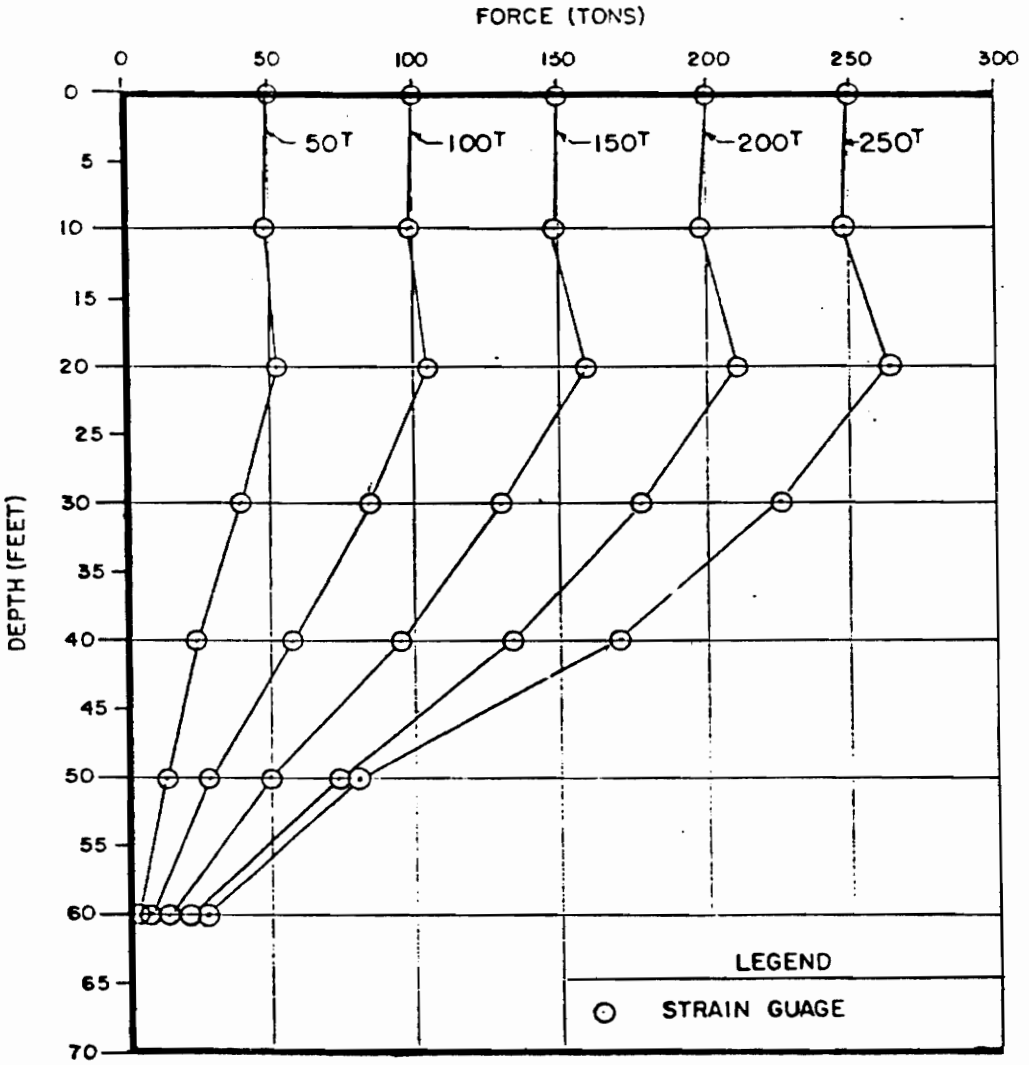

FIGURE 2.4 LOAD - DISTRIBUTION CURVES FOR TEST PILE TP-3

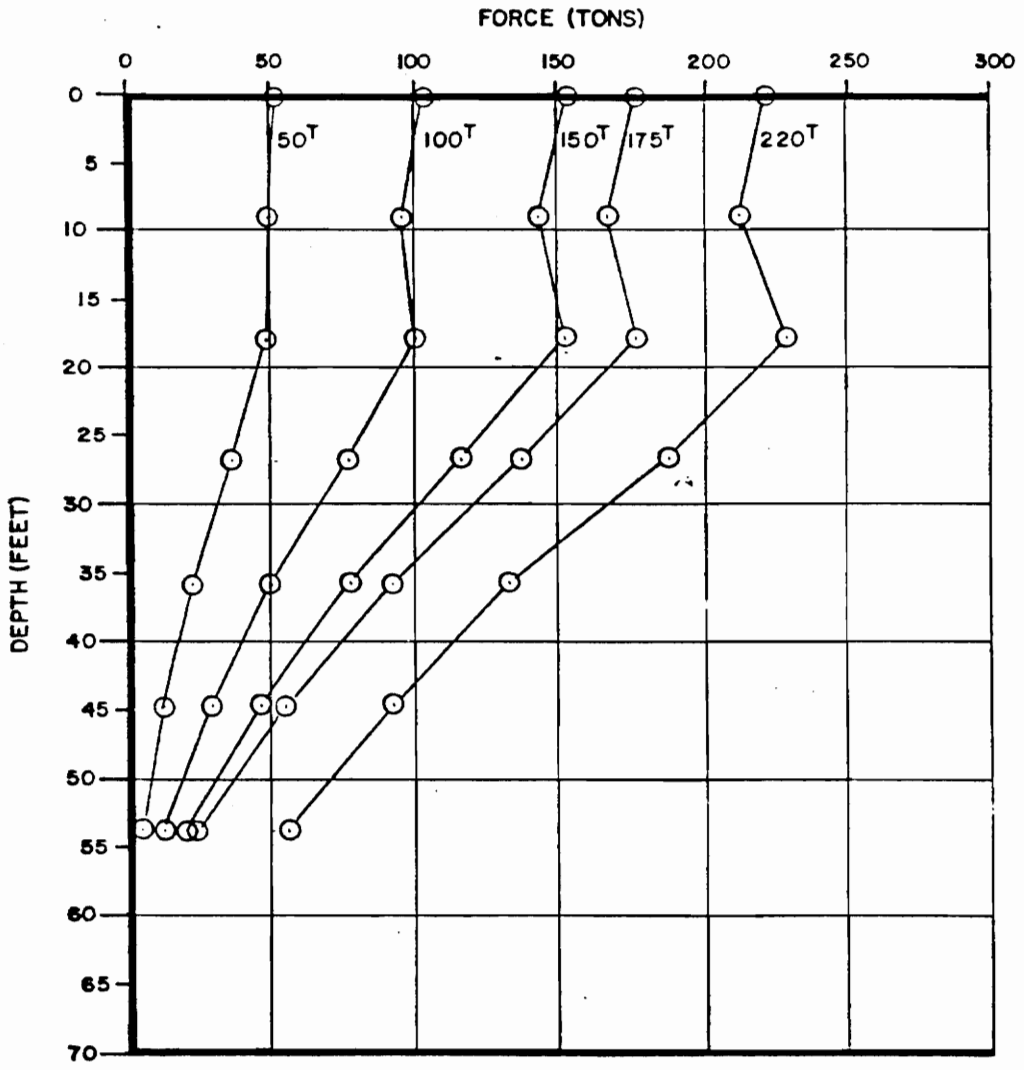

FIGURE 25 LOAD-DISTRIBUTION CURVES FOR TEST PILE TP-4

settlement begins to exceed 0.05 inches per ton of additional load (15).

2.6 Analysis of Test Data

Comparison of the embedded length and soil medium of test piles TP-3, TP-4 amd TP-5 indicate that the increased capacity of pile TP-5 was derived mainly from a greater side friction developed from granular fill soils that extend to a greater depth than at the locations of piles TP-3 and TP-4. At the three pile locations, fill soils (Stratum A) extended below the ground surface to depths of approximately 7, 4 and 29 feet for piles TP-3, TP-4 and TP-5 respectively. Underlying the fill soils at the locations of piles TP-3 and TP-4 are soft clays and silts of the Norfolk formation extending to depths of 19 and 14 feet respectively from the ground surface. These were not present in the area of pile TP-5 since the soils of the Yorktown formation directly underlie the fill. Piles TP-4 and TP-5 were embedded approximately 44 feet within the Yorktown formation; pile TP-3 was embedded 42 feet. The strain guage data from piles TP-3 and TP-4 would indicate that the shallow fill soils and the soft clay and silt soils of the Norfork formation contribute little to the overall capacity of the pile.

Variations in the ultimate load capacity of piles

TP-3 and TP-4 may be due in part to variations in soil conditions along the pile shaft and tip. However, the differences in loading procedures used for these two piles may also account for the difference in the ultimate load capacity. Analysis of the load-distribution curves indicate that the measured load at a depth of approximately 20 feet below the ground surface is greater than the actual applied load. This signifies that negative skin friction developed at the soil-pile interface at this depth. Martin (14) discussed several possible explanations which may have caused this to occur. The first was that the piles were not driven perfectly plumb causing a bending stress to be developed within the pile. Secondly, it was possible that not all of the strain guages were embedded exactly along the central axis of the pile. Another possible cause was an imposed load caused by the dead weight of the load frame that was adjacent to the pile. Corrections of the load distribution curves at the limit load attributed to possible stresses imposed by the weight of the load frame are shown in Figures 2.6 and 2.7 for piles TP-3 and TP-4 respectively. Since the effects of possible eccentricity could not be measured during testing, corrections for this factor were not applied.

Based on the corrected load distribution curve for pile TP-3, the unit shaft resistance was found to vary from 0.7 to 1.4 tsf in the upper stratum of the Yorktown

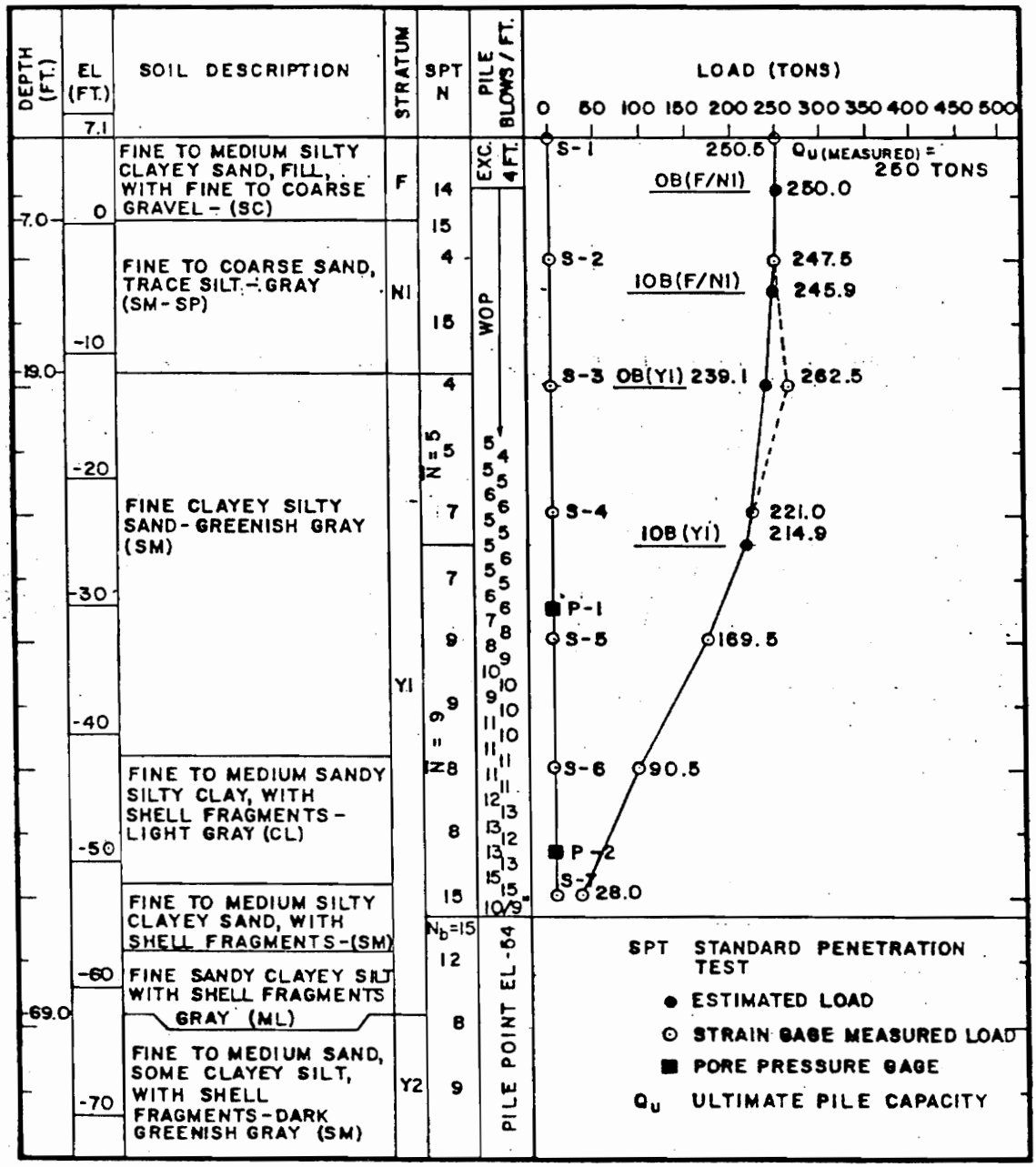

FIGURE 2.6 CORRECTED LOAD-DISTRIBUTION CURVE AT THE ULTIMATE LOAD FOR TEST PILE TP-3 (After Martin, et al., 1987)

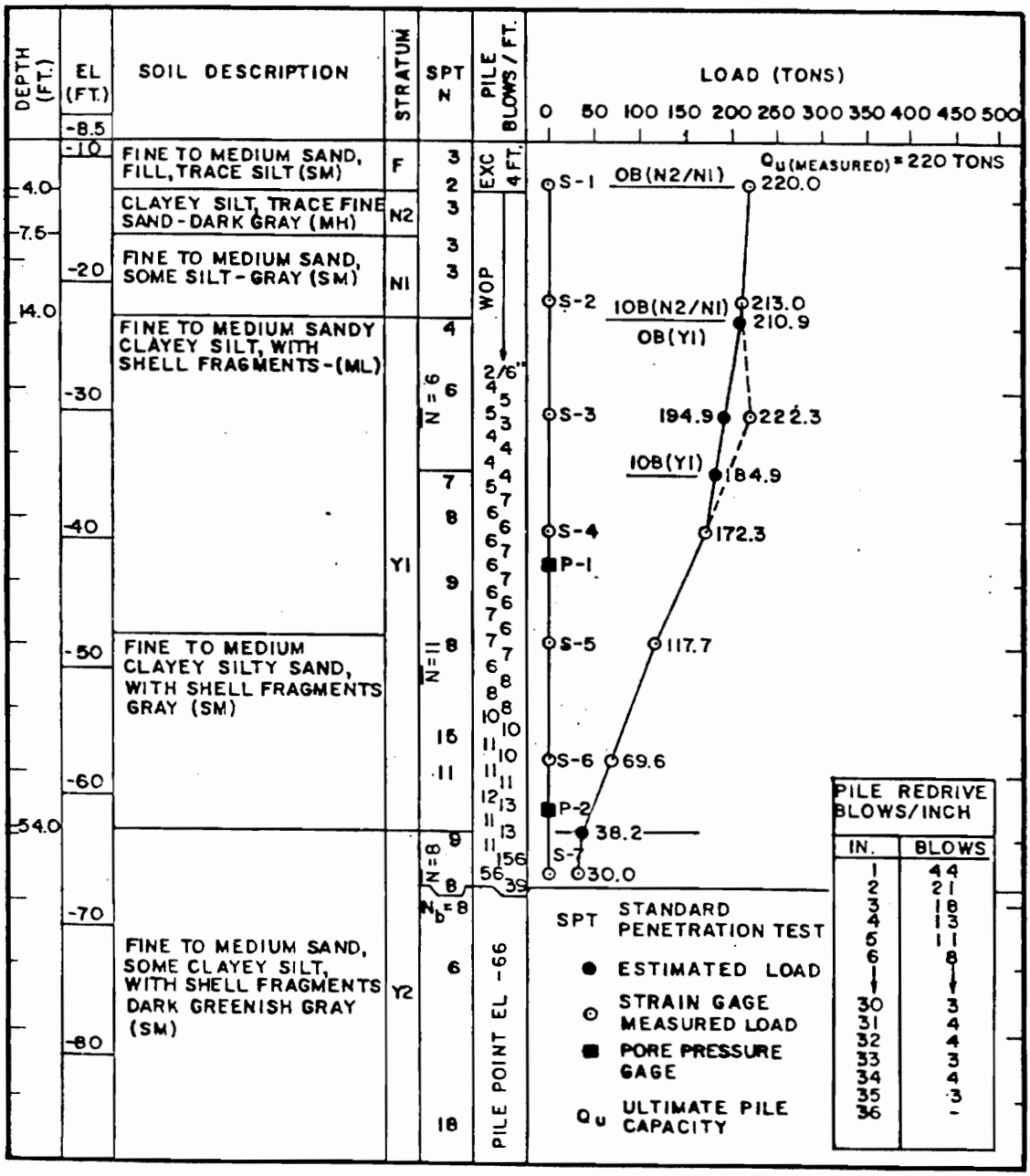

FIGURE 2.7 CORRECTED LOAD-DISTRIBUTION CURVE AT THE ULTIMATE LOAD FOR TEST PILE TP-4 (After Martin, et al., 1987)

formation. The load distribution curve for pile TP-4 also produced similar results. Unit shaft resistance varied between 0.6 to 1.2 tsf within Stratum C1. These variations are attributed to changes in relative densities throughout this stratum.

Unlike pile TP-3 which was embedded totally within Stratum C1, the last five feet of pile TP-4 was embedded within the more granular soil of Stratum C2. The load-distribution curve disclosed a unit shaft resistance of 0.5 tsf for Stratum C2.

The unit point resistance as reflected by the load-distribution curves for piles TP-3 and TP-4 were slightly different. The pile tip of TP-4 supported by Stratum C2 produced a unit point resistance of 28.7 tsf whereas the pile tip of TP-3 which was supported by the finer grain soils of Stratum C1 produced a lower unit point resistance of 20.6 tsf.

Although the point resistance for pile TP-4 was greater than pile TP-3, the ultimate load capacity was slightly less as determined from the load-settlement data. This was most likely due to variation in unit skin resistance throughout Stratum C1.

Chapter 3

SOIL SAMPLING AND IN-SITU TESTING

3.0 Introduction

One of the requirements in the determination of pile capacity and behavior is the analysis of subsurface conditions, index properties and strength-deformation characteristics of the soil medium in which the pile is embedded. In the preceding chapter, results of subsurface investigations and pile load tests were presented. However, these data were insufficient to perform the finite element method of analysis undertaken in this study. Therefore, it was necessary to conduct additional soil investigations.

Soil sampling was performed within a single bore hole using both "disturbed" and "undisturbed" methods; specifically, split spoon and Shelby tube samplers. Standard Penetration Tests and Menard Pressuremeter Tests were also performed. The purposes of these sampling procedures and tests were twofold: to obtain representative samples of the soil medium in which the piles were embedded for use in soil laboratory tests and secondly, to determine the in-situ strength and deformation characteristics of the soil medium.

The soil sampling and in-situ tests were limited

to a single test boring performed just prior to installation of production piles at the site on April 24, 1984. The location selected was approximately 21 feet south of pile TP-4 as shown on Figure 3.1. The areas near test piles TP-3 and TP-5 were not accessable at the time of this study.

The soil boring was drilled by Foundation Testing Services of Bethesda, Maryland. The borehole was drilled by a 3.5 inch hollow stem auger attached to a truck mounted drill rig, Model CME-45B. The boring extended from the ground surface to a depth of 75.0 feet. Since the load bearing capacity of piles is attributed primarily to Strata C1 and C2 soils within the Yorktown formation, sampling was limited to these soils. In-situ tests incorporated within the test boring program included Standard Penetration Tests and Menard pressuremeter tests.

3.1 Soil Sampling and Standard Penetration Tests

The boring operation included sampling subsurface soils of the Yorktown formation from a depth of 14.5 to 75.0 feet below the ground surface. Both split spoon and Shelby tube samplers were used at intervals of approximately 10 feet. The subsurface soils of the Norfolk formation were not sampled since they were found to have little impact on pile behavior for reasons already stated.

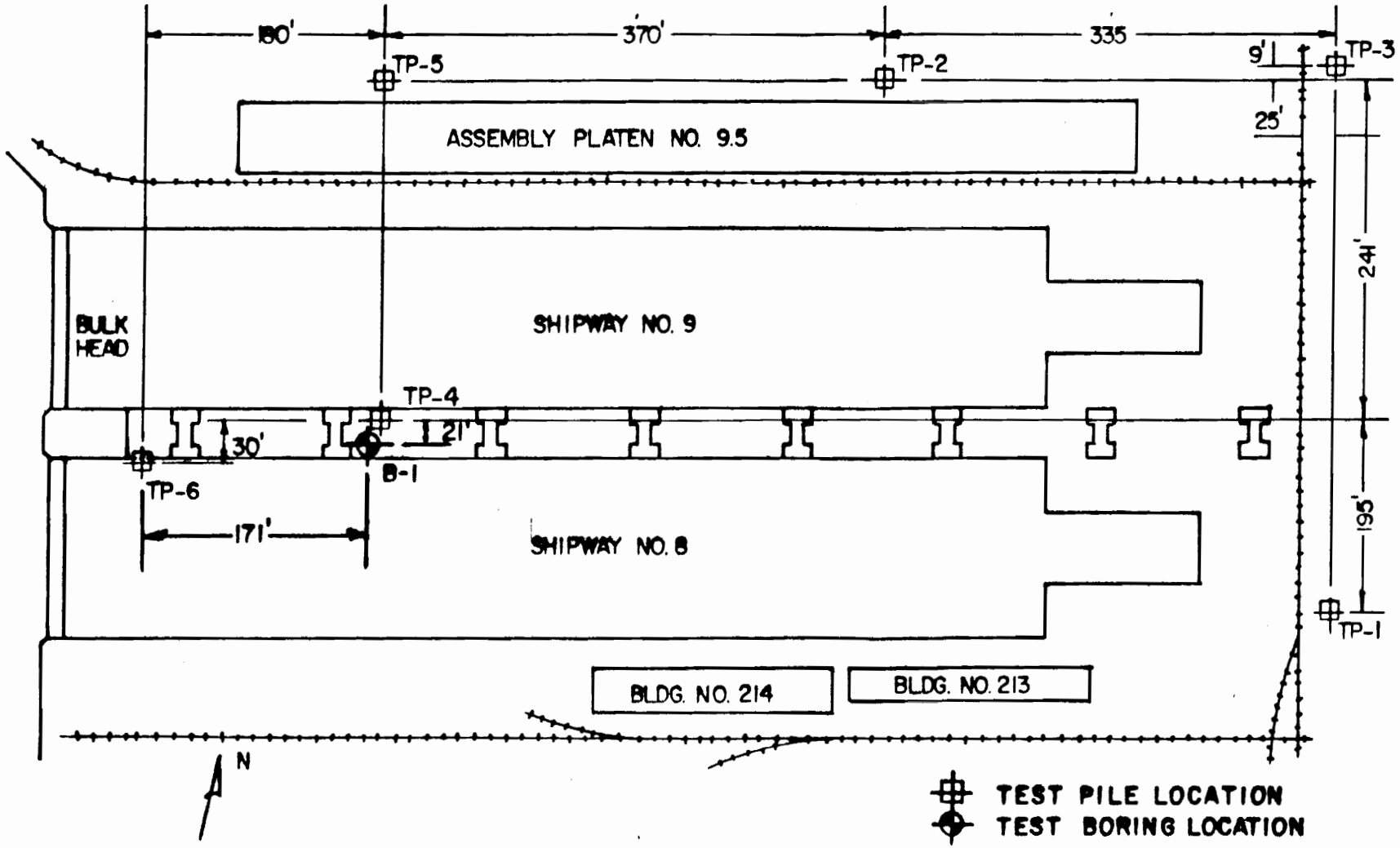

FIGURE 3.1 TEST BORING LOCATION PLAN

The "standard" split spoon sampling method was performed in accordance with the procedures set forth in ASTM D-1586: Standard Method of Penetration Test and Split-Barrel Sampling of Soils. The sampler used had dimensions of 2.0 inches O.D. and 1.375 inches I.D. and was driven with a 140 lb. weight falling 30 inches to a depth of 18 inches. The number of blows required to drive the sampler every 6.0 inches was recorded. The first 6.0 inches of driving seated the sampler at the bottom of the borehole whereas the number of blows required to drive the sampler an additional 12 inches represented the Standard Penetration Test value of the soil. This value, also referred to as the SPT N value, was then used to ascertain the relative density of the soils. The soil sample retained within the sampler was visually classified in accordance with ASTM D-2487: Uniform Soils Classification System and recorded in the Test Boring Log, Figure 3.2. The soil samples were then placed in air-tight glass jars and brought to the soil laboratory for further testing.

After the split spoon sample was obtained, the borehole was advanced 2.0 feet. At this point, a 3.0 inch I.D. thin walled metal tube (Shelby tube) with a maximum 30 inch recovery capacity was pushed under the weight of the cathead attached to the drill rig. The Shelby tube, with its larger diameter, thin wall, tapered edge and method of installation resulted in soil samples that were less

PROJECT: LANDLEVEL SHIPBUILDING FACILITY
NEWPORT NEWS SHIPBUILDING AND DRY DOCK COMPANY
NEWPORT NEWS, VIRGINIA

BORING NO. B-1
SHEET NO. 1 OF 1
DATE STARTED 4-21-81
FINISHED 4-21-81
DRILLER: N. STEDHAM
INSPECTOR: J. DOUGLAS

GROUND SURFACE ELEVATION: ± 12.2
GROUND WATER ELEVATION ENCOUNTERED: ± 10.3
GROUND WATER ELEVATION AFTER ___ HRS: —
CASING SIZE 5-1/2" O.D.
DRIVE SAMPLER DIA. 2" O.D. WT. 140# FALL 30"

	DEPTH (FT)		BLOW COUNT ON SPOON PER 6"		SOIL DESCRIPTION	REMARKS
						SUBSURFACE FROM GROUND SURFACE TO 14.5 FT NOT SAMPLED
C1	14.5	77.7	2-2-2	S	FINE TO MEDIUM SANDY CLAYEY SILT (ML), WITH SHELL FRAGMENTS, MOIST - GRAY	P.M. TEST NO. 1: 15' - 17'
				3"		
	23.5	-70	2-5-4	S	FINE TO MEDIUM SILTY SAND (SM) WITH SHELL FRAGMENTS, MOIST - GRAY	P.M. TEST NO. 2: 25' - 27'
				3"		
	33.0	-60	3-5-6	S	FINE TO MEDIUM SANDY CLAYEY SILT (ML), WITH SHELL FRAGMENTS, MOIST - GRAY	P.M. TEST NO. 3: 35' - 37'
				3"		
	43.0	-50	3-4-4	S	FINE TO MEDIUM SILTY SAND (SM), WITH SHELL FRAGMENTS, MOIST - GRAY	P.M. TEST NO. 4: 45' - 47'
		-40	6-14-14	S	DO, WITH HIGH CONCENTRATION OF SHELL FRAGMENTS	P.M. TEST NO. 5: 55' - 57' P.M. TEST NO. 6: 57' - 59'
C2	60.0	-30			FINE TO MEDIUM SAND, SOME SILT (SM), WITH SHELL FRAGMENTS, MOIST - DARK GREEN	
			4-4-6	S		P.M. TEST NO. 7: 65' - 67' (MEMBRANE RUPTURED) P.M. TEST NO. 8: 68' - 70' (CONTROL UNIT MALFUNCTION) P.M. TEST NO. 9: 72' - 74' (MEMBRANE RUPTURED)
		-20	3-3-9	S		
	75.0				BORING TERMINATED AT 75.0 FT	

S SPLIT SPOON SAMPLER LOCATION — PRESSUREMETER TEST LOCATION
3" SHELBY TUBE SAMPLER LOCATION — PRESSUREMETER TEST/SHELBY TUBE LOCATION

FIGURE 3.2 TEST BORING LOG

disturbed than those collected by the split spoon sampler. The tube was detached from the drill rods; the top and bottom openings of the tube were then sealed in wax. The depths at which the Shelby tube samples were collected are shown on the Test Boring Log, Figure 3.2.

For "bulk" soil samples, a 3.0 inch I.D. split spoon sampler was used. The split spoon sampler was continuously driven from the bottom of the borehole to its full length (2 feet) by the 140 lb. hammer attached to the drill rig. Blow counts were not obtained when the split spoon was being driven. The soils obtained within the split spoon were removed and placed in burlap bags. One bulk sample from Strata C1 and C2 was obtained.

Standard Penetration Test values of 8 and 9 were recorded for the granular soil of Stratum C1 which indicates they are of a firm density. An SPT value of 28 was recorded at a depth of approximately 55 feet below the ground surface. Most likely, this resulted from a heavy concentration of shell fragments encountered at this depth. The fine grained soils of Stratum C1 were determined to be of a soft to stiff consistency based upon SPT values of 2 and 11. The SPT values of 10 and 12 for the granular soils of Stratum C2 reflect that they too are of a firm density.

3.2 Menard Pressuremeter Tests

The pressuremeter test was first conceived by F. Kogler of Germany in 1933 and subsequently developed by M. Louis Menard in 1956 as a means of determining the in-situ strength-deformation characteristics of soils. The test involves the expansion of a cylindrical probe beneath the ground surface in order to measure the relationship between pressure and the resultant deformation of the soil. Soil properties are then calculated from the test data utilizing elastic-plastic or rheological theory.

3.2.1 Pressuremeter Test Apparatus

There are several types of pressuremeters, however, the probe, control unit and tubing are common to all as illustrated in Figure 3.3. Details concerning the make-up of each of these components can be found in reference (1). In this study, Menard Pressuremeter Model No. GC was used. This unit is best suited for soils of a soft to stiff consistency.

The probe, which is inserted within the borehole, applies a radial pressure along the walls of the borehole and simultaneously measures the increase in volume of the hole. At both ends of the probe are guard cells inflated by compressed bottled gas to the same pressure as the

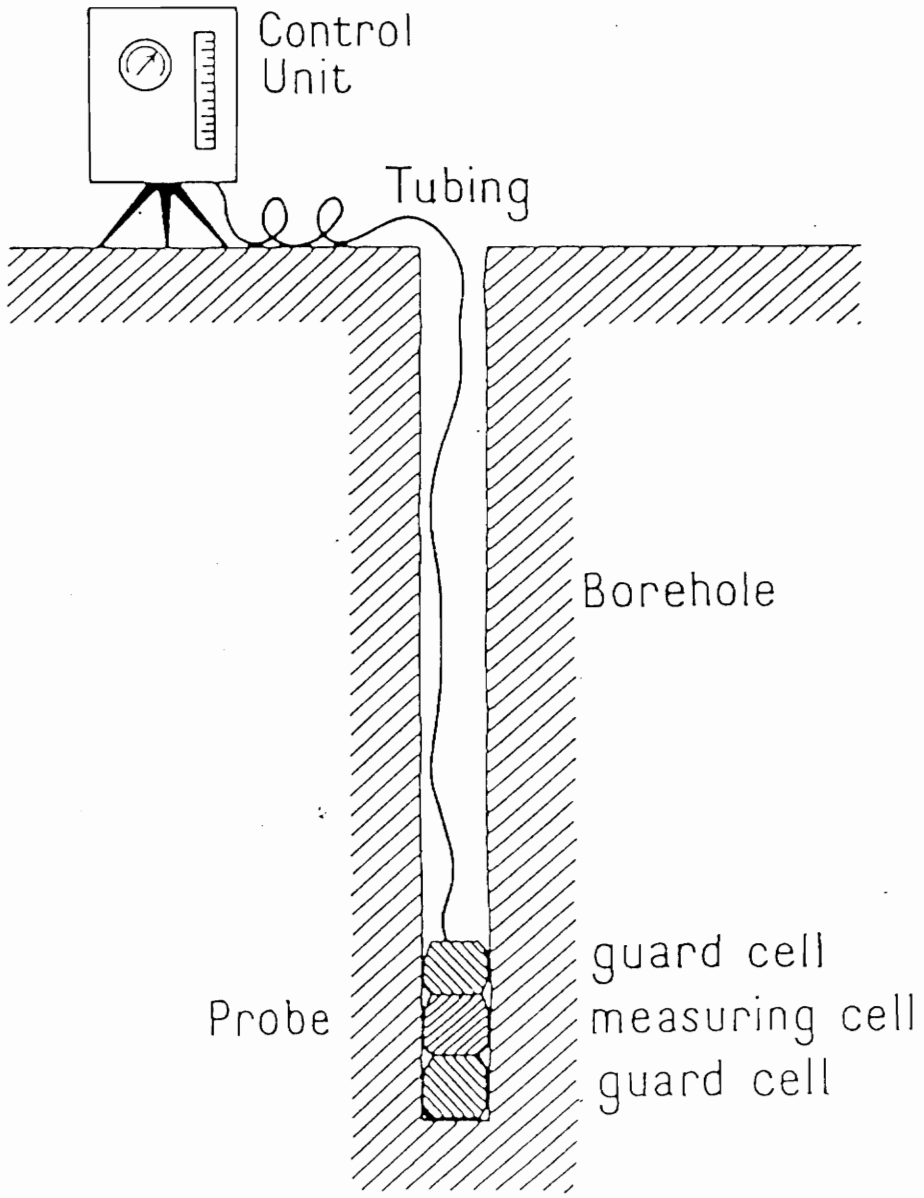

FIGURE 3.3 PRINCIPLE COMPONENTS OF THE MENARD PRESSUREMETER

measuring cell. This insures that deformation is radial. An outer sheath of heavy rubber, neoprene or rubber with steel straps is attached to the probe to protect the measuring cell from puncture. In the subsurface investigation performed for this study, a steel strap sheath was used due to the high concentration of shell fragments.

The control unit, consisting of a graduated water cylinder (volumeter) and regulator, controls and monitors expansion of the probe through tubing that conveys the water and gas from the control unit to the probe.

Equal increments of pressure are applied to the probe and the stress levels are held constant for a fixed length of time, usually one minute. Volume changes are recorded at intervals of 15, 30 and 60 seconds for each load application. The plot of the volumeter reading for each pressure increment typically results in a curve of the shape illustrated in Figure 3.4a. This curve represents readings derived from the control unit. Certain corrections for errors caused by the apparatus are required in order to plot the actual pressure-volume response of the soil. These corrections account for pressure gains and losses introduced by the test apparatus itself. The degree of correction required depends upon the particular type of pressuremeter used.

The plot of the corrected volume and pressure

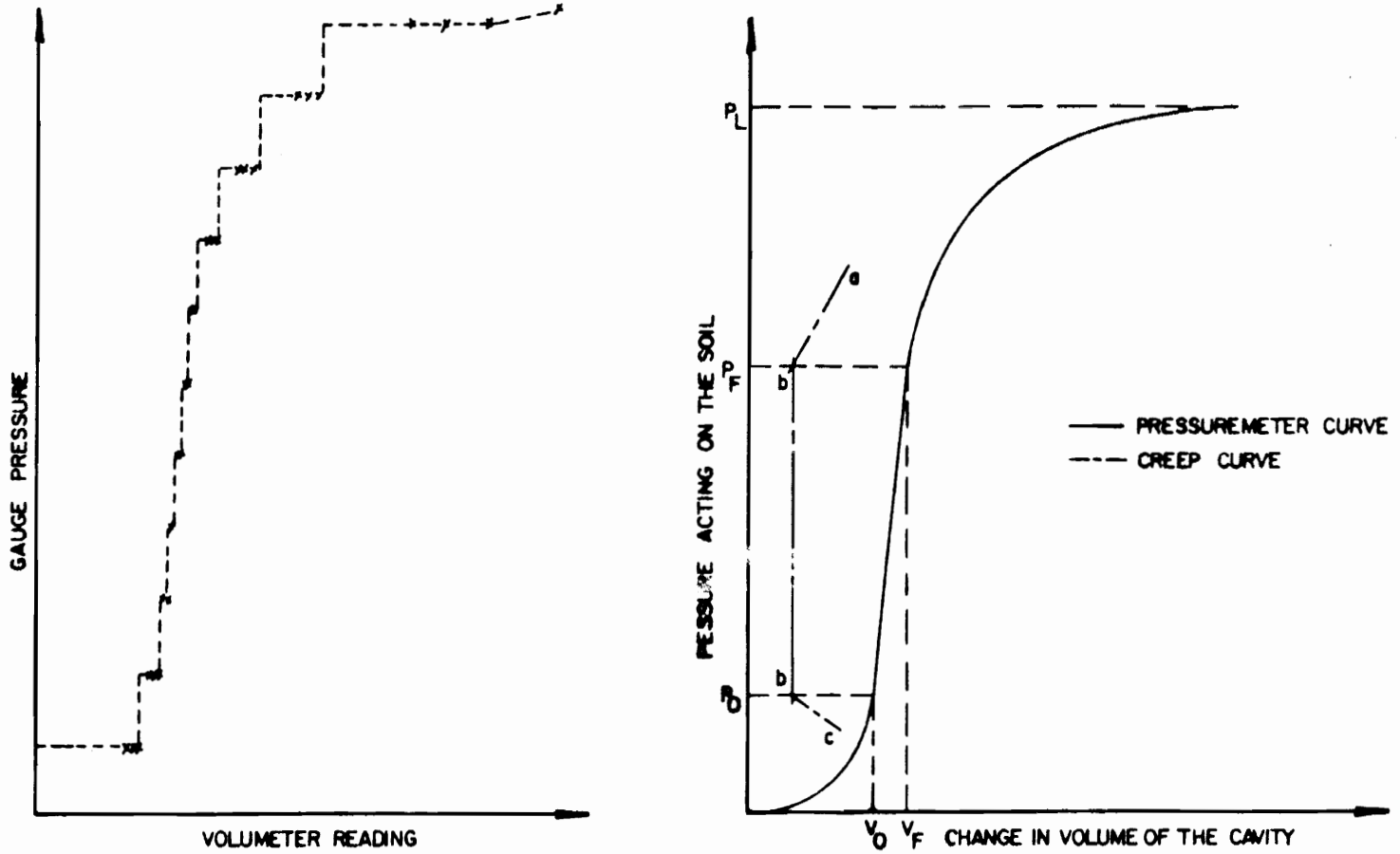

FIGURE 3.4 TYPICAL CORRECTED AND UNCORRECTED PREBORED PRESSUREMETER CURVES

data typically result in a curve of the shape illustrated in Figure 3.4b. Theoretically, there are three phases to the pressuremeter curve. The initial portion of the curve represents adjustment of the soil along the sidewalls of the borehole to its original state before the borehole was drilled. The pressure (Po) at this phase approximates the at-rest horizontal earth pressure of the soil. The corresponding volume (Vo) defines the initial size of the cavity.

In the second phase, the soil enters a pseudo-elastic state in which the curve behaves linearly with increased pressure changes beyond Po to the final pressure (Pf). The pressure (Pf) and corresponding volume (Vf) signify the start of yield conditions along the walls of the borehole. In the psuedo-elastic state, soil strain is assumed to conform to the laws of elasticity expressed by the equation:

$$G = V\ (\Delta p/\Delta v) \qquad 3.1$$

where the shear modulus (G) equals the volume (V) of the cavity corresponding to a particular change in pressure (Δp) and change in volume (Δv). While the slope ($\Delta p/\Delta v$) of the pressuremeter curve is constant from Vo to Vf, the volume (V) is not. Therefore, the value of the shear modulus (G) depends on the location along the line Vo to Vf

at which it is computed. Menard proposed that the volume at the midpoint (Vm) between Vo and Vf be used to compute the shear modulus. The midpoint volume (Vm) is computed as follows:

$$Vm = Vo + (Vo + Vf)/2 \qquad 3.2$$

The Menard shear modulus (Gm) is then calculated as follows:

$$Gm = Vm(\Delta p/\Delta v) \qquad 3.3$$

The value of Gm can also be determined directly from the pressuremeter data by plotting Δp versus $\Delta v/V$ in which Gm equals the slope of the curve between Vo to Vf.

For linear isotropic soils, the shear modulus may be converted to Young's Modulus (E) as follows:

$$E = 2(1 + \nu)G \qquad 3.4$$

For the above relationship, Menard recommended that a standard value of 0.33 be used for Poisson's ratio (ν). The resulting deformation modulus is referred to as the Menard pressuremeter modulus (Epm) for a soil and is expressed by the formula:

$$Epm = 2.66(Gm) \qquad 3.5$$

During the final phase, pressure increases above the initial yield pressure (Pf) result in an increased rate of volume change in the plastic deformation region and eventually becomes asymptotic. The pressure along the horizontal asymptote is referred to as the limit pressure (Pl) which is used to estimate the shear strength of the soil. In general, the limit pressure is taken as the pressure required to double the initial volume of the cavity.

Due to the limited number of data points resulting from this process, it is difficult to accurately interpret the values of Po and Pf from the pressuremeter curve. In order to facilitate the determination of these values, the change in volume that occurs between the 30 second and one minute reading versus the corresponding pressure change is plotted as illustrated in Figure 3.4b. This is referred to as the "creep curve" and the value of Pf as the "creep pressure". The pressure (Po) and pressure (Pf) correspond to the intersection of the two lines a-b and b-c formed by the creep curve.

In practice, interpretation of pressuremeter data is rather complex and therefore not usually suitable as a means of direct measurement. The influence of soil disturbance in forming the testhole and the inability to

determine drainage conditions during testing are among a number of factors that can distort results (1). Thus, the pressuremeter test is used mainly as a correlative tool to determine the strength-deformation characteristics of soil supported by other types of in-situ and soil laboratory tests.

3.2.2 Pressuremeter Test Procedures and Results

The borehole was drilled with a truck-mounted drill rig (Model CME-45B) equipped with a 3.5 inch I.D. hollow stem auger. The auger was advanced to the desired depth with a plug insert attached to the drill rods. Upon removal of the plug, a 3.0 inch I.D. Shelby tube was pushed at the bottom of the hole to form the cavity for the pressuremeter test. Since the most critical phase of pressuremeter testing occurs when opening the testhole, a Shelby tube was used to minimize soil disturbance. The probe was attached to the drill rods and positioned within the cavity.

In order to determine the in-situ strength-deformation characteristics of soils within Strata C1 and C2, nine tests were performed by Schnabel Engineering Associates at depths indicated on the Test Boring Log, Figure 3.2. Five were conducted within Stratum C1 at intervals of approximately 10 feet and the remaining four

within Stratum C2 at closure intervals less than five feet.

All nine tests were conducted within borehole B-1 drilled at the location shown in Figure 3.1. The elevation and description of the soil type within the borehole are also indicated in the Test Boring Log in Figure 3.2.

The pressuremeter and creep pressure curves from six of the nine pressuremeter tests are included in Appendix A. These data represent the corrected volume and pressure readings after one minute and reflect the change in volume which occurred between the 30 second and one minute readings.

From the pressuremeter data, the values of Po, Pf, Pl, and Epm for pressuremeter tests PM-1 through PM-6 were determined. These are shown in Table 3.1. The change in the values of Po, Pf and Pl as a function of depth are illustrated in Figure 3.5. Similarly, Figure 3.6 shows the change in Epm and SPT values.

Insufficient data was collected from tests PM-7 through PM-9 because the rubber membrane of the measuring cell ruptured; in addition, the pressure gauge malfunctioned during test PM-8. These difficulties resulted in pressuremeter data only for soils of the upper Yorktown formation.

The values of Po, Pf and Pl were found to increase linearly with depth. The value of Po, which approximates the total horizontal stress of the soil,

TABLE 3.1 SUMMARY OF MENARD PRESSUREMETER TEST DATA, LANDLEVEL SHIPBUILDING FACILITY, NEWPORT NEWS SHIPBUILDING AND DRY DOCK COMPANY, NEWPORT NEWS, VIRGINIA

Pressuremeter Test No.	Depth (ft)	Po kg/cm^2	Vo cm^2	Pf kg/cm^2	Vf cm^2	Pl kg/cm^2	Pl* kg/cm^2	Gm tsf	Epm tsf
1	15-17	1.9	241	7.0	345	13.5	11.7	54	143
2	25-27	4.2	219	8.0	318	16.0	11.8	41	108
3	35-37	2.1	182	10.5	380	16.5	14.4	46	121
4	45-47	4.5	281	10.5	374	21.6	17.1	72	192
5	55-57	5.0	282	12.7	497	20.0	15.0	42	112
6	57-59	7.0	307	12.9	397	30.2	23.2	75	199

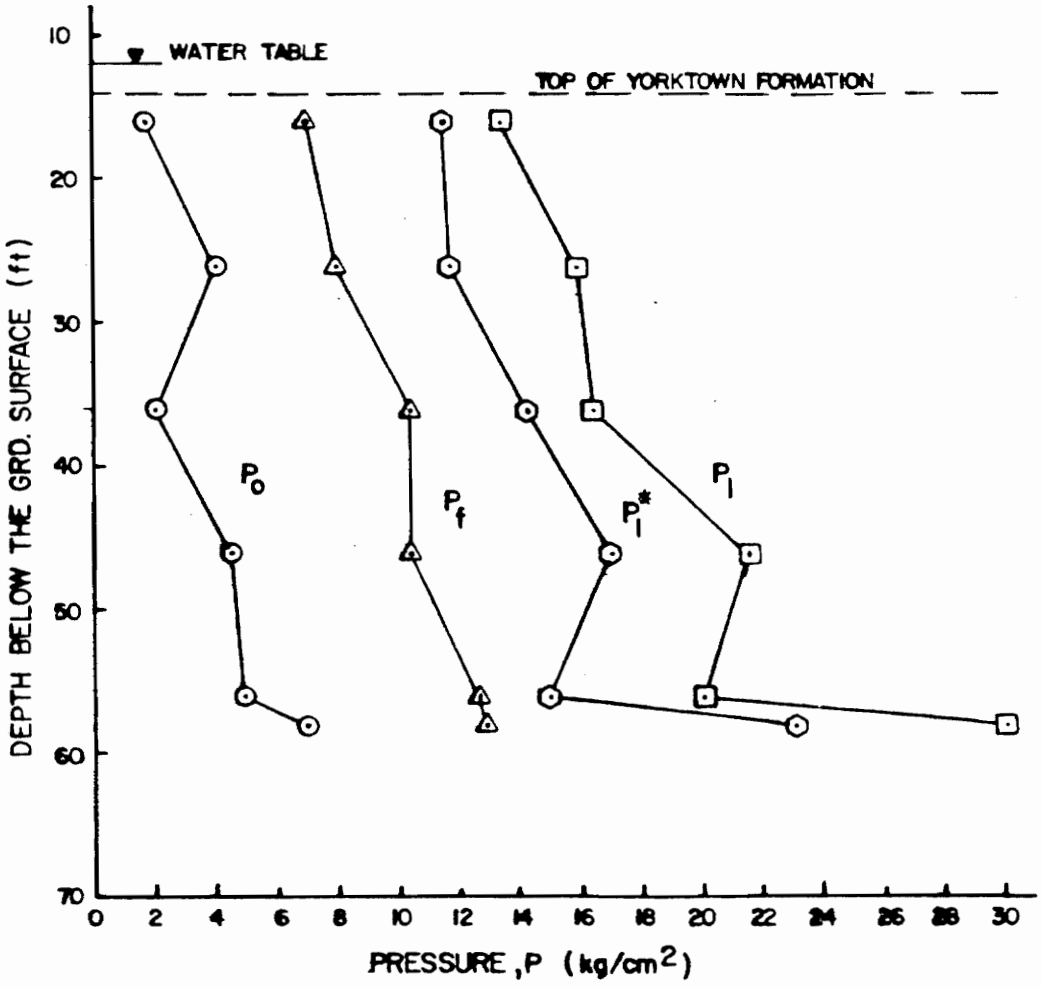

FIGURE 3.5 PROFILE OF P_o, P_f, P_l^*, AND P_l VALUES

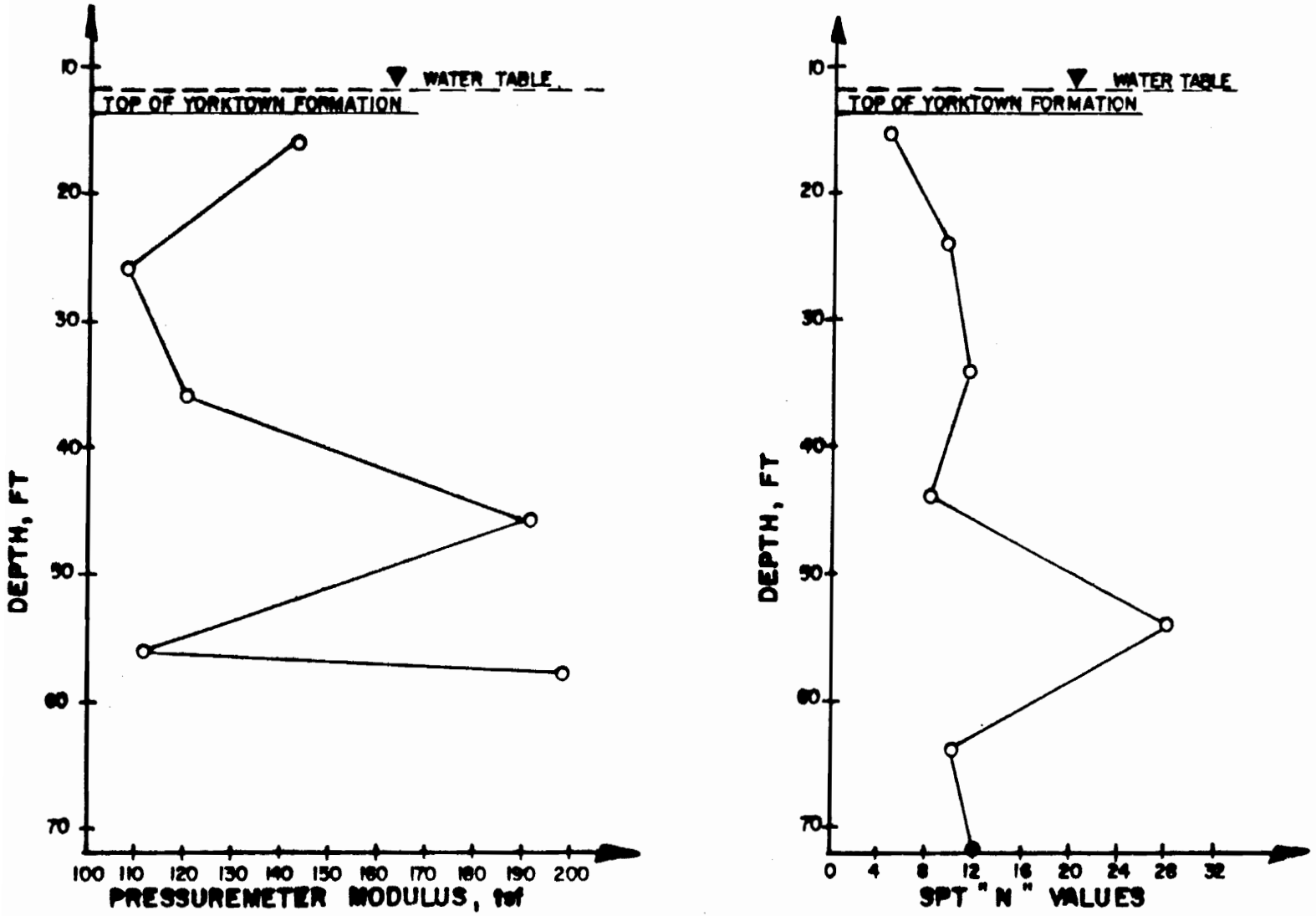

FIGURE 3.6 PRESSUREMETER MODULUS AND SPT "N" VALUES VERSUS DEPTH

varied between 1.9 to 7.0 tsf. This variance most likely resulted from the following: soil disturbance when forming the cavity; changes in soil type; and the inability to precisely determine the values of Po from the pressuremeter curve. In this regard, however, if it is assumed that the walls of the borehole did not undergo any substantial yield, then the values of Po can be used to determine the coefficient of at-rest earth pressure (Ko) as follows (1):

$$K_o = (Po - u)/\gamma' z \qquad 3.6$$

In this relationship, the porepressure (u), the depth below the ground surface (z) and effective unit weight (γ') of the overburden soil at that depth must also be determined. Considering the fact that soils of the Yorktown formation are granular and the manner in which the borehole was prepared, it would be realistic to assume that yielding of the borehole walls did occur.

The values of Pf also increased with depth from 7 to 12.9 tsf. It is interesting to note that studies performed by Lukes and DeBussey (1976) disclosed an equivalent relationship between the preconsolidation pressure (Pc) and the Pressuremeter failure pressure (Pf). Using this relationship, the over-consolidation ratio (OCR) for soils within the upper Yorktown formation is approxmiately 3.5. Consolidation test data obtained by

Schnabel Engineering for samples within this stratum yielded an OCR value of 3.2. Thus, the indicated values of Pf correlate well with values of Pc.

With regard to using the value of Pl from pressumeter data to determine the shear strength of soils, studies have revealed that only the undrained shear strength of cohesive soils can be determined with any degree of accuracy (9). In the relationship developed by Menard, the undrained shear strength (Su) is expressed as follows:

$$Su = (Pl-Po)/2K \qquad 3.7$$

where K is a variable coefficient that reflects soil type, relative density and soil structure. Gibson and Anderson (9) suggested a similar relationship for determining the undrained shear strength using the cohesive strength (c) of the soil and Poisson's ratio (ν) as follows:

$$Su = \frac{Pl-Po}{1 + \ln\{Epm/[2c(1+\nu)]\}} \qquad 3.8$$

In both equations, the value of Su is determined in part by the difference in the value of Pl and Po. This is referred to as the net limiting pressure (Pl*):

$$Pl^* = Pl-Po \qquad 3.9$$

The change in net limiting pressure with depth for the upper Yorktown formation is illustrated in Figure 3.5. The value of Pl* varies almost linearly throughout the soil stratum which indicates an increase in the shear strength of the soils in relation to depth. However, an accurate determination of shear strength was not deemed possible based solely on the data presented herein.

The change of the pressuremeter modulus (Epm) with depth is illustrated in Figure 3.6. The value of Epm varies between 110 and 140 tsf throughout the upper Yorktown formation except at depths of 46 and 58 feet. At these depths, values of 191 and 199 tsf respectively were recorded. Most likely, this resulted from heavy concentrations of shell fragments. This view is further supported by the sudden increase in SPT values versus depth as illustrated in Figure 3.6.

As discussed previously, the value of Epm cannot be compared directly with Young's Modulus. In order to obtain a reasonable value of Young's Modulus of a soil, Menard suggested that the value of Epm be divided by a rheologic coefficient (α) which considers both soil type and the degree of consolidation. For overconsolidated sand, Menard recommended a coefficent value of 0.5 which results in the Young's Modulus corresponding to twice the value of Epm. Using this value, Young's Modulus for granular soils of the Yorktown formation ranged between 216

and 288 tsf.

In brief, the pressuremeter data collected in conjunction with this study suggests:

1. The soil throughout the Yorktown formation is preconsolidated and has an OCR value of 3.5 based on the values of Pf.

2. Shear strength of the soil generally increases linearly with depth. This was evidenced by the increase in net limit pressure (Pl*) found throughout the Yorktown formation.

3. Insufficient data was available to allow for a reasonable determination of the actual strength of the soil.

4. Young's Modulus (E) values range from 216 to 288 tsf for the granular soils of the upper Yorktown formation.

5. Further pressuremeter testing within this soil formation must be conducted if a better correlation of pressuremeter data and soil properties is to be made.

Chapter 4

SOIL LABORATORY TESTS

4.0 General

The answer to a problem in Geotechnical engineering is normally obtained by first determining the properties of the soil in question and then employing these properties in predictive solutions. Often, soil properties can be effectively determined by soil laboratory testing.

Soil sampling and in-situ tests were performed in order to identify the soil type and relative density of the soil medium being investigated to include its in-situ strength-deformation characteristics. For further evaluation of the properties of the various soil types, soil laboratory tests were conducted. These were performed on the six Shelby tube samples obtained from the test boring for the following purposes: soil identification; determination of key strength characteristics; and establishment of hyperbolic soil parameters.

The strength properties of the soil medium are an important part in evaluating pile behavior. In this connection, Menard pressuremeter tests were conducted to obtain the in-situ strength-deformation characteristics of the soil. However, the data obtained was not deemed adequate to accurately determine the strength

characteristics. For this reason, triaxial tests were performed to better evaluate the strength characteristics of the soil medium. Along the soil-pile interface, it was not possible to determine the strength properties by conventional triaxial test methods. For this case, a soil-concrete interface test program was developed and is discussed later in this report.

4.1 Basic Soil Properties and Classification

The moisture content, natural density, Atterberg Limits, and grain size distribution were determined for each of the six Shelby tube samples obtained from the test boring. The term natural density refers to the soil density within the Shelby tube which may vary from the actual in-situ density due to disturbance of the soil during sampling and transport. The classifications presented herein are based upon ASTM D-2487: Classification of Soils For Engineering Purposes. The laboratory results and description of the samples tested are summarized in Table 4.1.

In general, the samples obtained from Stratum C1 were found to consist of fine to medium sandy clayey silt (ML) and silty sand (SM) with varying amounts of shell fragments. At a depth of approximately 55 ft. below the ground surface, the soils contained high concentrations of

TABLE 4.1
SUMMARY OF SOIL PROPERTIES
BORING NO. B-1

Sample Depth Elev.	Sample Type	Description of Soil Specimen	Stratum Design-ation	Natural Moisture (%)	Natural Density (pcf)		Atterberg Limit			% Passing No. 200 Sieve
					Dry	Wet	LL	PL	PI	
175'-20' / 74.7-72.2	Tube	Fine to medium sandy clayey silt to silty sand w/shell frag-ments - gray (ML-SM)	C1	26	98	124	22	27	5	50
27.5'-30' / 64.7-62.2	Tube	Fine to medium silty sand w/shell frag-ments - gray (SM)	C1	31	92	121	-	30	-	47
37.5'-40' / 54.7-52.2	Tube	Fine to medium sandy clayey silt w/shell fragments - gray (ML)	C1	32	89	118	30	35	5	66
44.5'-47' / 47.7-45.2	Tube	Fine to medium silty sand w/shell frag-ments - gray (SM)	C1	28	97	124	-	30	-	42
54.5'-57' / 37.7-35.2	Tube	Fine to medium clayey silty sand, w/ a high concentration of shell frag.-greenish gray (SM)	C1	24	104	129	-	-	-	32
64.5'-67' / 27.7-25.2	Tube	Fine to medium sand, some silt - dark greenish gray (SM)	C2	27	95	122	NP	NP	NP	20
16'-59' / 76.2-33.2	Bulk	Fine to medium clayey silty sand w/shell frag. - gray (SM)	C1	-	-	-	25	17	8	47
60'-74' / 32.2-18.2	Bulk	Fine to medium sand, some silt - dark greenish gray (SM)	C2	-	-	-	NP	NP	NP	23

NP = non-plastic

cemented shell fragments greater than 50 percent by weight. For Stratum C1, the percent finer by weight than the No. 200 sieve ranged from 32.69 to 66.36 percent. The Liquid Limit of the samples tested ranged from 21.95 to 30.0 and Plasticity Index values from 4.55 to 5.0 indicating that the soil fines are of low plasticity. The natural wet density of the soils within this stratum varied from 118.12 pcf to 128.97 pcf and dry densities ranged from 89.44 pcf to 104.39 pcf. The moisture content ranged from 23.58 to 32.08 percent.

Soil samples obtained from Stratum C2 consisted of uniformly graded fine to medium silty sand (SM). The soils were non-plastic and contained 19.89 percent finer by weight than the No. 200 sieve. Only one Shelby tube sample was obtained from within this stratum; natural wet and dry densities of 121.6 pcf and 95.4 pcf respectively were determined. Also, the moisture content was 27.4 percent.

The subsurface conditions with respect to changes in moisture content, natural density and percent fines versus depth within test boring B-1 are indicated in Figure 4.1. For soils within Stratum C1, the following results were obtained: an average moisture content of 28.3 percent; natural wet density of 123.2 pcf; and 47.3 percent finer by weight than the No. 200 sieve.

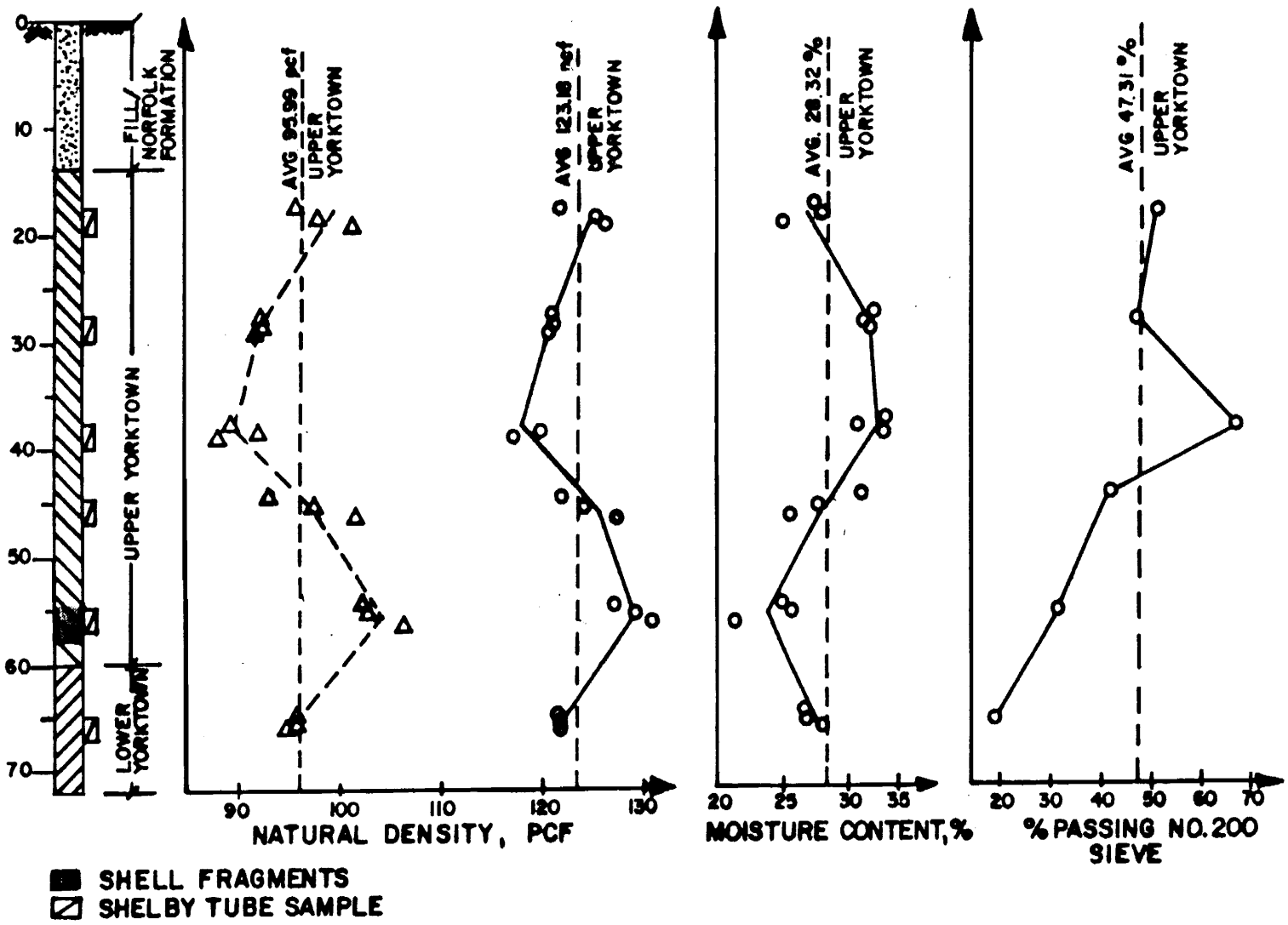

FIGURE 4.1 SUBSURFACE PROFILE OF SOIL PROPERTIES

4.2 Triaxial Testing of Soil Samples

The strength characteristics of a particular soil type is dependent upon the state of the soil before and during shearing to include drainage conditions and consolidation of the soils. Along the soil-pile interface and at the pile tip, shearing of the soils were assumed to behave under consolidated-drained (CD) conditions. The soil medium away from the pile perimeter beyond the soil-pile interface was assumed to behave under the consolidated-undrained (CU) condition. Therefore, a CU triaxial test was performed on a Shelby tube sample representing soils of the upper Yorktown formation (Stratum C1). Below the pile tip, the soil medium was considered to represent that of Stratum C2 in the case of the model pile. Hence, a representive Shelby tube sample was tested under consolidated-drained (CD) conditions.

Duncan et al. (1980) outlined procedures for determining stress-strain and volume change parameters that represent the non-linear and stress dependent stress-strain and volume change behavior of soil. These parameters are based upon hyperbolic stress-strain relationships which provide a framework that encompasses the most important characteristics of stress-strain behavior: non-linearity; stress-dependency; and inelasticity. Nine parameters are employed in the hyperbolic stress-strain relationship used

to determine soil behavior (Table 4.2).

Triaxial tests were conducted to obtain the hyperbolic parameters for the soil types which exist along the pile perimeter and tip for use in the finite element method of analysis. The hyperbolic parameters obtained from the test data were internal angle of friction (Φ); cohesion (c), modulus exponent (n), modulus number (K), failure ratio (Rf), bulk modulus number (Kb) and bulk modulus exponent (m). The test conditions that were imposed and descriptions of the soil samples from Strata C1 and C2 follow:

Stratum C1

From the five Shelby tube samples collected, only one contained enough soil after extrusion that was suitable for testing. This sample was obtained from a depth of approximately 37.5 to 40 feet below the ground surface. It consisted of fine to medium sandy clayey silt (ML). The soil properties associated with this sample are given in Table 4.1. Three triaxial compression tests were performed at confining pressures of 10, 40 and 70 psi. Each test was performed under consolidated-undrained conditions to account for the effect of excess porepressure on the stress-strain behavior of the soil. This effect was assumed to occur for soils along the pile perimeter during loading. A low strain rate of 0.002 in/min was applied to the samples tested. The data obtained from each test are

TABLE 4.2 SUMMARY OF THE HYPERBOLIC PARAMETERS
(After DUNCAN, et al., 1980)

Parameter	Name	Function
K, K_{ur}	Modulus number	Relate E_i and E_{ur} to σ_3
n	Modulus exponent	
c	Cohesion intercept	Relate $(\sigma_1-\sigma_3)_f$ to σ_3
ϕ, $\Delta\phi$	Friction angle parameters	
R_f	Failure ratio	Relates $(\sigma_1-\sigma_3)_{ult}$ to $(\sigma_1-\sigma_3)_f$
K_b	Bulk modulus number	Value of B/P_a at $\sigma_3 = P_a$
m	Bulk modulus exponent	Change in B/P_a for ten-fold increase in σ_3

shown in Appendix B.

Stratum C2

One Shelby tube sample was collected from this stratum at a depth between 64.5 to 67 ft. below the ground surface. The soil consisted of fine to medium sand with silt (SM). Three triaxial compression tests were also performed on this sample at confining pressures of 10, 40 and 70 psi. The test sample represented soils at the pile tip for which drainage was assumed to have occured during loading. Thus, each sample was tested under consolidated-drained conditions. In order to facilitate drainage, a low strain rate of 0.005 in/min was applied. The data obtained from each of the samples tested are included in Appendix C.

The confining pressures imposed were selected based upon horizontal earth pressures determined from the Menard pressuremeter tests which indicated a range between 29 psi to 99 psi.

The procedures used to determine the desired hyperbolic parameters were those established by Duncan et al. (1980). From the triaxial test data, stress versus strain curves corresponding to a particular confining pressure (σ_3) were developed as shown in Figure 4.2 in which the ultimate deviatoric stress (σ_1-σ_3) for each value of σ_3 was determined. In addition, the initial Young's Modulus (E_i) which varies with values of σ_3 was determined from the initial slope of the stress-strain curve. Using

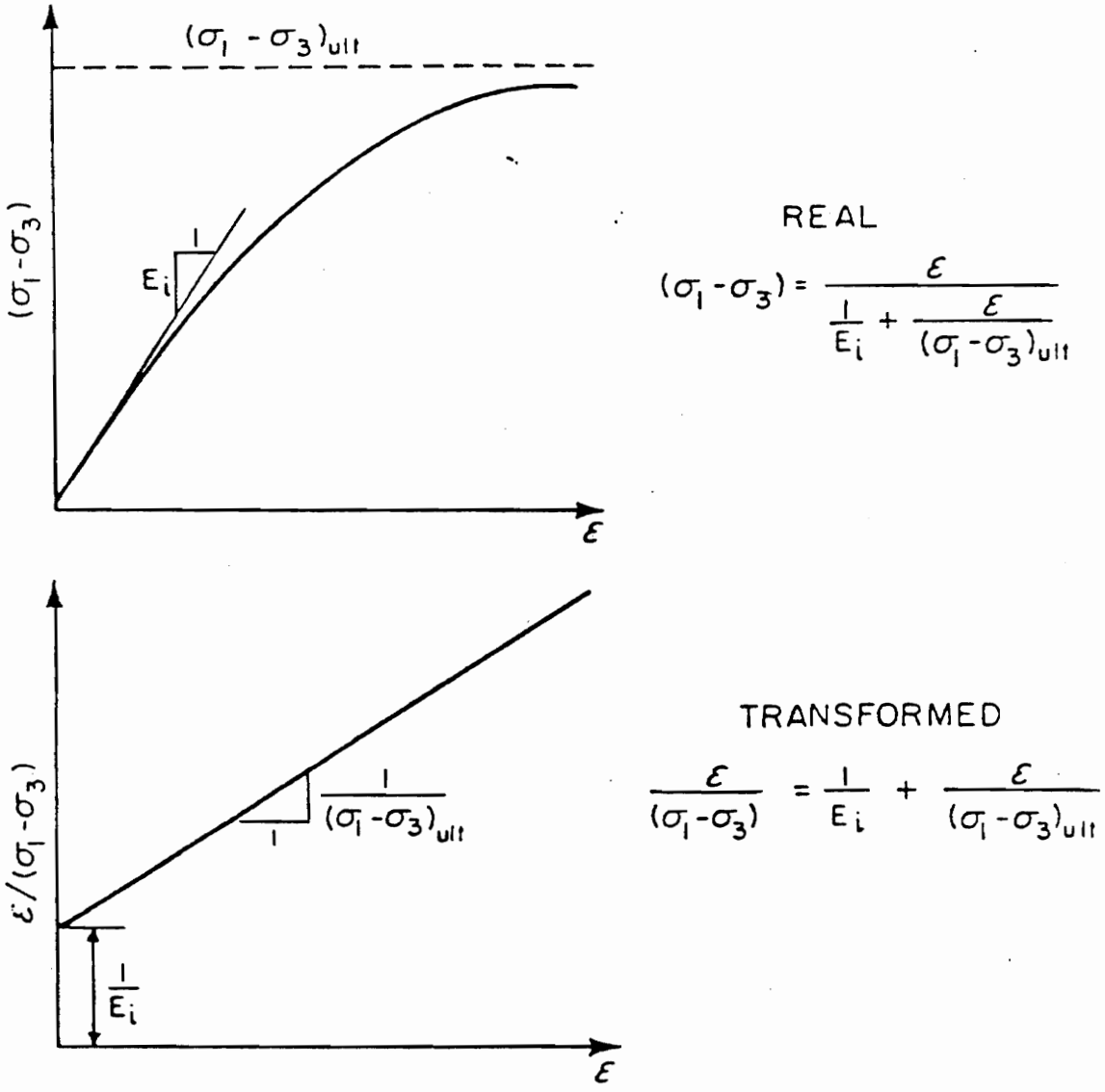

FIG. 4.2 HYPERBOLIC REPRESENTATION OF A STRESS-STRAIN CURVE
(After Duncan, et al., 1980)

Mohr-Columb theory, the shear strength parameters of internal angle of friction (ϕ,ϕ') and cohesion (c,c') are shown in Figure 4.3. The slope and Y-intercept of the failure envelope constructed tangent to each Mohr circle represents the value of ϕ and c respectively. For the undrained test condition, excess porepressure measured during testing was included as part of the total shear strength (σ_t) based on the following relation:

$$\sigma_t = \sigma' + u \qquad 4.1$$

where σ equals the effective shear strength and u the pore pressure. By subtracting out the value of u, the Mohr circle shifts to the left for positive pore pressure and to the right for negative pore pressure. The slope and Y-intercept of the failure envelope represent the effective internal angle of friction (ϕ') and cohesion (c') respectively.

In determining the best-fit hyperbola for the stress-strain curve, values of $\in/\sigma_1-\sigma_3$ calculated from the test data for strains ($\in$) where 70 and 90 percent of the strength has been mobilized and plotted to form a straight line curve as shown in Figure 4.2. The slope and Y-intercept of the line represents the inverse values of $(\sigma_1-\sigma_3)$ult and E_i, respectively. At this point, the failure ratio (Rf) can be determined by the equation:

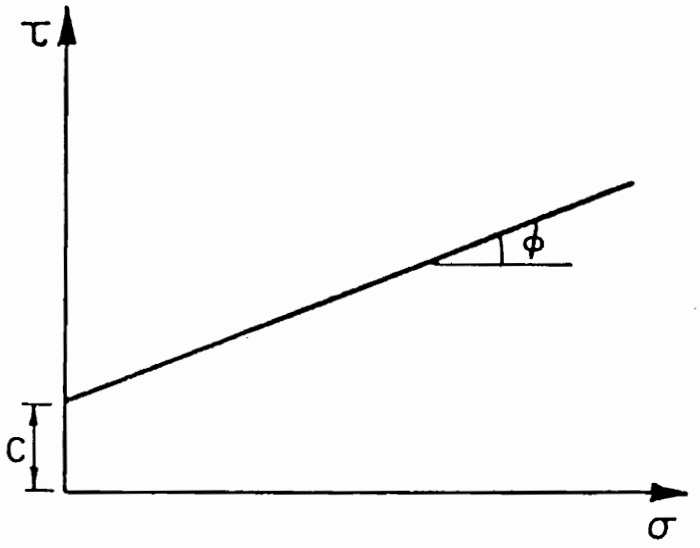

$$(\sigma_1 - \sigma_3)_f = \frac{2C \cos\phi + 2\sigma_3 \sin\phi}{1 - \sin\phi}$$

$$(\sigma_1 - \sigma_3)_f = R_f (\sigma_1 - \sigma_3)_{ult}$$

FIGURE 4.3 VARIATION OF STRENGTH WITH CONFINING PRESSURE
(After Duncan, et al., 1980)

$$R_f = \frac{(\sigma_1-\sigma_3)ult}{(\sigma_1-\sigma_3)f} \qquad 4.2$$

where $(\sigma_1-\sigma_3)f$ represents the deviatoric stress at failure which is always less than $(\sigma_1-\sigma_3)ult$. The variation of Ei with σ_3 is represented by the following equation:

$$E_i = KPa(\sigma_3/Pa)^n \qquad 4.3$$

where Pa is atmospheric pressure. For determining values of K and n, values of (Ei/Pa) versus (σ_3/Pa) were plotted on log-log scale as shown in Figure 4.4. The slope of the line represents the value of n and the Y-intercept the value of K.

The relationship between changes in Young's Modulus with stress is represented by the instantaneous slope of the stress-strain curve, referred to as the tangent modulus (E_t). Duncan et al. (1980) formulated that the appropriate value of the tangent modulus can be calculated for any stress condition (σ_3 and $\sigma_1-\sigma_3$) by the following expression:

$$E_t = \left[1 - \frac{R_f(1-\sin\phi)(\sigma_1-\sigma_3)}{2c\cos\phi + 2\sigma_3\sin\phi}\right]^2 KPa\left(\frac{\sigma 3}{Pa}\right)^n \qquad 4.4$$

In order to account for the non-linear volume change for

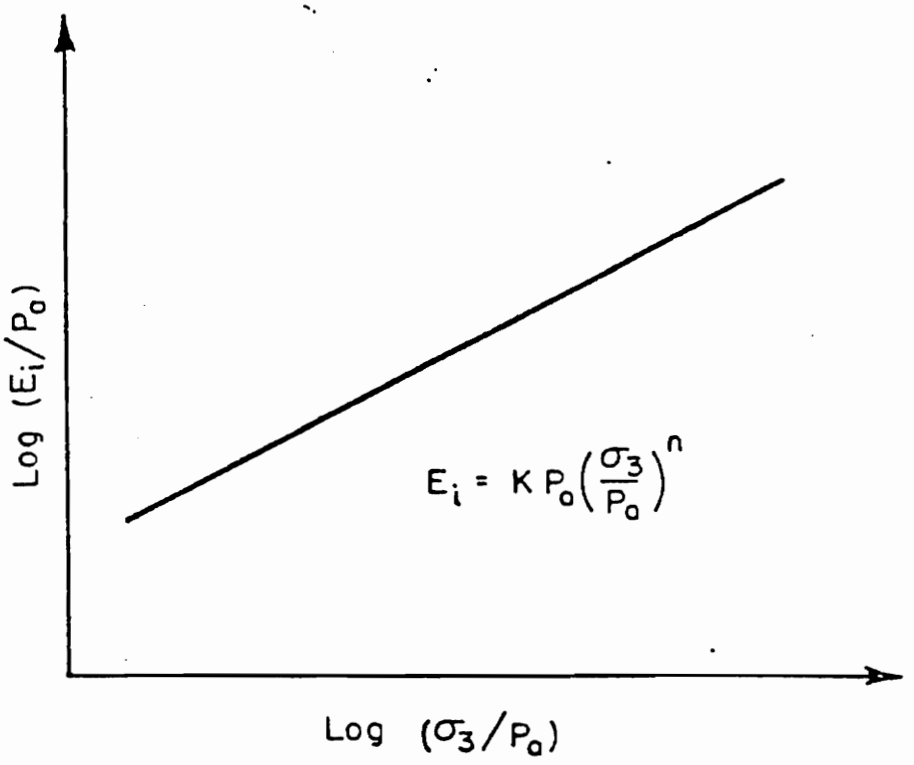

FIGURE 4.4 VARIATION OF INITIAL TANGENT MODULUS WITH CONFINING PRESSURE **(After Duncan, et al., 1980)**

most soils, as illustrated in Figure 4.5, the bulk modulus (B) is used. It is assumed that the bulk modulus is independent of the deviatoric stress ($\sigma_1-\sigma_3$) and varies with confining pressure (σ_3) to provide a reasonable approximation to the shape of these volume curves. According to the theory of elasticity, the bulk modulus (B) is defined by the equation:

$$B = \frac{\Delta\sigma_1 + \Delta\sigma_2 + \Delta\sigma_3}{3\epsilon_v} \qquad 4.5$$

where $\Delta\sigma$ represents changes in principle stress and ϵ_v the changes in volumetric strain corresponding to $\Delta\sigma$.
For the conventional triaxial test σ_3 remains constant, therefore, equation 4.5 may be expressed as:

$$B = (\sigma_1-\sigma_3)/3\epsilon_v \qquad 4.6$$

Bulk modulus values may be calculated using any value of ($\sigma_1-\sigma_3$). However, the bulk modulus will vary depending upon the value of ($\sigma_1-\sigma_3$) selected for soils which undergo volume change as a result of changes in shear and normal stress. The report by Duncan et al. (1980) outlines two criteria for selecting the value of ($\sigma_1-\sigma_3$) to calculate the bulk modulus. They are based on a number of studies of volume change behavior for a variety of soil types. The two criteria are: (1) If a horizontal tangent along the

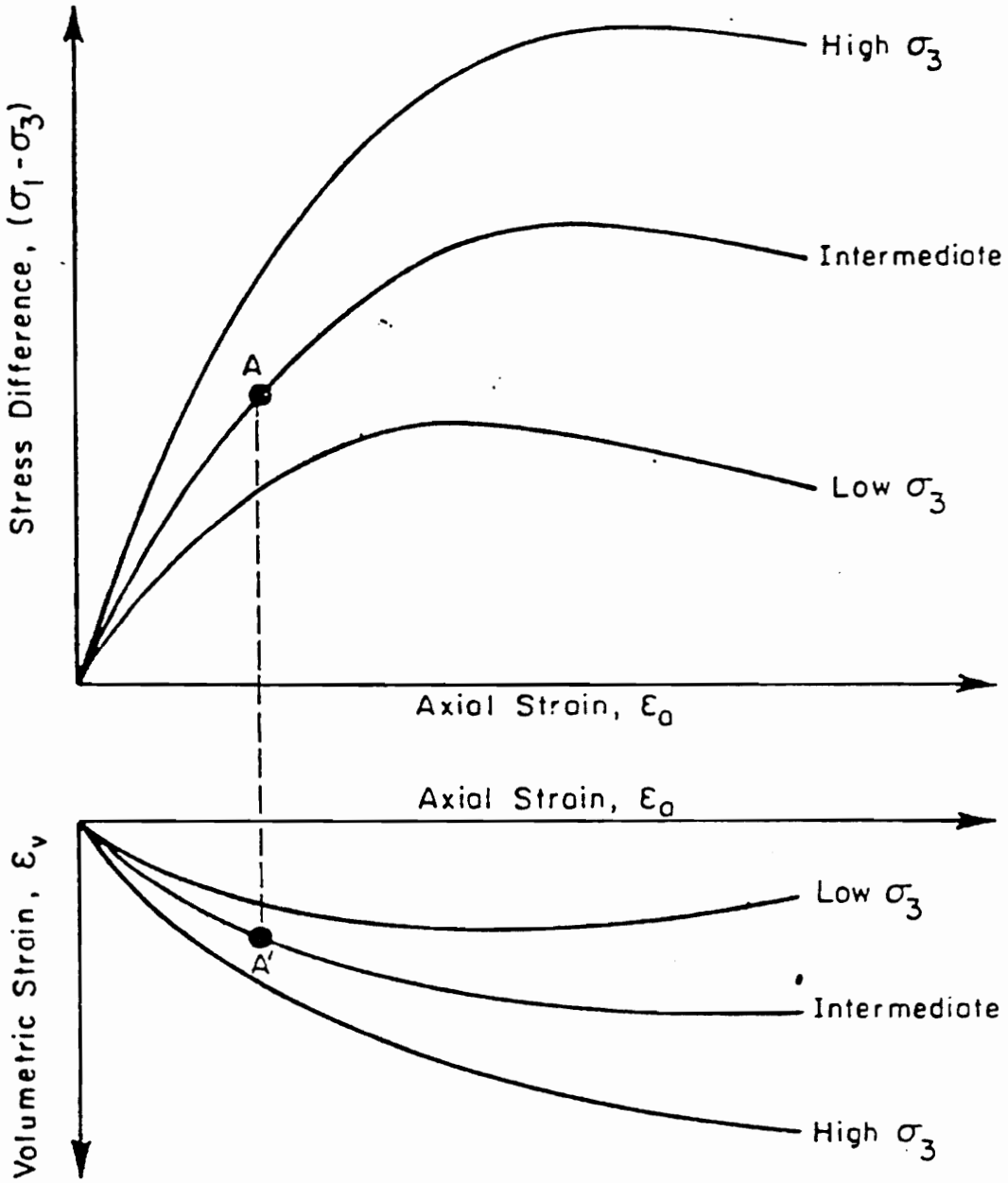

FIG. 4.5 NONLINEAR AND STRESS-DEPENDENT STRESS-STRAIN AND VOLUME CHANGE CURVES **(After Duncan, et al., 1980)**

volume change curve is not reached at the point at which 70 percent of the stress has been mobilized, then $(\sigma_1-\sigma_3)$ and corresponding ϵ_v values at the 70% stress level should be used and (2) If the horizontal tangent is reached at 70% of strength mobilization along the volume curve, then use the values of $(\sigma_1-\sigma_3)$ and corresponding ϵ_v value at the point on the volume curve where it becomes horizontal.

The bulk modulus varies with changes in confining pressure (σ_3). Hence, to determine the variation of B with σ_3 the following expression may be used.

$$B = K_b Pa(\sigma_3/Pa)^m \qquad 4.7$$

In this expression, values for atmospheric pressure (Pa), confining pressures (σ_3), bulk modulus exponent (m) and bulk modulus number (K_b) are required. This expression is simular to that for defining the variation in values of Ei resulting from changes in σ_3 values as presented in Equation 4.3. For the values of K_b and m, B/Pa versus σ_3/Pa are plotted on log-log scale as shown in Figure 4.6. The slope of the line formed represents the value of m and the Y-intercept, the value of K_b.

4.3 Summary of Results

The determination of hyperbolic parameters for

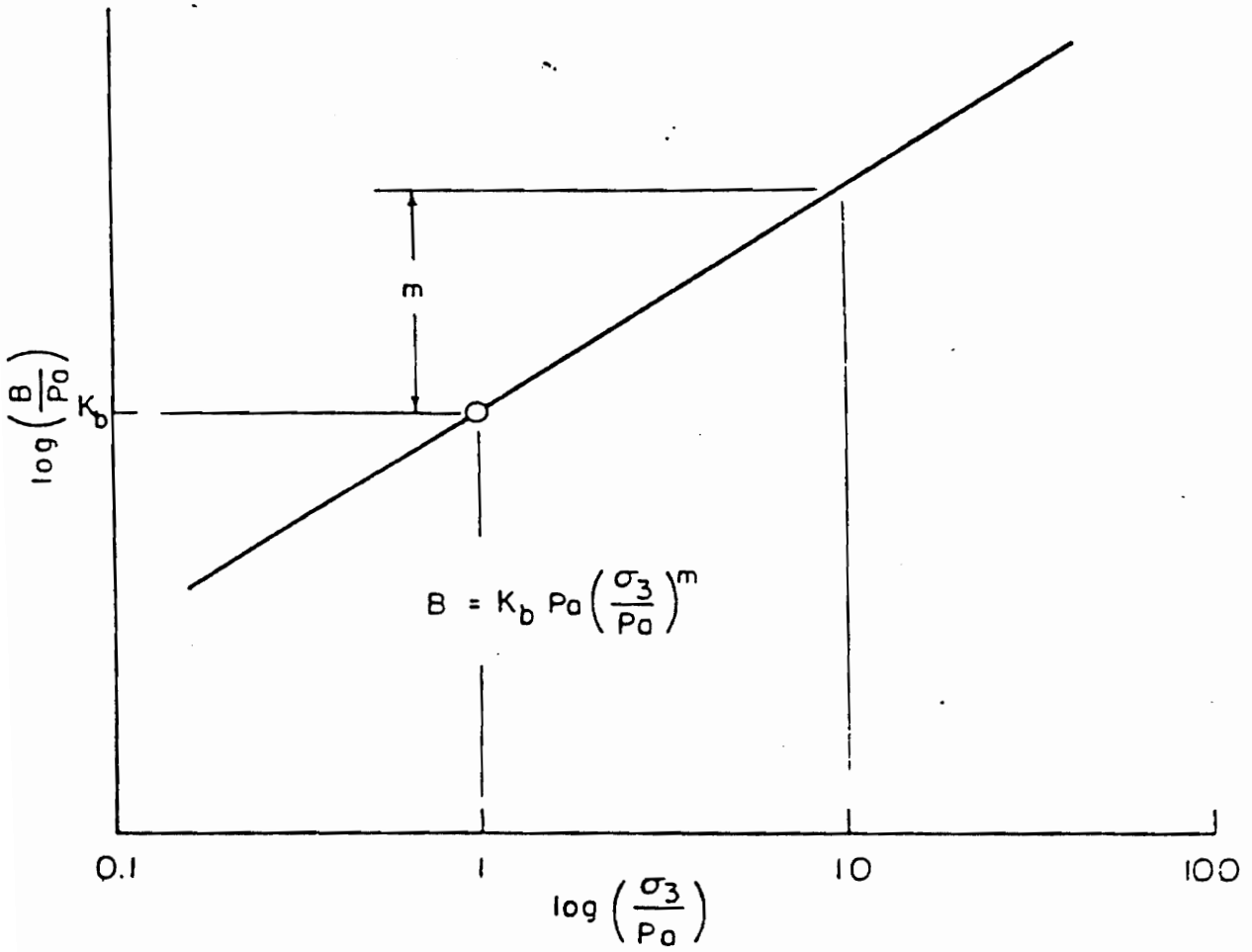

FIG. 4.6 VARIATION OF BULK MODULUS WITH CONFINING PRESSURE **(After Duncan, et al., 1980)**

both samples tested are included in Appendices B and C; the results are shown in Tables 4.3 and 4.4. Not surprisingly, as confining pressure increased the values of E_i and $(\sigma_1-\sigma_3)ult$ also increased under both test conditions. For the consolidated-drained (CD) test, with a 60 psi increase in σ_3, the value of Ei and $(\sigma_1-\sigma_3)ult$ increased about four-fold. Smaller changes in the values of E_i and $(\sigma_1-\sigma_3)ult$ due to similar changes in $_3$ were recorded for the sample tested under consolidated-undrained (CU) conditions. For this case, a 60 psi increase in σ_3 resulted in an approximate twofold increase in the values of E_i and $(\sigma_1-\sigma_3)ult$. Obviously, the soil type and conditions in which the soil specimens were tested were the main factors that caused this difference.

The strength characteristics of the soil types varied under similar values of σ_3. At low confining pressure (10 psi), the value of $(\sigma_1-\sigma_3)ult$ was similar. However, at a σ_3 value of 70 psi, the values of $(\sigma_1-\sigma_3)ult$ for soil at the pile tip were almost double that obtained for the sample which represented soils along the pile perimeter. The specimen representing soil at the pile tip exhibited a greater internal angle of friction (ϕ') and smaller value of cohesion (c') than that obtained for both the effective and total stress for the specimen representing soil along the pile perimeter. This is to be expected since soils at the tip were more granular than

TABLE 4.3 SUMMARY OF STRENGTH AND HYPERBOLIC PARAMETERS DETERMINED FOR THE SOIL SAMPLES TESTED THAT WERE OBTAINED FROM THE UPPER YORKTOWN FORMATION

DESCRIPTION: Fine to medium sandy clayey silt, gray			Classification: ML		Stratum: Cl	
Boring No. B-1	Depth: 37.5'- 40'	Test Method: CU - Triaxial				
σ_3 (psi)	$(\sigma_1-\sigma_3)$ (psi) ult.	Cohesion c (psi)	Internal Angle of Friction ϕ	Ei (psi)	R_f	K	n
10	34.7	c = 13	ϕ = 10.5°	3125	0.58	70	0.5
40	52.0	c' = 9.5	ϕ' = 19.0°	4348	0.55		
70	62.4			8333	0.61		

Rf avg. 0.58

Ei avg. 5269 psi

TABLE 4.4 SUMMARY OF STRENGTH AND HYPERBOLIC PARAMETERS DETERMINED FOR THE SOIL SAMPLES TESTED THAT WERE OBTAINED FROM THE LOWER YORKTOWN FORMATION

DESCRIPTION: Fine to medium sand, some silt, greenish gray			Classification SM					Stratum: C2		
Boring No. B-1		Depth: 64.5'- 67'		Test Method: CD - Triaxial						
σ_3 (psi)	$(\sigma_1-\sigma_3)_f$ (psi)	Cohesion c (psi)	Internal Angle of Friction ϕ	Ei (psi)	R_f	K	n	B (psi)	K_b	m
10	33.2	c' = 4.0	$\phi' = 28^0$	813	0.71	22	0.47	595	18	0.46
40	88.2			1644	0.83			1872		
70	104.8			2018	0.79			1460		

Rf avg. 0.78

Ei avg. 1492 psi

those along the pile perimeter.

The failure ratio (R_f) used to relate $(\sigma_1-\sigma_3)_{ult}$ and $(\sigma_1-\sigma_3)_f$ varied little with changes in confining pressure for both test conditions. However, the variation in values of R_f relative to variation in soil types and test conditions were significant. For the consolidated-undrained (CU) condition, a mean R_f value of 0.6 was obtained and for the consolidated-drained (CD) condition, the R_f value was 0.8.

Chapter 5

SOIL-CONCRETE INTERFACE TEST PROGRAM

5.0 Introduction

Analysis of soil-structure interaction using the finite element method requires a knowledge of the stress-deformation characteristics at the soil-pile interface. Accordingly, a soil-concrete interface test program was developed to provide a means of determining the strength-deformation characteristics along the soil-pile interface.

For the concrete piles analyzed herein, the soil medium was representative of the upper Yorktown formation (Stratum C1). The assumption was made that the soils at the interface undergo remolding during both installation and loading of the pile. The representative sample was placed in a remolded state in contact with a precast concrete block of both smooth and rough surface textures. Shearing along the soil-concrete interface was accomplished by a strain-controlled direct shear apparatus.

The objectives of the soil-concrete interface test program were to determine the strength and hyperbolic parameters of the soil. The parameters of interest were: the interface angle of friction (ϕ_i); adhesion (Ca); initial shear stiffness modulus (K_{si}); modulus number (K_j); and the modulus exponent (n).

5.1 General Theory

Previous studies have shown that the strength-deformation characteristics between soil types and solid surfaces are dependent upon several factors: the physical properties and gradation of the soil; the moisture content of the soil and the solid surface; the normal stress; density of the soil; the material type; and surface texture of the solid (11).

Utilizing the results of direct shear tests for numerical solutions require an analytical model of the shear stress versus the relative displacement curve. As with the stress-strain curve developed from triaxial tests, Clough and Duncan (1971) have shown that the stress-displacement curves from direct shear tests can be approximated by a hyperbola during primary loading. This hyperbola can be represented by an equation of the form:

$$\tau = \frac{\Delta s}{1/K_{si} + \Delta s/\tau_{ult}} \qquad 5.1$$

in which τ is the shear strength, Δs the relative displacement, K_{si} the initial shear stiffness modulus, and τ_{ult} representing the ultimate shear strength. The transformed linear hyperbolic equation of the form shown below represents a linear relationship between $\Delta s/\tau$ and Δs.

$$\frac{\Delta s}{\tau} = \frac{1}{K_{si}} + \frac{\Delta s}{\tau_{ult}} \qquad 5.2$$

Therefore, to obtain the best fit hyperbola for the stress-displacement curve, the values of $\Delta s/\tau$ versus Δs determined from the test data were plotted. The straight line which best fits the transformed plot corresponds to the best fit hyperbola of the stress-displacement curve as shown in Figure 5.1. Clough and Duncan (1971) have further shown that the transformed linear hyperbola can be achieved by a straight line which passes through the points at which 70 and 90 percent of the strength has been mobilized. Since Equation 5.2 represents that of a straight line, then the slope and Y-intercept of the transformed hyperbola represents the inverse values of τ_{ult} and K_{si} respectively.

The value of the internal angle of friction (ϕ_i) can be determined from the slope of the line which best fits the plot of τ_{ult} versus normal stress (σ_n). The shear stress value at failure (τ_f) is a function of normal pressure as expressed by the following equation:

$$\tau_f = \sigma_n \tan \phi_i \qquad 5.3$$

The value of τ_f is smaller than the value of τ_{ult} and are related by a factor, referred to as the failure ratio (R_f):

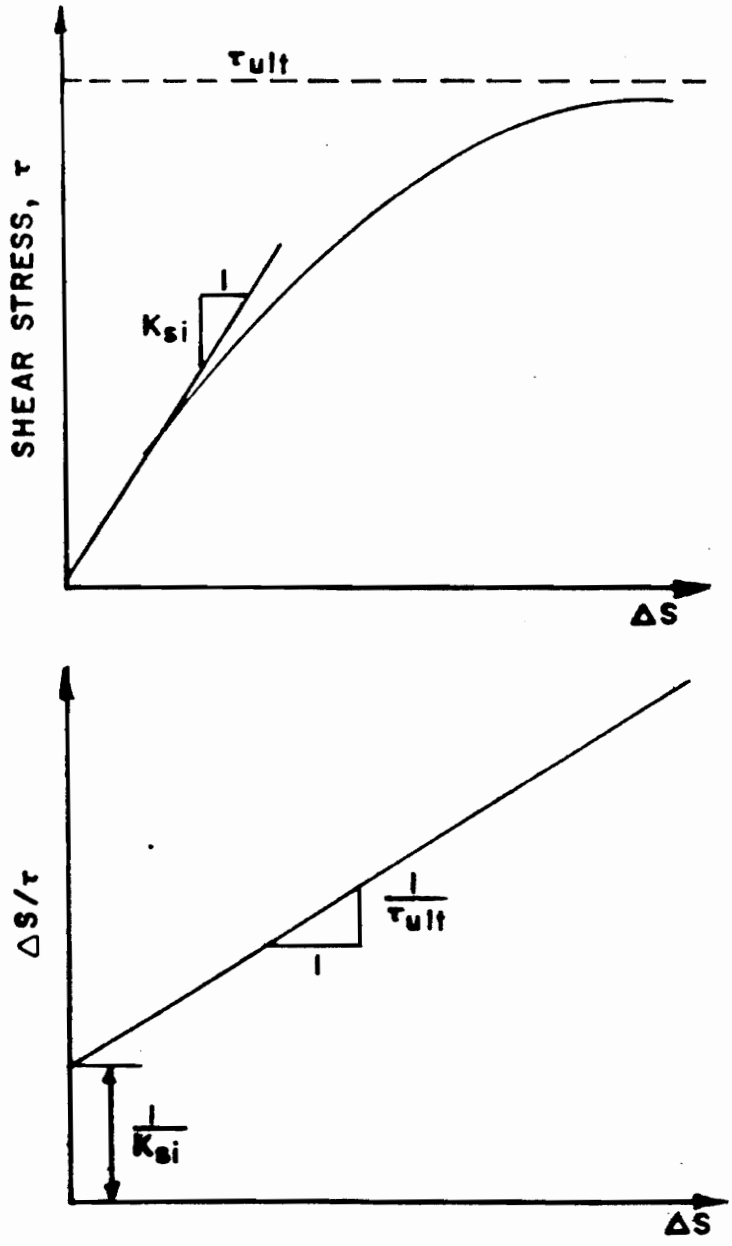

REAL

$$\tau = \frac{\Delta S}{\frac{1}{K_{si}} + \frac{\Delta S}{\tau_{ult}}}$$

TRANSFORMED

$$\frac{\Delta S}{\tau} = \frac{1}{K_{si}} + \frac{\Delta S}{\tau_{ult}}$$

FIGURE 5.1 HYPERBOLIC REPRESENTATION FOR DIRECT SHEAR TESTS

$$R_f = \tau_f/\tau_{ult} \qquad 5.4$$

This value is similar to the R_f value in Equation 4.2 which relates ultimate and failure deviatoric stresses derived from conventional triaxial testing.

The variation of K_{si} with σ_n at the interface can be expressed by the following equation as set forth by Clough (1969):

$$K_{si} = K_j\left[\gamma_w(\sigma_n/Pa)^n\right] \qquad 5.5$$

In this equation: γ_w represents the unit weight of water; Pa the atmospheric pressure; K_j the modulus number; and n the modulus exponent. The values of K_j and n can be found by first determining the value of K_{si} corresponding to the value of σ_n and plotting the value of K_{si}/γ_w versus σ_n/Pa on a log-log scale as shown in Figure 5.2. The slope and Y-intercept of the best-fit straight line through the data points represents the value of n and K_j respectively.

The relationship of the tangent shear stiffness modulus (K_{st}) to the normal stress (σ_n) is represented by the equation:

$$K_{st} = K_j\ \gamma_w\left(\frac{\sigma_n}{Pa}\right)^n\left(1-\left(\frac{R_f\ \tau}{\sigma_n\ \tan\ \phi_i}\right)^2\right. \qquad 5.6$$

This equation can be used to evaluate the non-linear and

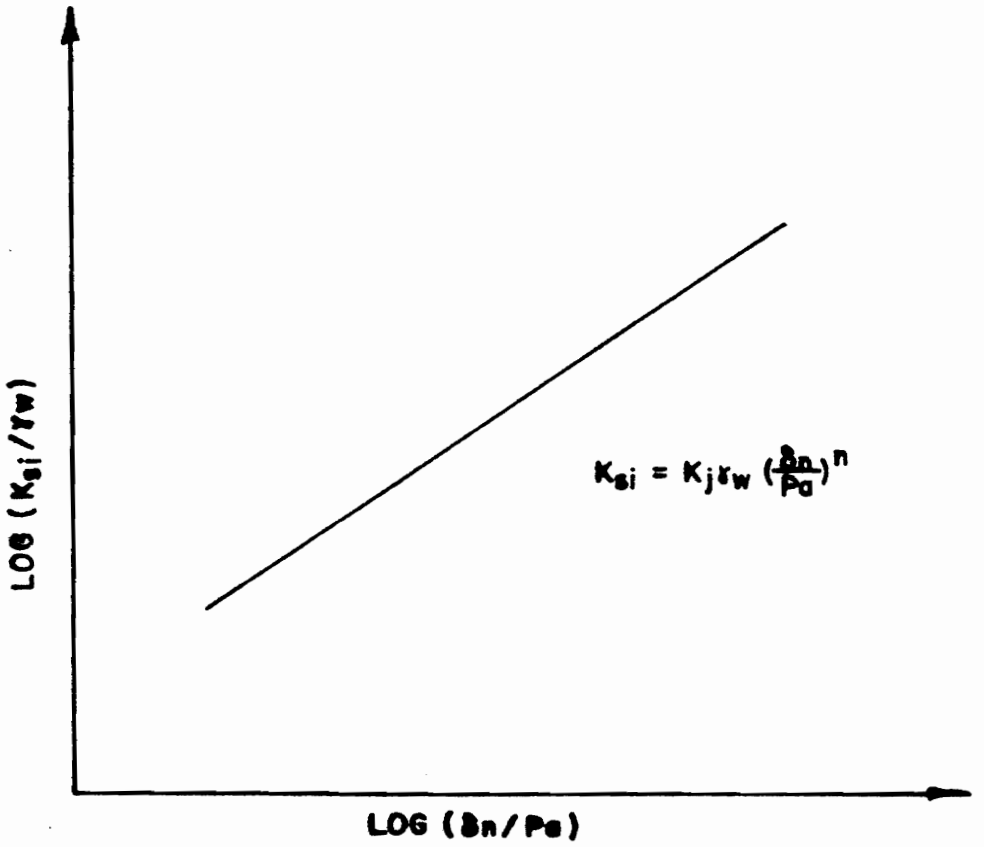

FIGURE 5.2 VARIATION IN INITIAL SHEAR STIFFNESS MODULUS WITH NORMAL STRESS

stress dependent behavior at the interface of the soils in contact with the solid body.

5.2 Test Apparatus

There are several shear devices which can be employed for interface testing: the direct shear apparatus in which the soil undergoes direct single shear along the zone between the two halfs of a square or circular box; the double ring shear apparatus which consists of a set of rings in which the soil can be tested in either direct single shear or double shear; and finally, the angular shear device comprised of rings that shear the soil in an angular manner. These three types of devices are illustrated in Figure 5.3. The direct shear apparatus was chosen for use in this test program because it facilitated sample preparation plus testing and was readily available.

The shear force can be applied to any of the above devices by two methods. The first involves the application of a known force and measuring the resultant deformation; this is referred to as a stress control test. The second method involves shearing the sample at a constant rate and measuring the resultant force; this is known as a strain control test. The major advantage of the strain versus stress control test is that ultimate shear and peak resistance can be determined more accurately.

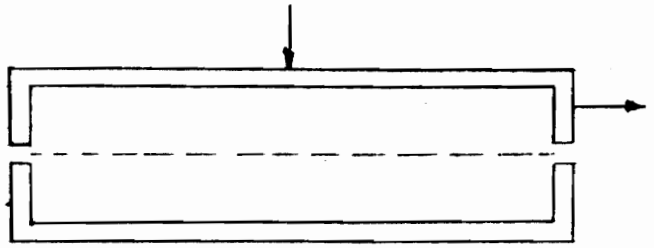

DIRECT SHEAR APPARATUS

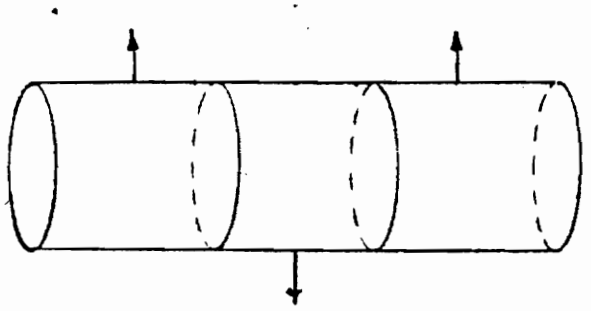

DOUBLE RING SHEAR APPARATUS

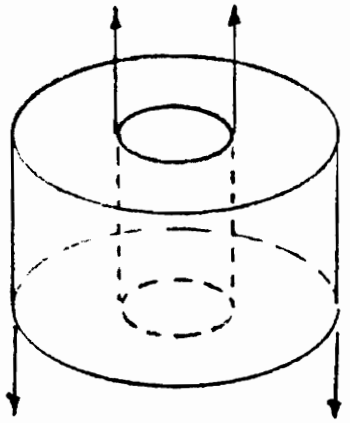

ANNULAR SHEAR APPARATUS

FIGURE 5.3 TYPICAL TYPES OF SHEAR APPARATUS

Since this data was necessary in modeling the stress-deformation behavior of the soil-concrete interface, the strain control method of testing was employed.

Direct shear interface testing was performed with a Wykeham-Farrance constant rate strain shear machine, (Model WF25000), with some minor modifications as illustrated in Figure 5.4. The machine was able to accommondate a 4.0 inch square shear box 2.0 inches in depth and the application of normal stresses up to 5.0 tsf by means of a loaded hanger arrangement. The specimen was sheared at a uniform rate of strain through a motor and gear box arrangement. Twenty-five strain rates, ranging from 0.0000192 to 0.048 inch per minute, were obtainable. The shear force was determined by a proving ring in contact with the upper half of the box.

The motor and gear box arrangement allowed the shear stress to be applied at a constant rate of strain in both the forward and reverse directions. The cyclic load imposed on the soil-structure interface required modification of the shear box, load piston and proving ring. The upper portion of the box was attached to the load piston and to the proving ring which allowed the soil to be sheared in a forward and reverse direction at a constant rate of strain.

The shear force in both directions was obtained by using two Wykeham Farrance proving rings of high tensile

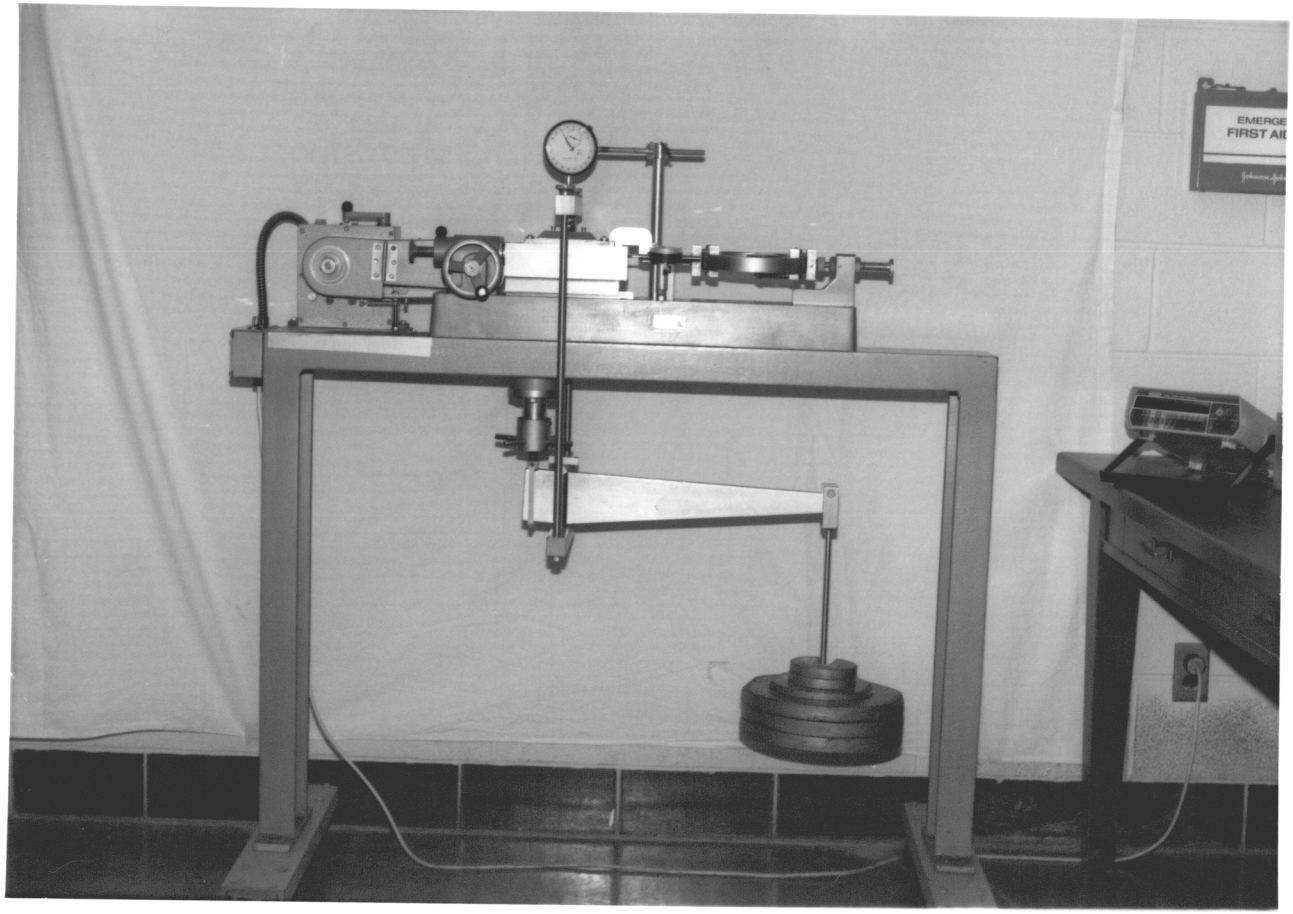

FIGURE 5.4 MODIFIED WYKEHAM-FARRANLE CONSTANT RATE STRAIN SHEAR MACHINE

steel with load capacities of 500 and 1000 lbs. These rings were calibrated with an electronic load cell for compression and tension.

Dial indicators were used to measure the vertical deformation and the horizontal displacement of the specimen within the shear box during shearing. Their respective accuracies were 0.0001 inch/div. and 0.001 inch/div. In addition to these two dial indicators, a third was attached to the proving ring to measure its displacement under loading in tension and compression; the accuracy attained was 0.0001 inch/div.

5.3 Precast Interface Concrete Blocks

The square, prestressed, precast concrete piles being analyzed were molded in a steel trough resulting in a smooth surface texture along three faces of the pile and one rough face. For the interface tests, two precast blocks were molded to simulate the smooth and rough surface textures of the pile. Both concrete blocks were of the same mix design and identical in size and shape. Each block was designed to replace the lower half of the shear box of the direct shear apparatus and remain stationary during interface testing.

The concrete for the precast interface blocks was designed for a 14 day compressive strength of 4000 psi.

The mix design consisted of Portland Cement, Type IV, with a water cement ratio of 0.57 and a slump of 4.0 inches. The fine and coarse aggregate employed in the design mix consisted of washed sand and crushed limestone respectively. The 1.0 inch thickness of each precast block limited the use of aggregate to a size finer than $^{3}/_{4}$ inch.

The concrete was placed within wooden molds with inside dimensions of 4.0 inches square and 1.0 inch in depth. Two $^{1}/_{2}$ inch diameter threaded bolts were embedded within the concrete block. The threaded ends of the bolt extended 1.0 inch from the side of the blocks to provide a means of securing the concrete blocks within the reservoir of the direct shear device. This precluded slippage during interface testing. Embedded at the surface of the concrete block were two metal plates and two threaded shafts extending the entire thickness of the block. The location of the plates and shafts corresponded to the threaded holes located within the upper half of the shear box. The hollow threaded shafts provided a means of securing the upper half of the shear box to the concrete block. The slide plate provided a smooth surface for ease of separating the upper shear box from the concrete block by use of adjustment screws.

The desired smooth surface texture of the concrete was achieved by first troweling to a smooth finish and placing a glass plate on the surface to further reduce

any irregularities. The rough surface texture was obtained by striking off the concrete with a piece of wood across the concrete surface. After allowing the concrete to set for 24 hours within a curing room, the concrete was removed from the mold, submerged in water and placed back into the curing room for 14 days.

The strength of the concrete was tested with two concrete cylinders, 6.0 inches in diameter and 12 inches in height, that were molded in accordance with ASTM C-31. The cylinders were placed in a curing room for 14 days at which time they were tested in accordance with ASTM C-39; the resultant compressive strength was 3750 psi.

5.4 Soil Selection and Preparation

The samples selected for interface testing consisted of a mixture of soils from the upper Yorktown formation. The soil type, moisture content, unit weight, grain size distribution and Atterberg Limits were determined since they have an effect on the stress-deformation behavior at the soil-concrete interface (11).

The sample classified as fine to medium silty sand with shell fragments (SM) in accordance with ASTM D-2487. Gradation analysis indicated the soil contained 47 percent material finer by weight than the No. 200 sieve. The fines exhibited a low plasticity based upon a Liquid

Limit of 25 and Plasticity Index of 7.6. By comparison, laboratory testing of soils from Stratum C1 disclosed a mean value of 47.3 percent material finer by weight than the No. 200 sieve.

The moisture content and soil density were based upon mean values derived from laboratory testing of samples obtained from various depths within Stratum C1. The mean values of the dry and wet unit weight of soils from Stratum C1 were 96 pcf and 123.2 pcf respectively; the average moisture content was 28.3 percent. For the latter, air dried soil was mixed with distilled water, placed in air-tight bags and allowed to cure for 24 hours within the moisture room to obtain the desired moisture content.

The soil sample was compacted within the upper shear box attached to the precast concrete blocks. Prior thereto, the moisture content of each test specimen was determined. Based on the moisture content of the sample and the volume of the upper shear box, a predetermined weight of soil sample was used. The soil was uniformily compacted to the desired wet and dry soil density of approximately 96 and 123 pcf respectively.

5.5 Interface Testing Procedures

Basically, direct shear interface testing involves three phases: preparation of the soil sample;

load application plus soil consolidation; and shearing of the specimen. The procedures that were followed for each of these phases are enumerated below:

Phase 1: Soil Preparation:

a. The upper half of the shear box was attached to the precast block using clamp screws.

b. The soil was compacted to the desired density within the upper half of the box; care was taken to assure that the soil was compacted uniformly and that the box was completely filled.

c. Filter paper was placed over the soil and trimmed to the inside dimensions of the box; a square porus stone and loading cap was placed on top of the paper.

Phase 2: Loading and Consolidation of Soil:

a. The concrete-shear box assembly was positioned within the reservoir attached to the direct shear apparatus; the concrete block was secured within the reservoir by adjusting the hex nuts on the threaded bolts extending from the side of the block. This prevented any movement of the block during testing. In placing the assembly within the reservoir, the key socket on the load arm attached to the upper half of the shear box had to slide over the key attached to the load ring; the assembly was then secured with the hex nut.

b. The load hanger, ball and yoke were positioned on top of the loading cap and the desired load applied to the hanger. Dial guages were attached to measure vertical and horizontal displacements as illustrated in Figure 5.5. The clamp screws which secured the shear box to the concrete block were removed and the spacing screws separating the upper shear box from the concrete block were adjusted. The separation distance corresponded to the largest grain size of the soil specimen and was measured with a feeler guage.

c. The four screws securing the load cap to the upper shear box were loosened and readings of vertical displacement were taken. The spacing screws were then removed and the reservoir was filled with distilled water.

d. Time readings of vertical displacement were continued; once secondary consolidation occurred, the sample was considered ready for shearing.

Phase 3: Shearing of Soil Specimen:

a. During shearing of the specimen, readings were taken of vertical movement with corresponding load ring readings at intervals of 0.005 inch of horizontal displacement until failure occured.

b. Once failure occured, the direction of shear was reversed and readings on all three guages were taken as in 3a above until the shear box returned to its original

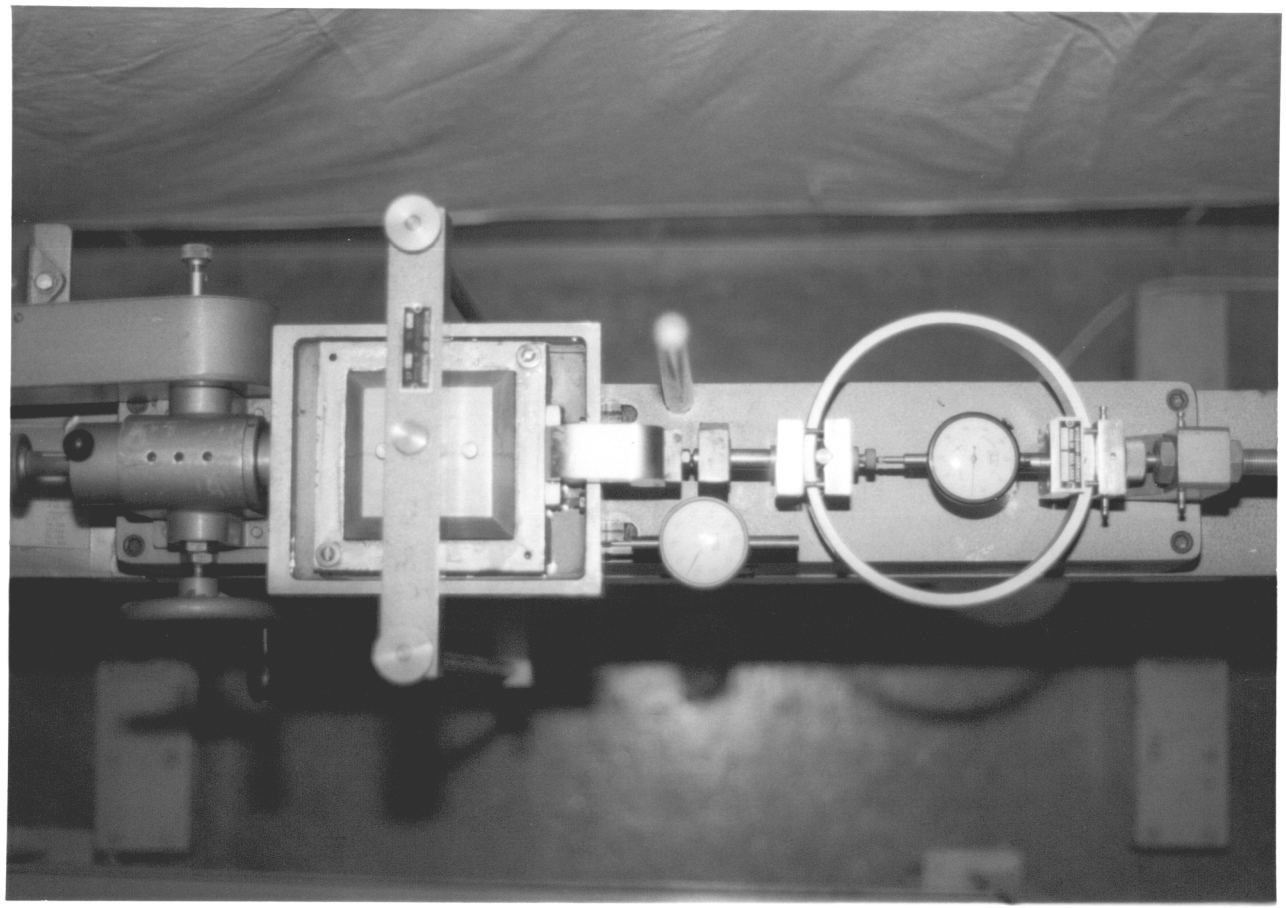

FIGURE 5.5 SHEAR BOX AND RESERVOIR ASSEMBLY FOR THE DIRECT SHEAR APPARATUS

position.

c. The sample was allowed to stand for 12 hours then the procedures in 3a and 3b above were repeated.

5.6 Results and Analysis of Interface Testing

The data obtained from the four interface tests permitted the determination of key stress-deformation properties plus the strength and hyperbolic parameters along the soil-pile interface. Two strength parameters were determined; the interface angle of friction (ϕ_i), and adhesion (Ca). The hyperbolic parameters that were determined consisted of the following: the shear stiffness modulus (K_{si}); failure ratio (R_f); modulus exponent (n); and modulus number (K). The stress versus horizontal deformation plus vertical deformation versus horizontal deformation curves for the four interface tests are included in Appendix D. The maximum shear and residual stresses plus the horizontal and vertical deformation for each load cycle for a given normal stress and surface texture are summarized in Table 5.1.

The maximum shear stress at failure (τ_f) increased approximately 300 percent with an increase in normal stress (σ_n) from 1.0 to 4.5 tsf. The values of τ_f upon unloading and reloading were within 3.0 percent of those obtained during the initial loading cycle at normal

TABLE 5.1 RELATIONSHIP OF NORMAL STRESS VERSUS HORIZONTAL AND VERTICAL DEFORMATION

Test Cycle	Stress-Deformation Parameters	Smooth Surface			Rough Surface
		1	2	3	4
Load	Maximum shear stress (τ_f), psi	13.15	24.04	40.22	24.02
	Horizontal displacement (ΔH_f), in	0.185	0.30	0.475	0.275
	Vertical displacement (Δv_f), in	0.00510	0.0196	0.0314	0.0226
	Residual shear stress (τr)	13.06	23.95		
	Horizontal displacement (ΔHr)	0.210	0.320	N/A	N/A
	Vertical displacement (Δvr)	0.00545	0.0203		
Unload	Shear stress (τu)	0	0	0	0
	Horizontal displacement (ΔHu)	-0.118	-0.06	-0.87	-0.06
	Vertical displacement (Δvu)	0.0082	0.0063	-	0.0025
Reload	Maximum shear stress (τ_f')	4.291	24.59	38.91	23.67
	Horizontal displacement ($\Delta H_f'$)	-0.325	-0.320	-0.425	0.30
	Vertical displacement ($\Delta v_f'$)	0.01035	0.0268	0.0308	0.0422
	Residual shear stress ($\tau r'$)	4.278			
	Horizontal displacement ($\Delta Hr'$)	-0.350	N/A	N/A	N/A
	Vertical displacement ($\Delta vr'$)	0.01035			
Unload After 12 Hrs	Shear stress ($\tau u'$)	0	0	0	0
	Horizontal displacement ($\Delta Hu'$)	0.015	0.064	0.010	0.076
	Vertical displacement ($\Delta vu'$)	0.0006	0.00445	0.0044	0.0039
Reload After 12 Hrs	Maximum shear stress (τ_f'')	13.03	23.90	40.32	25.30
	Horizontal displacement ($\Delta H_f''$)	0.235	0.345	0.400	0.270
	Vertical displacement ($\Delta v_f''$)	0.0067	0.0084	0.0104	0.00698
	Residual shear stress ($\tau r''$)	12.80	23.84		25.0
	Horizontal displacement ($\Delta Hr''$)	0.40	0.350	N/A	0.325
	Vertical displacement ($\Delta vr''$)	0.0067	0.0084		0.0068

stresses of 2.7 and 4.5 tsf. For the sample sheared at a normal stress of 1.0 tsf, the value of τ_f upon reloading was 67 percent of that obtained during the initial load cycle. At the end of the reload cycle, shearing of specimens was suspended for a period of 12 hours. After the 12 hour hold period, the test specimens were subjected to cyclic loads. The values of τ_f obtained during this reloading cycle were within 0.9 percent of the value of τ_f recorded for the initial load cycle.

The interface stress-deformation characteristics resulting from changes in the concrete surface texture were only available for interface tests conducted under a normal stress of 2.7 tsf. During the initial loading cycle, values of maximum shear strength of 24.04 psi and 24.02 psi were recorded for the smooth and rough surfaces respectively. Upon unloading and reloading the value of τ_f for the rough surface was 3.7 percent less than that obtained for the smooth textured block. The value of τ_f upon unloading and reloading the test specimens at the end of the 12 hour hold period was 5.5 percent greater.

Strength parameters were determined from the stress-deformation data obtained from the three smooth surface interface tests during initial loading. The values of maximum shear stress at failure (τ_f) versus normal stress (σ_n) for each test are plotted in Figure 5.6. From the slope and Y-intercept of the line which best fits the

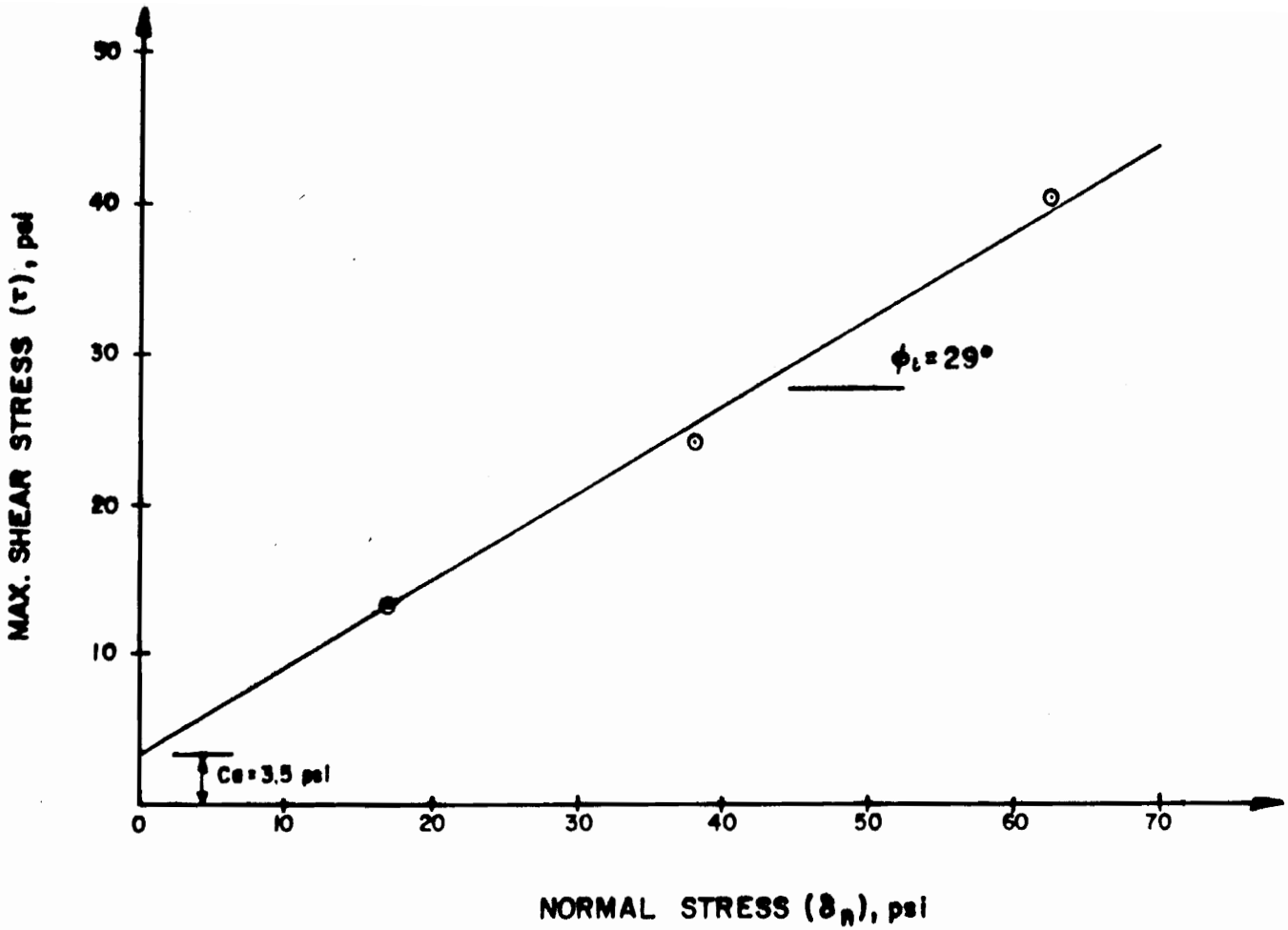

FIGURE 5.6 VARIATION IN SHEAR STRESS WITH CHANGES IN NORMAL LOAD FOR SMOOTH SURFACE SOIL- CONCRETE INTERFACE TESTS

data, an internal angle of friction (ϕ_i) of 29 degrees and adhesion (Ca) of 3.5 psi respectively were obtained.

The hyperbolic parameters of shear stiffness (K_{si}), failure ratio (R_f), modulus number (K_j), and modulus exponent (n) along the soil-pile interface were also determined based upon the stress-deformation data obtained from the three smooth surface interface tests during initial loading; the resulting values are summarized in Table 5.2. The stress-displacement curves are represented by the transformed linear hyperbola achieved by a straight line which passes through the points at which 70 and 90 percent of the strength has been mobilized. From this transformation, the ultimate shear stress (τ ult) values of 25.21, 36.36 and 52.14 psi were determined for normal loads of 13.69, 37.92 and 62.24 psi respectively. The failure ratio (R_f) value determined for each normal load resulted in an average R_f value of 0.65. The hyperbolic parameters based on the soil-concrete interface data have been incorporated in Appendix D.

TABLE 5.2 SUMMARY OF HYPERBOLIC PARAMETERS DETERMINED FROM SOIL-CONCRETE INTERFACE TESTING

DESCRIPTION: Fine to medium silty sand with shell fragments, gray				Classification: SM		Stratum: Cl	
Boring No. B-1		Depth: 14.5'- 60'		Test Method: Direct Shear Interface Testing			
σ_n (psi)	τ_f (psi)	Adhesion Ca (psi)	Internal Angle of Friction ϕ_i	Ksi (psi)	R_f	K_j	n
13.7	13.2	3.5	29°	215	0.52	270	0.34
37.9	24.0			288	0.66		
62.2	40.2			360	0.77		

Rf avg. 0.65

Ksi avg. 288 psi

Chapter 6

FINITE ELEMENT METHOD OF ANALYSIS

6.0 General

Finite element analysis of Geotechnical engineering problems has obtained greater acceptance with the growth in computer technology and the reduction of computer costs. Among its uses in this field are the analyses of deep foundation systems. Conventional methods for this purpose include: dynamic and static formulas; empirical static formulas based upon "N" values; and wave equations. These are designed to compute deformation and bearing capacity of piles, however, they generally cannot account for many of the variables that affect pile capacity and behavior. As noted earlier, in this category are: in-situ stresses; soil disturbance and induced stresses caused by pile driving; variations in soil strength and soil-pile interface properties; consolidation and negative skin friction plus cyclic load. In this regard, the finite element method has shown promise in handling many of these factors.

In this study, the application of the finite element method was used to ascertain the pile capacity and the behavior of a single concrete pile modeled after the piles and subsurface conditions at the Land Level

Shipbuilding Facility in Newport News, Virginia. The data derived therefrom permitted a comparative analysis to be made with the results from full scale pile tests conducted at that location. Essential to this undertaking was the determination of the soil strength-deformation characteristics and hyperbolic parameters of the soil media in which piles at this site are embedded. In addition, the strength-deformation characteristic and hyperbolic parameters along the soil-pile interface are required.

The program used for the analysis was the "soil-struct" axi-symmetric finite element program by Clough (1982) (4). The parameters that were obtained from this program included: the ultimate bearing capacity; the load-deformation behavior; and load-transfer characteristics of the pile.

6.1 Finite Element Procedures

Described below in outline fashion are the basic steps involved in the finite element method of analysis. These steps were also followed in the analysis performed for this study. Details regarding applications and procedures for the solution of various engineering problems are well documented in various publications (7,21).

The finite element method of analysis generally consists of five basic steps.

Step 1 - Discretization:

This initial step, as implied by the term, segments the region to be analyzed. In addition to segmenting the region, the boundary of the region is also delineated. In this study, the boundary was defined as the limits within the soil medium which are not affected by pile loading. The concrete pile and soil medium within the specified boundary were incorporated into a finite element mesh. Two types of "elements" were used: the two dimensional quadrilateral and the interface.

The two dimensional guadrilateral element (QM5) was developed by Doherty, Wilson and Taylor (1969). The shape of this element is shown in Figure 6.1a. It has four corner nodes plus an internal condensed node and was used to discretize the pile and the soil medium. The interface element allows for simulating movement at the junction between the pile and surrounding soil medium; it was defined by four nodes. Each of two pairs of nodes were assigned the same coordinates; thus, the interface element had no thickness as illustrated in Figure 6.1b.

Each element of the mesh is assigned various physical properties and its stiffness equation formulated. The individual elements are then aggregated to obtain the equations for the total structure being analyzed.

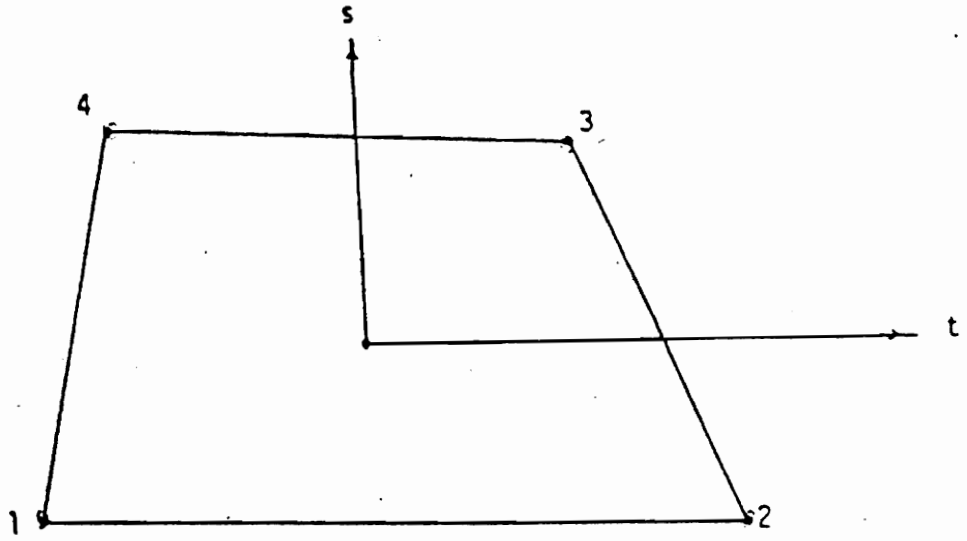

(a)

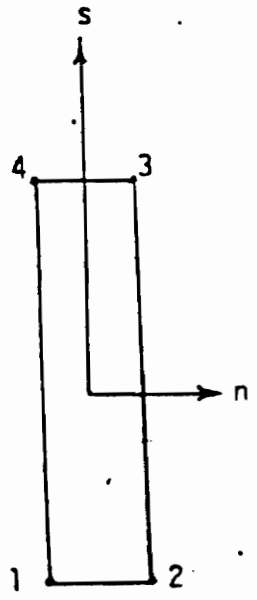

(b)

FIGURE 6.1 (a) 2-D QUADRILATERAL ELEMENT
(b) INTERFACE ELEMENT

Step 2 - Selection of Approximation Functions:

In a two dimensional analysis, the displacement within each element can be expressed as follows:

$$\begin{Bmatrix} u \\ v \end{Bmatrix} = [N]\{q\} \qquad 6.1$$

where: u = displacement in the x direction

v = displacement in the y direction

{q} = nodal displacement vector

[N] = matrix of approximation function

Both the displacement and geometry of the element are expressed by using the same matrix of approximation function, [N], which is dependent upon the type of element used in the analysis. Descriptions of various matrix of approximation functions corresponding to different types of elements are discussed by Doherty, Wilson and Taylor (1969).

Step 3 - Derivation of the Element Equations:

Using variational theory or the weighted residual method, the element stiffness equation is derived as follows:

$$[k]\{q\} = \{Q\} \qquad 6.2$$

In this relationship, [k] is the element stiffness matrix

which is determined from the following equation:

$$[k] = \iiint_V [B]^t[c][B]dv \qquad 6.3$$

where: $\{q\}$ = nodal displacement vector

$\{Q\}$ = load vector

$[c]$ = constitutive matrix

$[B]$ = transformation matrix

v = volume of the element

The constitutive matrix [c] is obtained from the stress-strain behavior of the soil. For soils along the pile perimeter and pile tip, hyperbolic stress-strain relations are used in which the tangent Young's Modulus (E_t) is changed for each load step of the calculation using the following formula:

$$E_t = \left[1 - \frac{R_f(1-\sin\phi)(\sigma_1-\sigma_3)}{2c\cos\phi + 2\sigma_3\sin\phi}\right]^2 \text{KPa} \left(\frac{\sigma_3}{Pa}\right)^n \qquad 6.4$$

Determination of non-linear stress dependent behavior at the soil-pile interface is based on the tangent shear stiffness modulus (K_{st}); it is determined using Equation 6.5 which was also discussed in Chapter 5.

$$K_{st} = Kj\gamma_w\left(\frac{\sigma_n}{Pa}\right)^n \left[1 - \frac{R_f\ \tau}{\sigma_n \tan\phi_i}\right] \qquad 6.5$$

Step 4 - Assembling Element Properties To Form Global Equations:

In the previous step, Equation 6.3 was obtained for each element in the structure. In this step, these equations are combined to form a stiffness relationship for the entire system by adding the matrix equation for each element in the following manner:

$$[K]\{r\} = \{R\} \qquad 6.6$$

where: $[K]$ = global stiffness matrix

$\{r\}$ = global nodal displacement vector

$\{R\}$ = global nodal force vector

Before the set of simultaneous equations can be solved, the geometric boundary conditions are introduced into the system.

Step 5 - Solve For The Primary And Secondary Unknowns:

The nodal displacement $\{r\}$ represents the primary unknown and is computed by Equation 6.6. The secondary unknown stress (σ) and strain ($\in$) within each element can be found using the following relationships wherein the vector of nodal displacement, (q), is known.

$$\{\in\} = [B]\{q\} \qquad 6.7$$

and:

$$\{\sigma\} = [c]\{\in\} = [c][B]\{q\} \qquad 6.8$$

6.2 Application and Results

The soil strata and pile type were modified for ease of application of the finite element method. The 14 inch square concrete pile was simulated by an equivalent circular pile with a tip and butt diameter of 15.84 inches. The model pile in this analysis assumed a 60 feet embedment within the Yorktown formation. For the actual case, only 42 and 44 feet of the total embedment length of test piles TP-3 and TP-4 respectively were embedded within the Yorktown formation. This simulation was considered reasonable since the Norfolk formation was found to contribute little to the bearing capacity of the piles.

The soil strata plus pile embedment of the test and model piles are depicted in Figure 6.2. The surface area at the pile tip and pile perimeter of the actual versus the model pile is presented in Table 6.1. The additional surface area along the pile perimeter resulting from deeper simulated embedment of the model pile in the Yorktown formation was introduced to account for the capacity attributed to the Norfolk formation in the case of the test piles.

The finite element mesh that was used to analyze

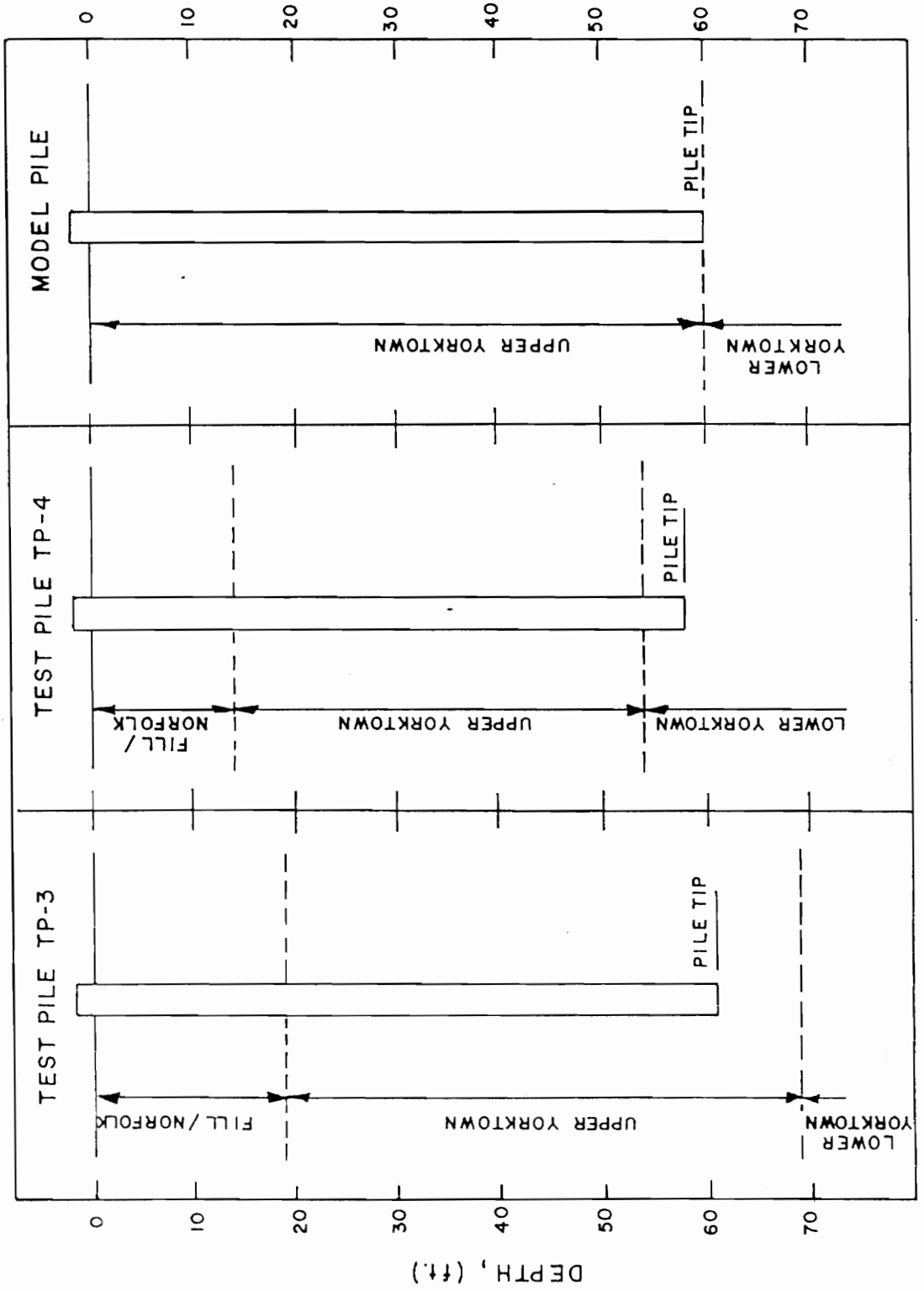

FIGURE 6.2 PILE EMBEDMENT PROFILES

TABLE 6.1 PILE SURFACE AREA, FT^2

	Test Pile TP-3	Test Pile TP-4	Model Pile
Pile Tip	1.4	1.4	1.4
Total Pile Perimeter	284.7	270.7	248.8
Pile Perimeter Embedded in the Yorktown Formation	196.0	205.3	248.8

the behavior of the soil and model pile is shown in Figure 6.3. It consisted of 293 nodes and 285 elements, 16 of which were interface elements. Four-node quadrilateral elements were used to discretize both the soil medium and the pile. At the interface of the pile and the surrounding soil medium, interface elements were used. Table 6.2 gives the material properties for the soil medium and the pile; the soil-pile interface properties are given in Table 6.3.

The pile was loaded in 30 ton increments to a maximum load of 300 tons. This corresponds to the maximum load obtainable in the pile load test. Before applying the load, the in-situ stresses were set-up in the soil plus the interface and pile elements. Initial stresses in the interface and the pile elements were set equal to those in the adjacent soil elements. The initial shear stress for all elements along the ground surface were set equal to zero.

6.3 Analysis of Results

The applied load versus pile butt displacement was determined at various increments by finite element analysis and compared with load-displacement data obtained from the pile load tests performed on test piles TP-3 and TP-4. The results are shown in Figure 6.4. The load-displacement response resulting from the model pile was

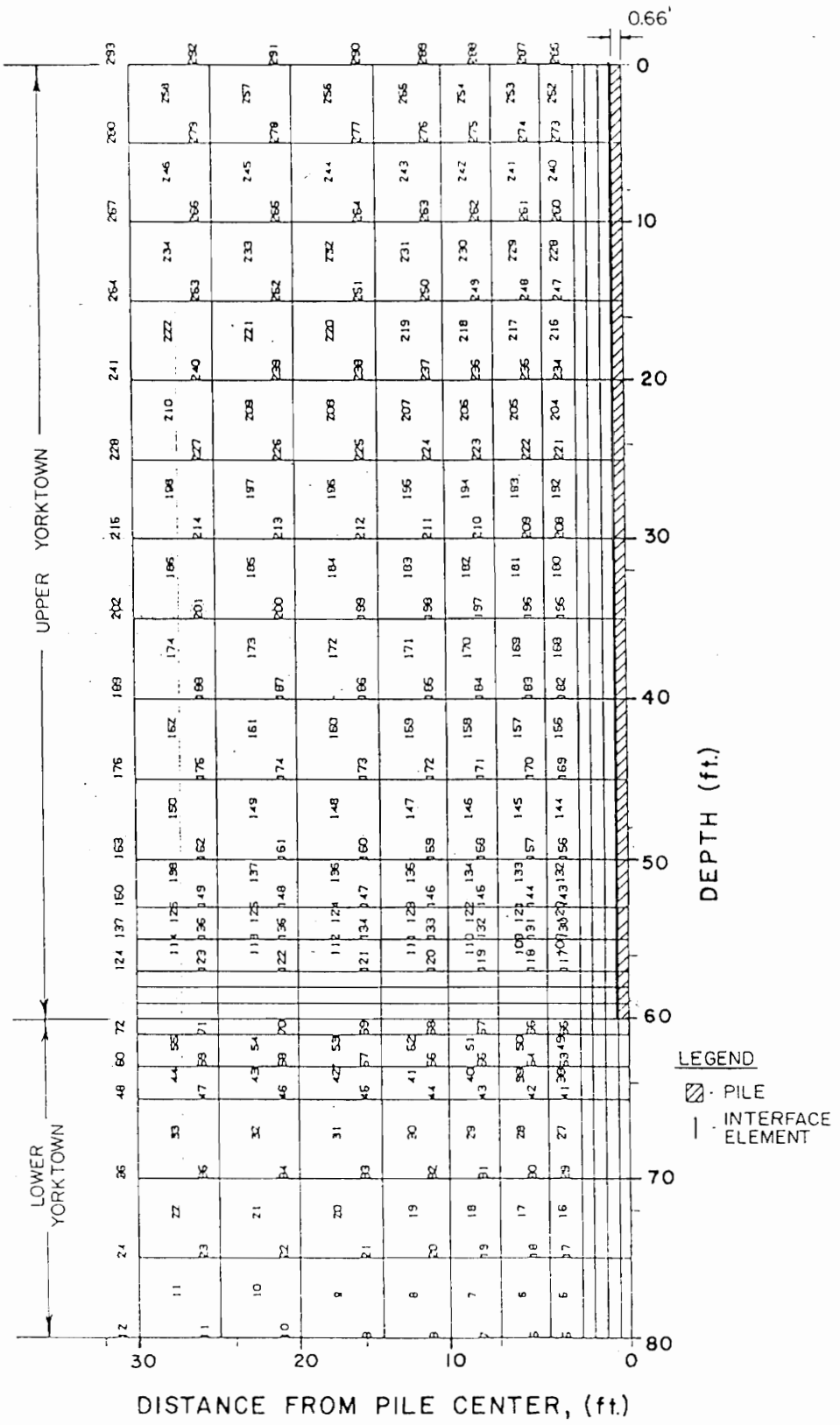

FIGURE 6.3 FINITE ELEMENT MESH

TABLE 6.2 MATERIAL PROPERTIES OF THE PILE AND SOIL MEDIUM USED IN THE FINITE ELEMENT ANALYSIS

Material Properties	Concrete Pile	Soil Along Pile Perimeter Above W. T.	Soil Along Pile Perimeter Below W. T.	Soil At Pile Tip
Poisson Ratio (ν)	0.2	0.3	0.3	0.3
Unit Weight (γ), pcf	150	123.0	60.8	59.6
Lateral Earth Pressure Coefficient (Ko)	-	0.5	0.5	0.5
Internal Angle of Friction (ϕ), degrees	-	28	28	28
Cohesion (c), psf	-	648	648	576
Failure Ratio (R_f)	-	0.70	0.70	0.76
Modulus Exponent (n)	-	0.50	0.50	0.68
Unload/Reload Coefficient	10	20	20	20
Youngs Modulus (E_i), psf	5.919E8	6.564E5	6.565E5	4.151E5

TABLE 6.3 MATERIAL PROPERTIES AT THE SOIL/PILE INTERFACE USED IN THE FINITE ELEMENT ANALYSIS

Shear Stiffness (Ks), psf	6.564E5
Cohesion (c), pcf	0
Internal Angle of Friction (Ø), degees	28
Tensile Strength, psf	0.10
Strength Factor (R_f)	0.69

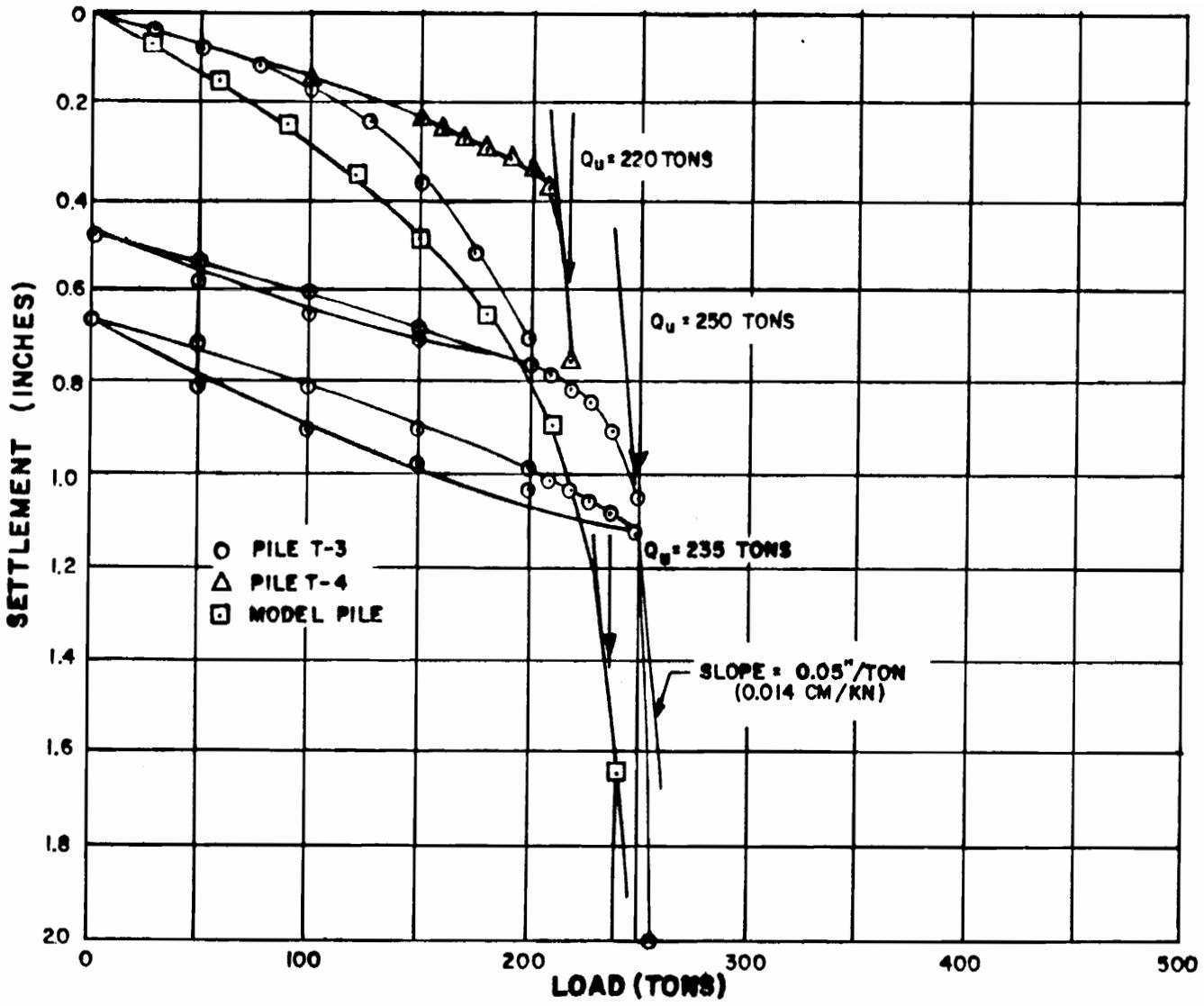

FIGURE 6.4 LOAD-SETTLEMENT CURVES FOR THE MODEL PILE AND TEST PILES TP-3 AND TP-4

similar to that exhibited by test pile TP-3 to within 0.1 inches throughout the initial load cycle to failure. Test pile TP-4 exhibited less displacement at the pile butt compared to both test pile TP-3 and the model pile. As previously discussed, difficulties were encounted during the load test with pile TP-4 and resulted in preloading and subsequent redriving prior to load testing. In addition, pile TP-4 was embedded about five feet within the firm granular soils of the lower Yorktown formation whereas test pile TP-3 was embedded in the soft fine grain soils of the upper Yorktown formation only. This was also the simulated case for the model pile. Due to the above conditions, greater amounts of compressive residual loads may have developed at the pile tip prior to load testing compared to test pile TP-3 and the model pile. This would result in less measureable displacement for a given load up to plunge failure.

The ultimate capacity of the model and test piles were determined by the Norlund method (15). This resulted in the following ultimate bearing capacity values: 235 tons for the model pile; 250 tons for TP-3; and 220 tons for test pile TP-4.

The ultimate load capacity of the model pile was also determined by general static analysis. The static analysis which was used employed soil mechanics and bearing capacity theory for determining the ultimate load capacity

of a single pile from measured soil properties. The ultimate load capacity of a single pile (P_u) is generally expressed as the sum of the ultimate pile shaft resistance (P_{su}) plus ultimate base resistance (P_{bu}) minus the weight of the pile (W_p) as shown below:

$$P_u = P_{su} + P_{bu} - W_p \qquad 6.9$$

The ultimate base resistance (P_{bu}) is defined by Vesic (1975) by the following expression.

$$P_{bu} = A_b(cNc^* + qNq^*) \qquad 6.10$$

where:

A_b = cross-sectional area of the pile tip

c = cohesion

q = mean normal ground stress

N_q = bearing capacity factor

N_c^* = bearing capacity factor

The value of the mean normal ground stress (q) is a function of the at-rest lateral earth pressure (K_o) and vertical stress (q_v). It is determined by the following equation:

$$\bar{q} = \frac{1 + 2K_o}{3}\left(q_v\right) \qquad 6.11$$

Vesic (1975) established that bearing capacity factors are

a function of the internal angle of friction (ϕ) and rigidity index (I_r) of the soil. The rigidity index value of 10 used in this analysis was obtained from Vesic (1975) for sand and silt soils. Using correlation tables given by Vesic (1975), values of 27.40 and 15.57 were determined for N_c^* and N_q^* respectively.

The ultimate shaft resistance (P_{su}) can be computed by integration of the soil-pile shear strength, $_s$, over the surface of the pile shaft (19) as shown below:

$$P_{su} = {}_o\int^L p\tau_s dL \qquad 6.12$$

where: p = pile perimeter

τ_s = soil-pile shear strength

L = pile length

The shear strength is similar to Columb's expression for analyzing sliding of a rigid body in contact with soil as shown by the following equation:

$$\tau = Ca + q_s \tan \phi_i \qquad 6.13$$

where: Ca = adhesion

$\tan \phi_i$ = coefficient of friction at the soil-pile interface

q_s = normal stress on the shaft.

The normal stress on the shaft (q_s) is equal to the vertical stress (q_v) multipled by a coefficient of skin pressure (k_s) which is similar to the at-rest earth pressure coefficient (K_o).

Based upon the statistical method of analysis described above and use of the soil properties given in Table 6.2, ultimate shaft and base resistance values of 145 tons and 47 tons respectively were computed for the model pile. Neglecting the weight of the pile, the ultimate load capacity of the model pile was 192 tons. This is a conservative estimate of pile capacity as compared to the results from both the finite element analysis and pile load tests.

In the finite element method, the stress at the centroid of each element that constituted the model pile were determined for each load increment. The load-distribution curves developed from these data at applied loads of 60, 150 and 210 tons are presented in Figure 6.5. Load distribution curves that were developed for test piles TP-3 and TP-4 are also presented in Figure 6.5.

At an applied load of 150 tons, the load-distribution curves exhibited by the model pile and test pile TP-4 were similar; whereas, a greater variance resulted for test pile TP-3. Variations of the load-distribution curve of the model pile compared with those of the test piles are attributed to the fill and soils of the

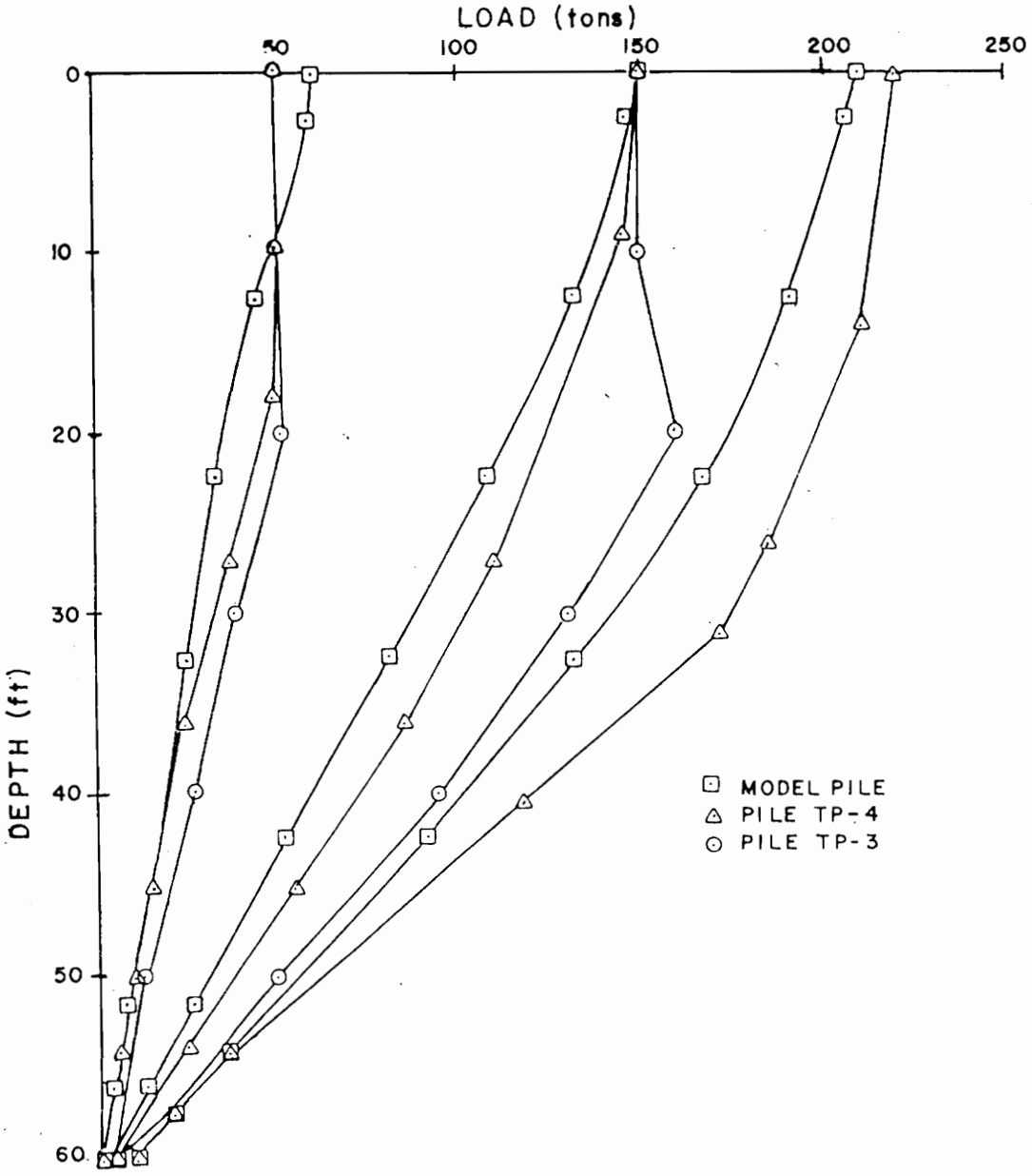

FIGURE 6.5 LOAD-DISTRIBUTION CURVES FOR THE MODEL PILE AND TEST PILES TP-3 AND TP-4

Norfolk formation which contributed little to capacity and therefore were not considered in the model case. In addition, the differences may have resulted from residual stresses developed during driving of the test piles which was not considered in the finite element method. It is possible to account for such residual stresses in the finite element method of analysis but this was not attempted.

The degree of correlation between the model pile and actual pile behavior are further illustrated in Figure 6.6 by a plot of the applied load mobilized as point and side friction resistance throughout the initial load cycle. The shear stress recorded for each interface element was divided by the surface area of the pile segment for each element and summed to obtain the shaft resistant values presented. The tip resistance is the difference between the shaft resistance and gross load applied. The general trend of each curve is similar indicating a greater percentage of the applied load is maintained by shaft resistance than by tip resistance with all three curves linearly increasing at a porportional rate up to about 210 tons. Beyond the 210 ton load, the percent mobilized at the pile tip increased at a higher rate than along the pile perimeter.

The percentage of load mobilized as shaft and tip resistence for the model pile and test pile TP-3 were

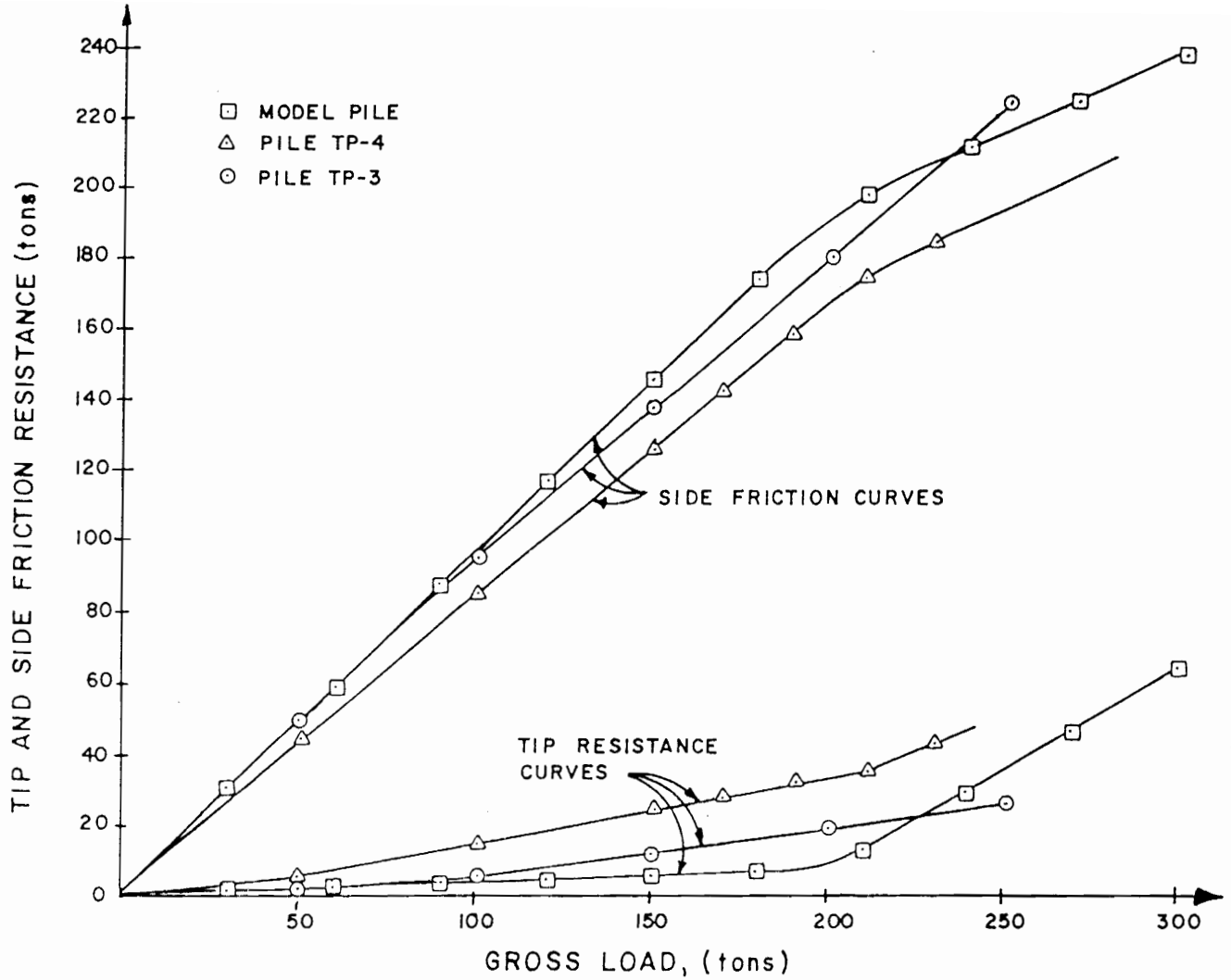

FIGURE 6.6 GROSS LOAD VERSUS TIP AND SIDE FRICTION RESISTANCE FOR THE MODEL PILE AND TEST PILES TP-3 AND TP-4

similar. When compared to test pile TP-4, a slightly lower percentage of load was mobilized as shaft resistance and a higher percentage as tip resistance. This difference is believed to be the result of additional side friction resistance derived from the additional surface area within the bearing stratum of the model and test pile TP-3 as compared with test pile TP-4.

The percentage of shaft resistance and tip resistance mobilized at the limit load for the test piles and the model pile determined from both the finite element method and static analysis are shown in Table 6.4. The percentage of shaft resistance mobilized at the limit load for test pile TP-3 and the model pile were similar. Test pile TP-4 contained less shaft resistance and greater tip resistance at the limit load as compared with the other two cases. This may be the result of the embedment of pile TP-4 in the granular soils of the lower Yorktown formation. The static analysis used to compute the ultimate load capacity of the model pile described herein resulted in a greater percentage of tip resistance and less shaft resistance mobilized at the limit load than was determined by the finite element analysis. In the finite element analysis, the initial Young's Modules was used for soils at the pile tip. Due to pile driving, the soils at the tip are subjected to load/unload conditions. Therefore, the use of the unload/reload modulus value may be better suited

TABLE 6.4 PERCENT SHAFT AND TIP RESISTANCE MOBILIZED AT THE LIMIT LOAD FOR TEST PILE TP-3, TP-4, AND THE MODEL PILE

	LIMIT LOAD (TONS)	SHAFT RESISTANCE (%)	TIP RESISTANCE (%)
TEST PILE TP-3	250	90	10
TEST PILE TP-4	220	82	18
MODEL PILE BY FINITE ELEMENT ANALYSIS	235	89	11
MODEL PILE BY STATIC ANALYSIS	192	76	24

for use in this analysis. This would result in higher stiffness values for soils at the pile tip. The result would lead to a greater percentage of the applied load, in the case of the model, mobilized at the tip as was the case for the test piles.

The distribution of the unit skin friction along the shaft of the model pile computed by the finite element method at the limit load of 210 tons is shown in Figure 6.7. It shows an increase in unit skin friction along the pile shaft with increased depth to a point 10 feet above the pile tip and then decreases sharply to the tip grade. The behavior of the curve correlates well with the load-distribution curves for this pile as illustrated in Figure 6.5. Vesic (1975) explains that this type of load-transfer is due to compression and creep of soils along the pile shaft under newly applied stress.

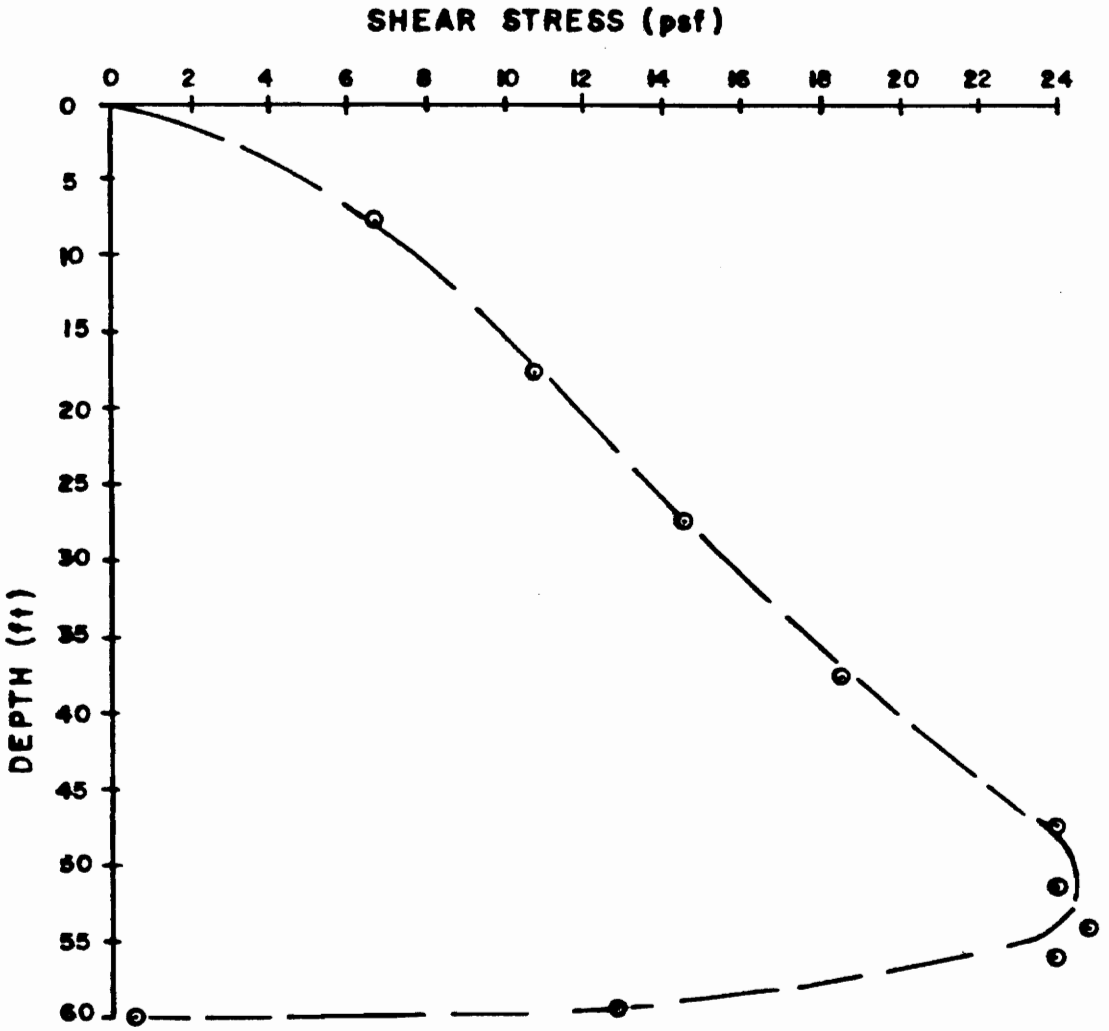

FIGURE 6.7 VARIATION IN UNIT SKIN FRICTION RESISTANCE ALONG THE SOIL-PILE INTERFACE FOR THE MODEL PILE AT THE ULTIMATE LOAD

CHAPTER 7

SUMMARY AND CONCLUSIONS

7.0 Summary

The finite element method was used to determine the load-capacity and behavior of a single concrete pile that was modeled after full scale instrumented piles used during the design phase of the foundation system for the Land Level Shipbuilding Facility located in Newport News, Virginia. The principal function of this facility is the construction of Naval ships and submarines. Hence, the foundation was designed for heavy loads over an extremely large area. The final design involved over 10,000 prestressed precast concrete piles capable of handling 100 tons each.

The objective of the study was to compare the results obtained from the finite element method with those derived from full scale pile load tests that were conducted for the Shipbuilding Facility. The outcome of this comparative analysis formed the basis for assessing the feasibility and effectiveness of the finite element method in the design of deep foundation systems in the Tidewater area of Virginia.

Before the comparative analysis could be accomplished, it was necessary to ascertain the subsurface

conditions in the immediate vicinity of the test piles. Moreover, the conditions and manner in which the pile test program was conducted was of extreme importance. All available information relevant to this aspect of the study was addressed.

Despite the extensive soil investigative program undertaken by the design firm for the foundation, the data generated did not provide all the soil parameters required for the finite element method. Thus, soil sampling and in-situ tests were conducted to include soil laboratory tests to determine index properties and strength-deformation characteristics of the soil medium and for the soil-pile interface. The specific tests, types of apparatus used, the results and analyses thereof were covered in detail. These are outlined below along with pertinent findings. The finite element method was described in general terms along with the steps used to ascertain specific elements of information needed to determine pile capacity and behavior. The results therefrom were then compared to those from the instrumented test piles.

7.1 Findings

In general, two geological formations, the Norfolk and Yorktown, underlie the Tidewater area. The younger Norfolk formation generally consists of fine

grained soils while the older Yorktown is comprised of more granular soils containing varying amounts of shell fragments; concentrations over 50 percent by weight are not uncommon. The soils of the Norfolk formation were found to contribute little to the bearing capacity of piles; it is derived primarily from the more granular soils of the Yorktown formation.

The upper stratum of the Yorktown formation generally consists of clayey and silty sand with interbedded layers of clay and silt. Typically, this stratum contains fines of greater than 35 percent but less than 65 percent by weight. The lower portion consists of sandy soils with less than 35 percent fines by weight. Due to these subsurface conditions and the fact that bedrock depths range from 2000 to 3000 feet below the surface, most large structures are supported on pile foundations embedded within the Yorktown formation.

The sensitivity of the soils makes accurate determination of pile capacity by conventional methods difficult, hence, pile test programs are often used during the design phase of deep foundations in the Tidewater area.

Pile load tests performed on three test piles of interest in this study indicated that pile capacities range between 230 to 320 tsf; these results are based on load-settlement data. Two test piles were instrumented with wire strain guages and monitored during the load tests.

Skin friction was found to vary from 0.6 to 1.4 tsf for soils within the upper stratum of the Yorktown formation. Variations in shaft resistance were attributed to changes in relative density as evidenced by variances in SPT values. Only one of the instrumented piles penetrated the lower Yorktown formation for which a shaft resistance of 0.5 tsf was determined.

Standard Penetration Tests disclosed a moderate variance in relative density within the upper stratum of the Yorktown formation; SPT values ranged between 4 and 28. This variance was not evidenced for soils of the lower Yorktown formation which had an average SPT value of 11.

The Menard pressuremeter tests resulted in the following findings regarding the upper Yorktown formation.

1. The soils are preconsolidated and have an estimated average OCR value of 3.5.

2. Shear strength increases with depth.

3. Young's Modulus (E), determined from the pressuremeter modulus (Epm), ranges from 216 to 288 tsf.

The pressuremeter data presented herein is inadequate for use in evaluating the strength-deformation characteristics of the soil. Further pressuremeter testing within the Yorktown formation must be conducted before the test data can be considered conclusive.

Triaxial tests, consolidated-undrained (CU) and consolidated-drained (CD), on undisturbed samples indicated

that the more granular soils of the lower Yorktown formation had a higher degree of effective internal angle of friction (ϕ') and a lower effective cohesion (c') than the more fine grained soils of the upper stratum. Under similar load conditions, shear strength was greater for soils within the lower stratum.

Direct shear tests were conducted to determine the strength-deformation characteristics along the soil-pile interface within the upper Yorktown formation. Three interface tests were performed using smooth surface concrete blocks at normal loads of 0.98, 2.75, and 4.48 tsf. One rough surface texture concrete block interface test was performed at a normal load of 2.75 tsf. The interface tests with the smooth textured block disclosed the following:

1. Maximum shear strength (τ_f) increased approximately 300 percent with an increase in normal stress (σ_n) from 1.0 to 4.5 tsf.

2. The value of (τ_f) determined upon reloading the test specimen was within 3.0 percent of that obtained during the initial load cycle for the 2.7 and 4.5 tsf normal load.

3. Upon reloading after a 12 hour hold, the value of τ_f was within 0.9 percent of the value of τ_f determined during the initial load cycle.

4. The roughness of the concrete surface had

little effect on the interface parameters.

5. It appeared that remolding of the soil does not greatly affect the shear-deformation characteristics even after the remolded soil stands for an extended period.

Typically, piles embedded within the Yorktown formation experience greater retap values after the pile driving is stopped for a period of 12 hours or less. This could be due to excess pore pressure and densification resulting from the initial driving of the pile.

Using the finite element method, a model of test piles TP-3 and TP-4 was developed. At applied loads of 150 tons, the load-distribution curves of the model pile and test pile TP-4 were similar. This was also the case with regard to point and side friction resistance. This same high degree of correlation was observed relative to the percentage of load mobilized as shaft and tip resistance between the model and test pile TP-3. The ultimate pile capacity of the model and the test piles were determined by the Norlund method. For the model pile, the ultimate bearing capacity was 235 tons versus 250 tons for TP-3 and 220 tons for TP-4. In yet another comparison, the ultimate load capacity determined by general static analysis resulted in a value of 192 tons compared to the 235 tons determined by the finite element method. This gives an indication of the conservative findings inherent in standard static analyses.

7.2 Conclusions

In this study, the results of the finite element method of analyzing pile capacity and behavior correlate well with data derived from the full scale test pile program conducted for the foundation system of the Land Level Shipbuilding Facility in Newport News, Virginia. This was evidenced by a number of parameters used to determine pile capacity and behavior, specifically: load distribution; point and side friction resistance; shaft and tip resistance and others.

The data required to determine pile capacity and behavior using the finite element method are readily determined from standard field and laboratory tests. Hence, this method is deemed feasible from the standpoint that extraordinary and costly data are not required.

Use of conventional static and dynamic formulas provided conservative values of pile capacity in comparison to those derived from full scale pile tests or the finite element method.

The finite element method shows promise for use in the design of deep foundation systems in the Tidewater area of Virginia as evidenced by the outcomes of this study. Additional use of the finite element analysis is required to better develop the soil parameters associated with the Yorktown Formation to improve its reliance and use

for the purpose of design. It has potential in the near term for use as a tool to expand the data base in predicting the capacity and behavior of piles in conjunction with other forms of predictive analyses such as pile load tests.

It is suggested that, in some cases, the finite element could be used in lieu of expensive full-scale pile tests.

REFERENCES

1. Baguelin, F., Jezequel, J.F., and Shields, D.H., "The Pressuremeter and Foundation Engineering," Tran Tech Publication, 1978.

2. Bowles, J.E., "Foundation Analysis and Design," Second Edition, McGraw-Hill, Inc., 1977.

3. Bowles, J.E., "Engineering Properties of Soils and Their Measurement," McGraw-Hill, Inc., 1978.

4. Clough, G.W., "User's Manual for Program Soilstruct Axisymmetric Version," Virginia Polytechnic Institute and State University, Blacksburg, Virginia, 1982.

5. Clough, G. W., "Finite Element Analyses of Soil-Structure Interaction in U-Frame Locks," dissertation presented to the University of California, Berkeley, 1969.

6. Clough, G.W., and Duncan, J.M., "Finite Element Analyses of Retaining Wall Behavior," Journal of Soil Mechanics and Foundation Division, ASCE, Vol. 97, No. SM12, December, 1971, pp. 1657-1673.

7. Deasai, C.S., and Christian, J.T., "Numerical Methods in Geotechnical Engineering," McGraw-Hill, Inc., 1977.

8. Duncan, J.M., "Strength, Stress-Strain and Bulk Modulus Parameters for Finite Element Analyses of Stress and Movements in Soil Masses," Report No. UCB/GT/80-01, Office of Research Services, University of California, Berkeley, California, August 1980.

9. Gibson, R.E. and Anderson, W.F., "In-Situ Measurements of Soil Properties with the Pressuremeter," Civil Engineering and Public Works Review, Vol 56, May 1961, pp. 615.

10. Holloway, D.M., Clough, G.W., and Vesic, A.S., "A Rational Procedure for Evaluating the Behavior of Impact-Driven Pile," Behavior of Deep Foundations, ASTM STP 670, Raymond Lundgren, Ed., American Society for Testing and Materials, 1979, pp. 335-357.

11. Kulhawy, F.H., "Stress-Deformation Behavior of Soil-Concrete Interfaces," Report No. B-49(1), Office of Research Services, Syracuse University, Syracuse, New York, September 1976.

12. Lambe, T.W., "Soil Testing for Engineers," John Kiley and Sons, Inc., 1951.

13. Lukes, G.L., Leclerc DeBussey, B., Pressuremeter and Laboratory Test Correlations for Clays," Journal of the Geotechnical Engineering Division, ASCE, Vol. 102, No. GT9, September 1976, pp. 945-963.

14. Martin, R.E., "Concrete Pile Design in Tidewater Virginia," Journal of Geotechnical Engineering Division, ASCE, Vol 113,
No. 6, June 1987, pp. 568-585.

15. Nordlund, R.L., "Bearing Capacity of Piles in Cohesionless Soils," Journal of the Soil Mechanics and Foundations Division, ASCE, Vol. 89, No. 3, March 1963, pp. 1-35.

16. Poulos, H.G., and Davis, E.H., "Pile Foundation Analysis and Design," John Willey and Sons 1980.

17. Schnabel Engineering Associates, P.C., Geotechnical Engineering Reports: Land Level Shipbuilding Facility, 1983.

18. Tomlinson, M.J., "Pile Design and Construction Practice,"
A Viewpoint Publication, 1977.

19. Vesic, A.S., "Principles of Pile Foundation Design," Soil Mechanics Series No. 38, Duke University, Durham, North Carolina, March 1975.

20. Winterkorn, H.E., and Fange, H.V., "Foundation Engineering Handbook," Van Nostrand Reinhold Company, 1975.

21. Zienkiewicz, O.C., "The Finite Element Method," Third Edition, McGraw-Hill, Inc., 1977.

APPENDIX A

Pressuremeter Curves

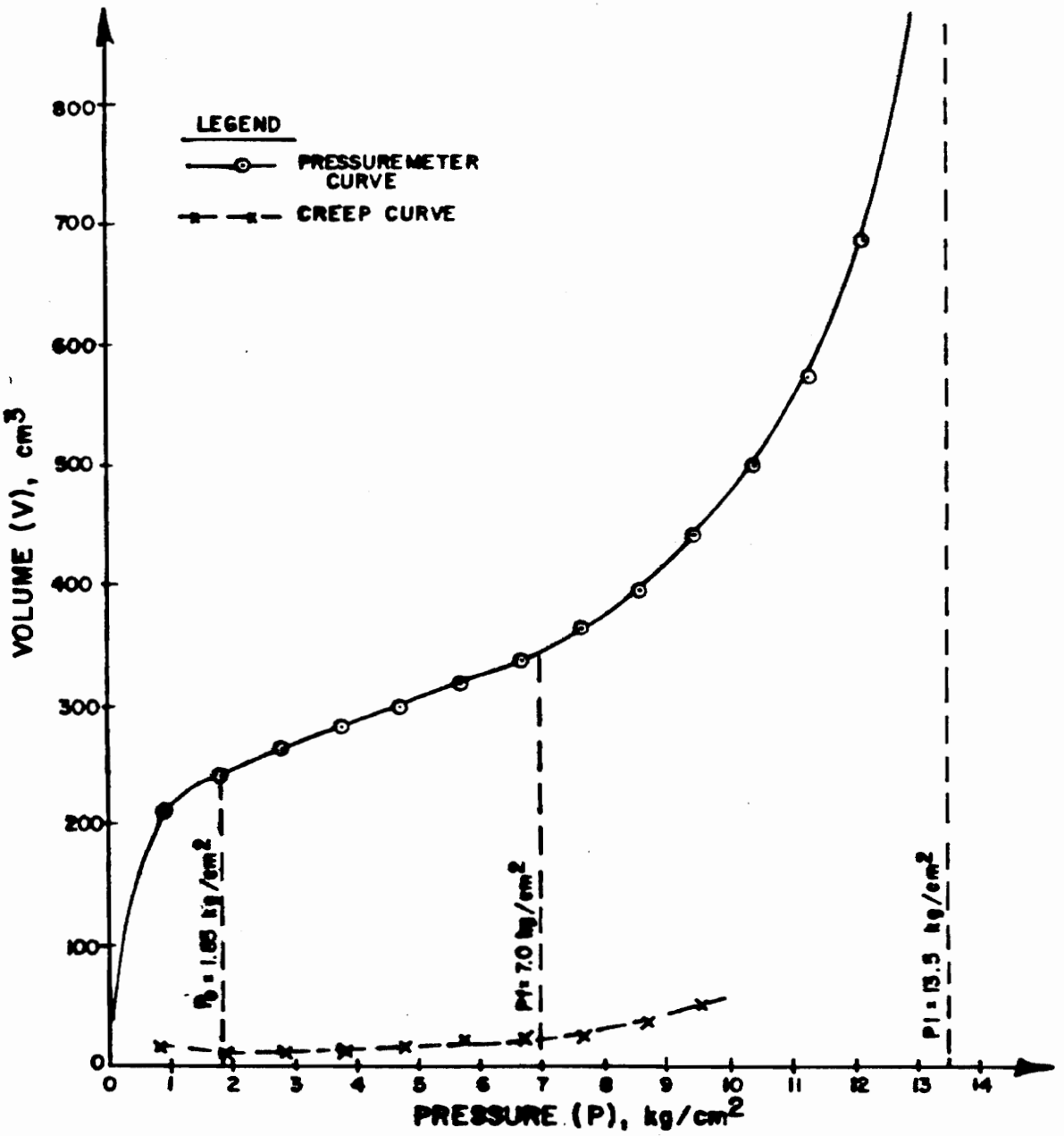

FIGURE A-1 PRESSUREMETER TEST NO. 1
(DEPTH 15'-17')

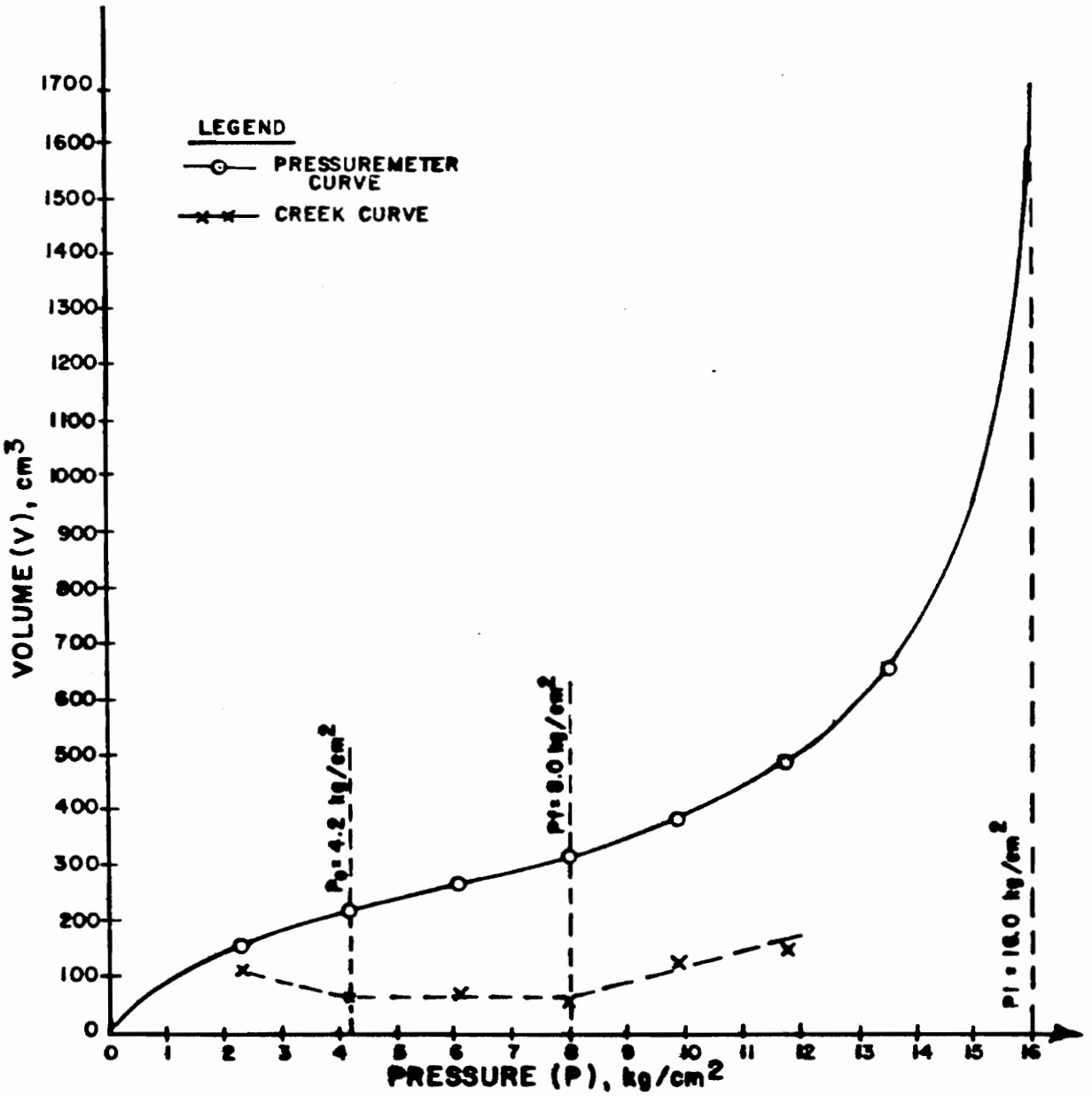

FIGURE A-2 PRESSUREMETER TEST NO.2
(DEPTH 25'-27')

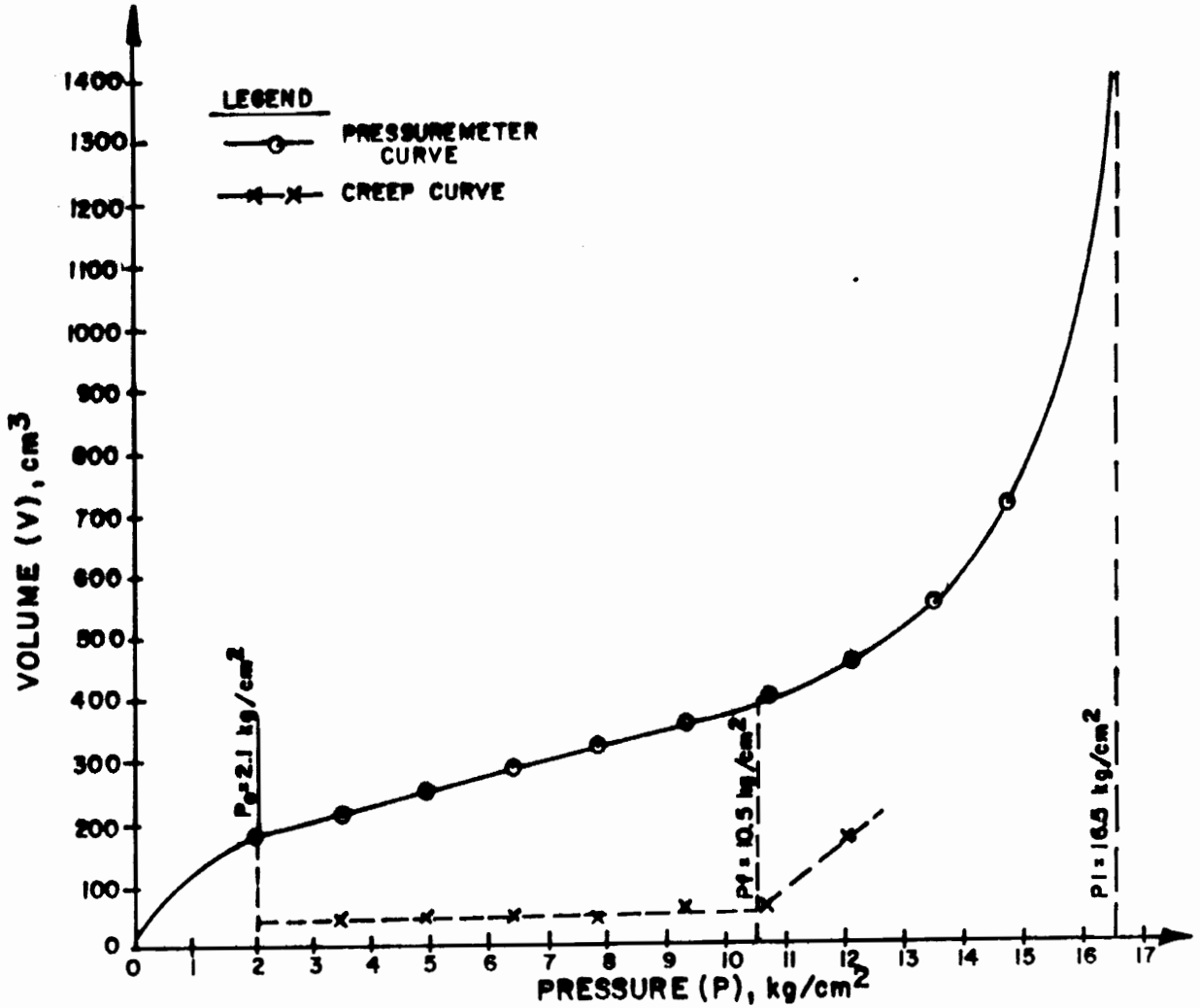

FIGURE A-3 PRESSUREMETER TEST NO. 3
(DEPTH 35'-37')

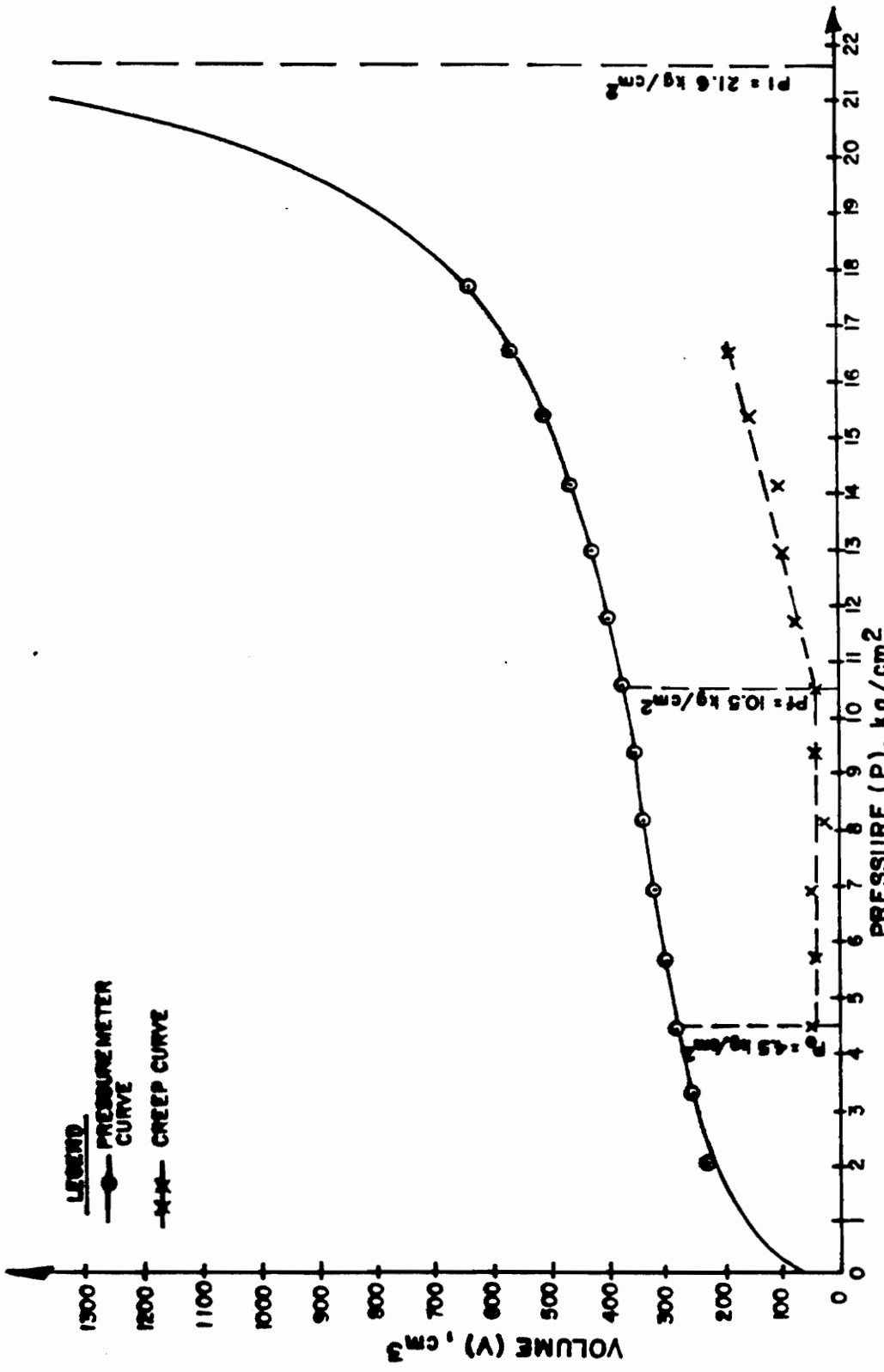

FIGURE A-4 PRESSUREMETER TEST NO.4
(DEPTH 45'-47')

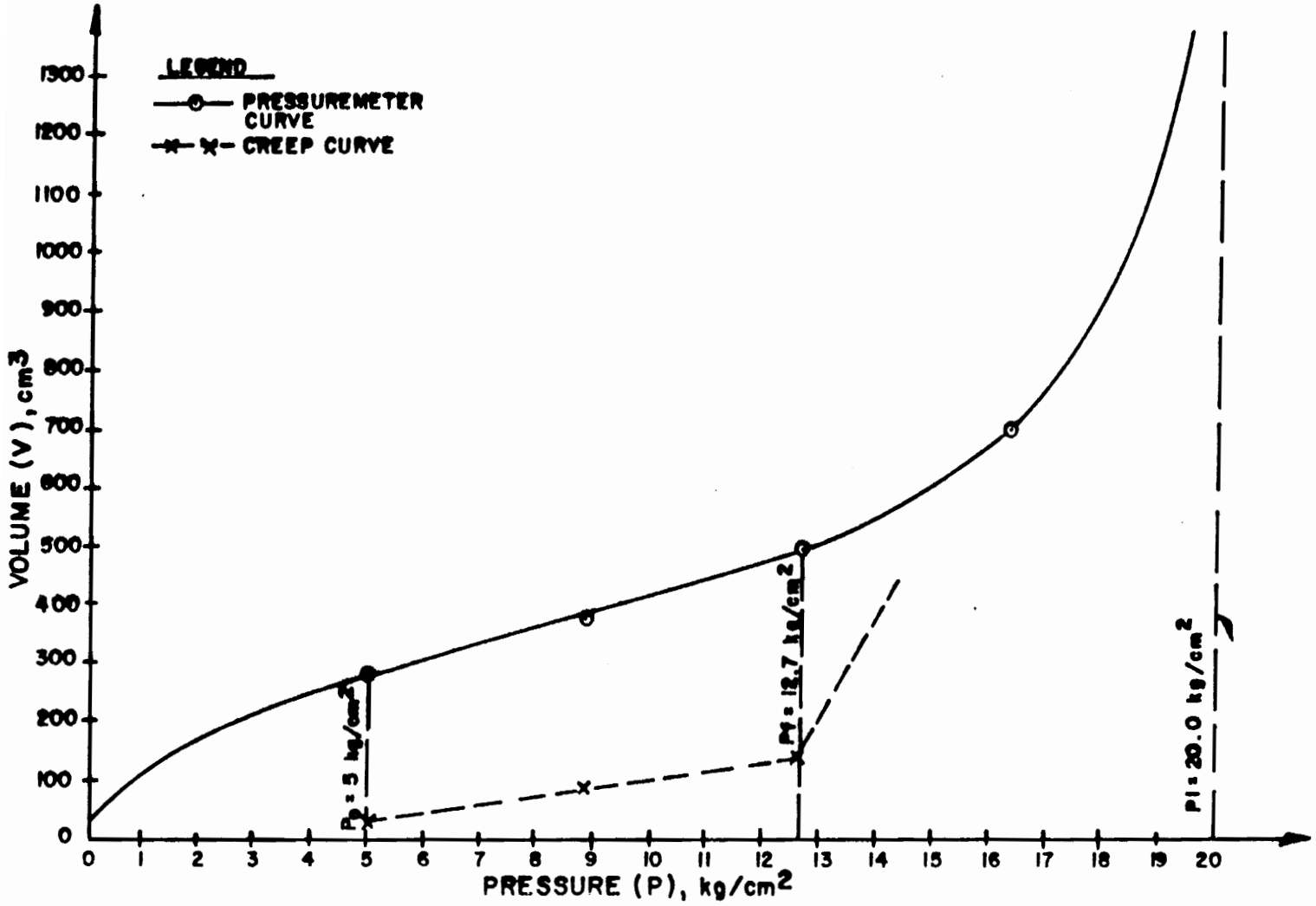

FIGURE A-5 PRESSUREMETER TEST NO. 5
(DEPTH 55'-57')

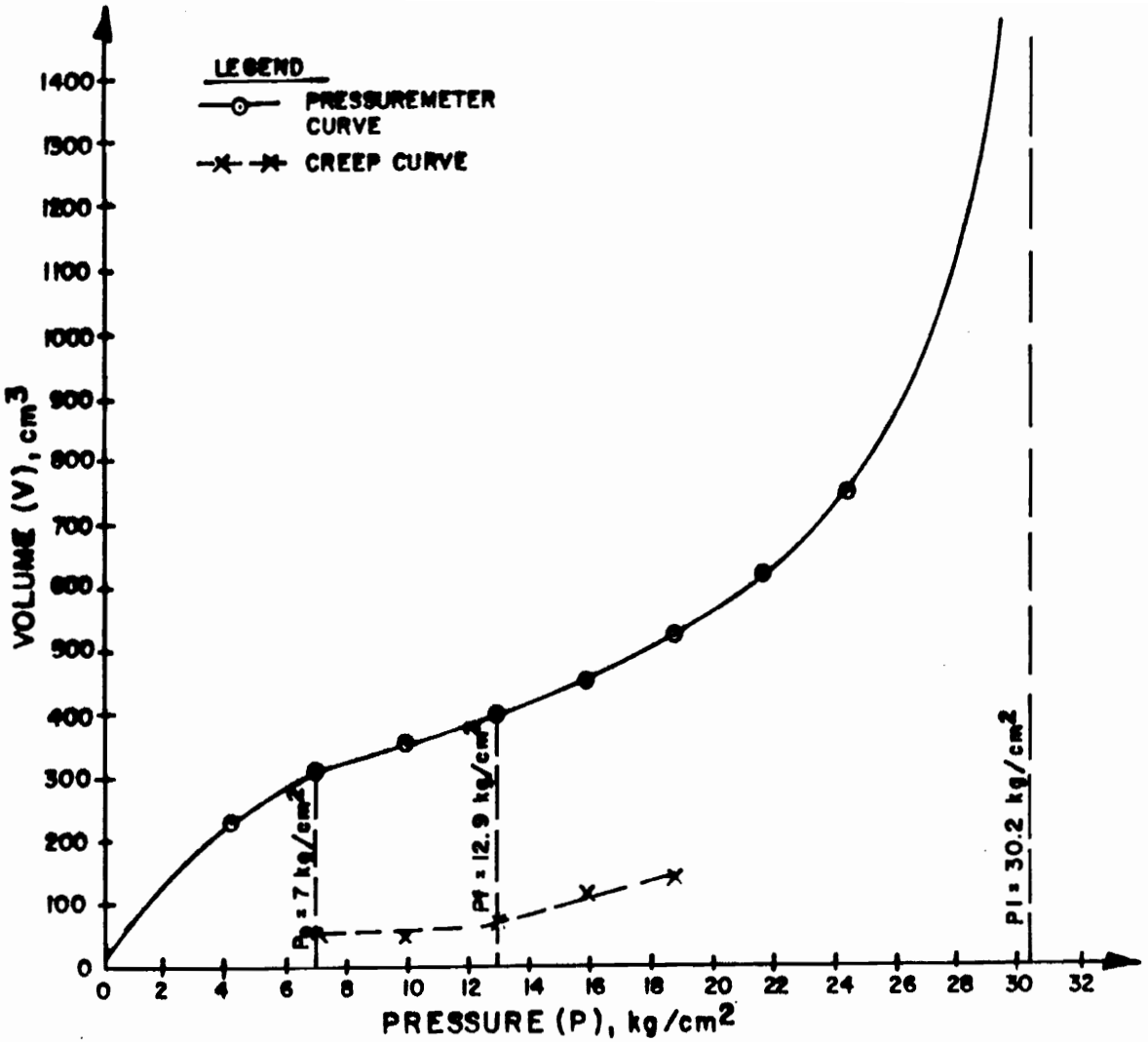

FIGURE A-6 PRESSUREMETER TEST NO. 6
(DEPTH 57'-59')

APPENDIX B

Results of CU-Triaxial Tests

Upper Yorktown Formation

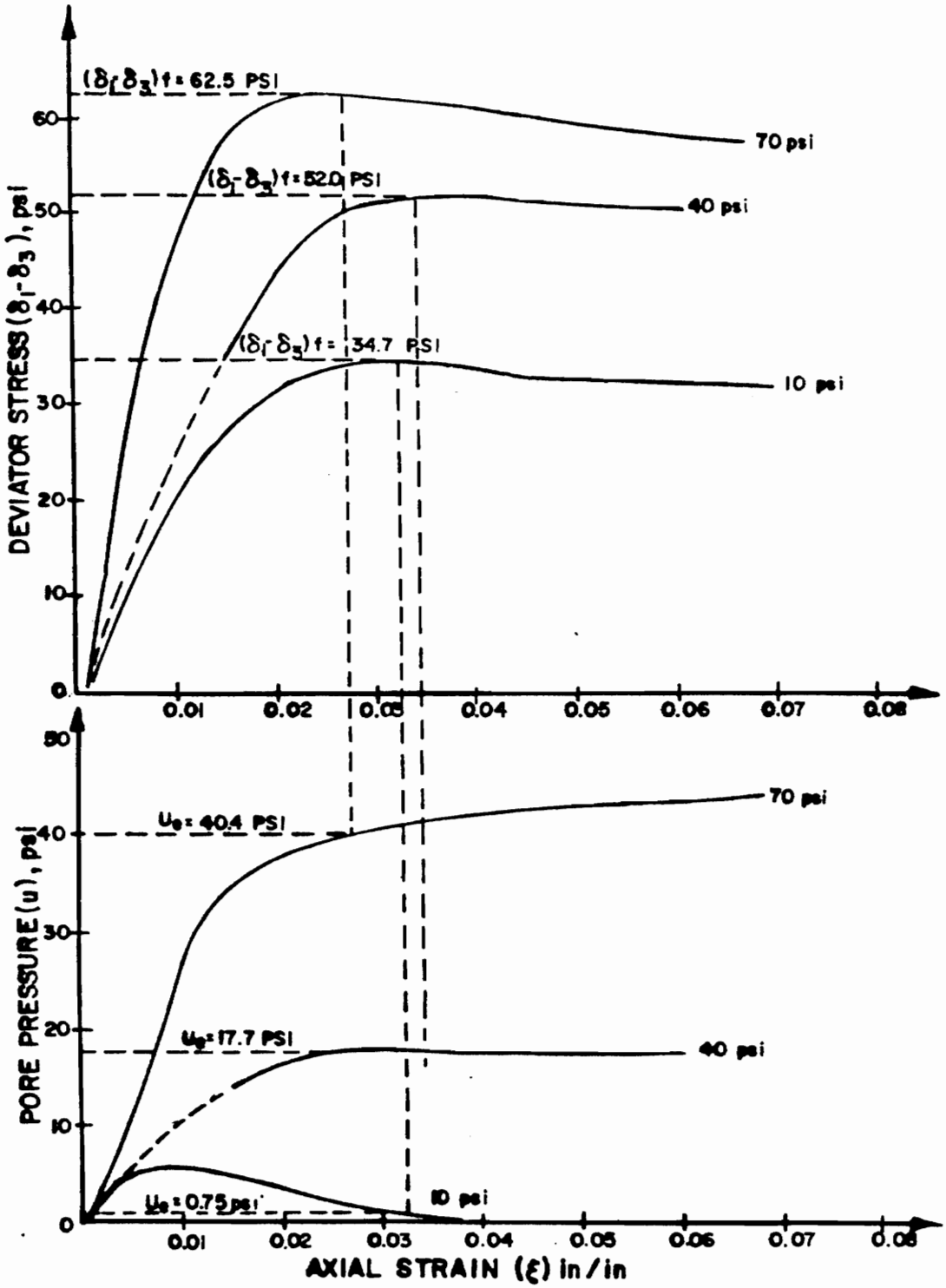

FIGURE B-1 CU-TRIXIAL TEST CURVES
UPPER YORKTOWN FORMATION
(DEPTH 37.5'-40.0')

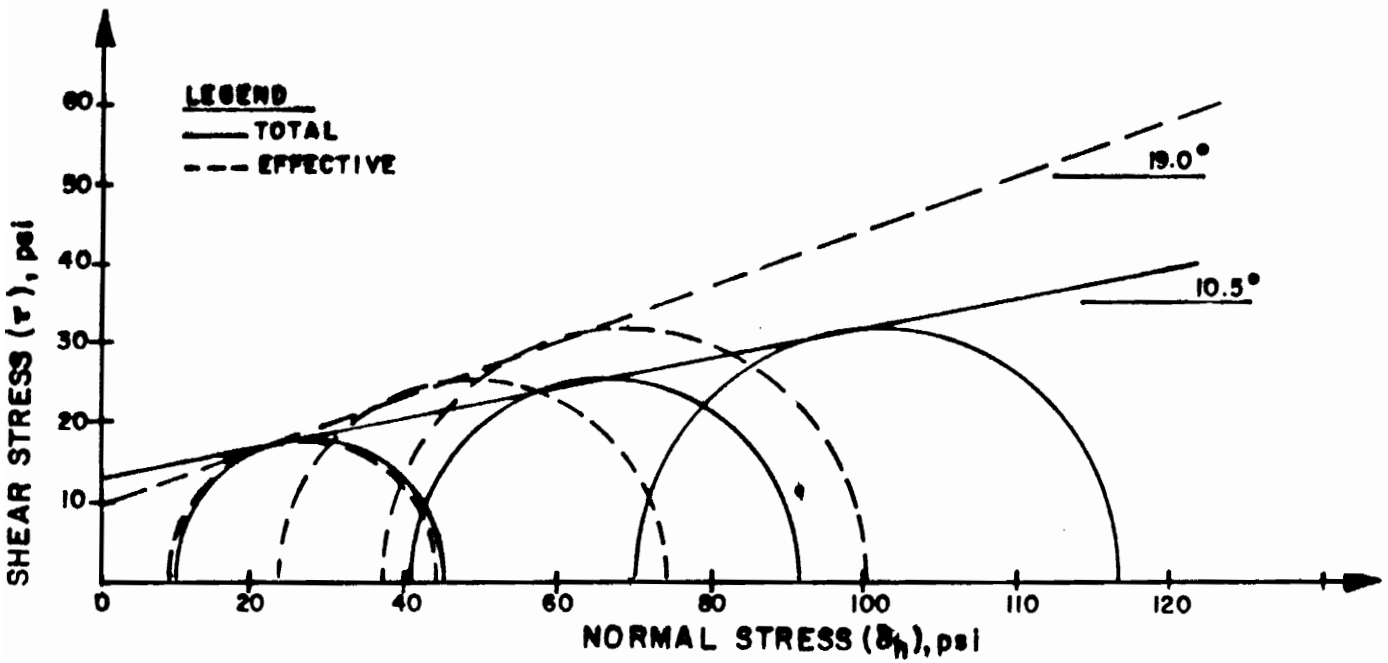

FIGURE B-2 CU-TRIAXIAL FAILURE CIRCLES
UPPER YORKTOWN FORMATION
(DEPTH 37.5'-40.0')

Soil: Stratum C1

Data for Deviatoric Modulus Parameters								Data for Bulk Modulus Parameters		
		70 % Stress Level			95 % Stress Level					
σ_3 ①	$(\sigma_1-\sigma_3)_f$ ②	$(\sigma_1-\sigma_3)$ ③	ε_a ④	$\frac{\varepsilon_a}{(\sigma_1-\sigma_3)}$ ⑤	$(\sigma_1-\sigma_3)$ ⑥	ε_a ⑦	$\frac{\varepsilon_a}{(\sigma_1-\sigma_3)}$ ⑧	$(\sigma_1-\sigma_3)_b$ ⑨	ε_v ⑩	$\frac{(\sigma_1-\sigma_3)_b}{3\varepsilon_v}$ ⑪
10	34.7	24.29	0.0128	5.27E-4	32.97	0.0230	6.98E-4	-	-	-
40	52.0	36.40	0.0150	4.10E-4	49.94	0.0260	5.26E-4	-	-	-
70	62.5	43.75	0.0093	2.13E-4	59.38	0.0173	2.91E-4	-	-	-

P_a = 14.5 psi

$\frac{\sigma_3}{P_a}$ ②	$\frac{1}{(\sigma_1-\sigma_3)_{ult}}$ ⑬	R_f ⑭	$\frac{E_i}{P_a}$ ⑮	$\frac{B}{P_a}$ ⑯
0.680	1.66E-2	0.58	212.6	-
2.721	1.05E-2	0.55	295.8	-
4.762	9.75E-3	0.61	566.9	-

$$\frac{1}{(\sigma_1-\sigma_3)_{ult}} = \frac{⑧ - ⑤}{⑦ - ④} \qquad R_f = ② \times ⑬$$

Average R_f = 0.58

$$\frac{E_i}{P_a} = \frac{2.0}{⑤ + ⑧ - ⑬ \times [④ + ⑦]} \cdot \frac{1}{P_a}$$

$$\frac{B}{P_a} = \frac{⑪}{P_a}$$

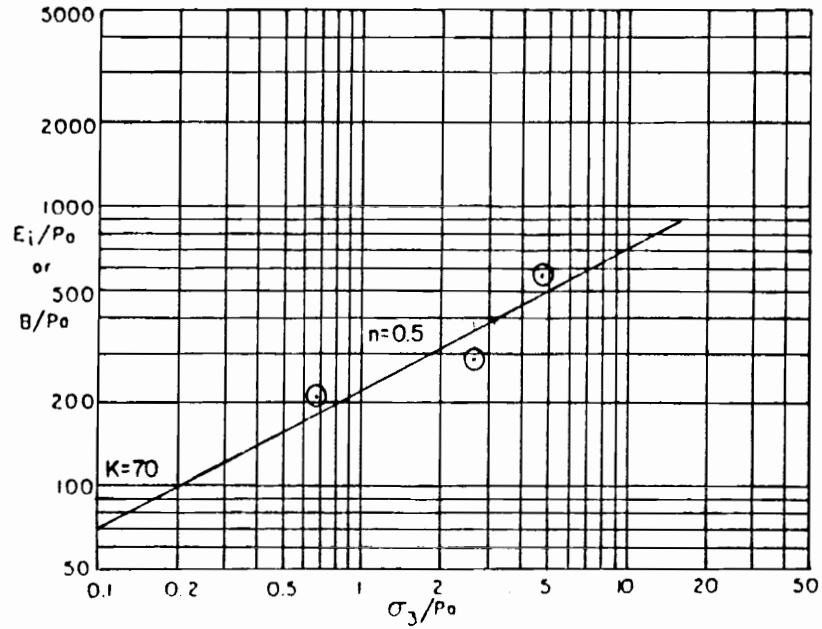

FIGURE B-3 DETERMINATION OF HYPERBOLIC PARAMETERS FROM CU-TRIAXIAL TEST

APPENDIX C

Results of CD-Triaxial Tests

Lower Yorktown Formation

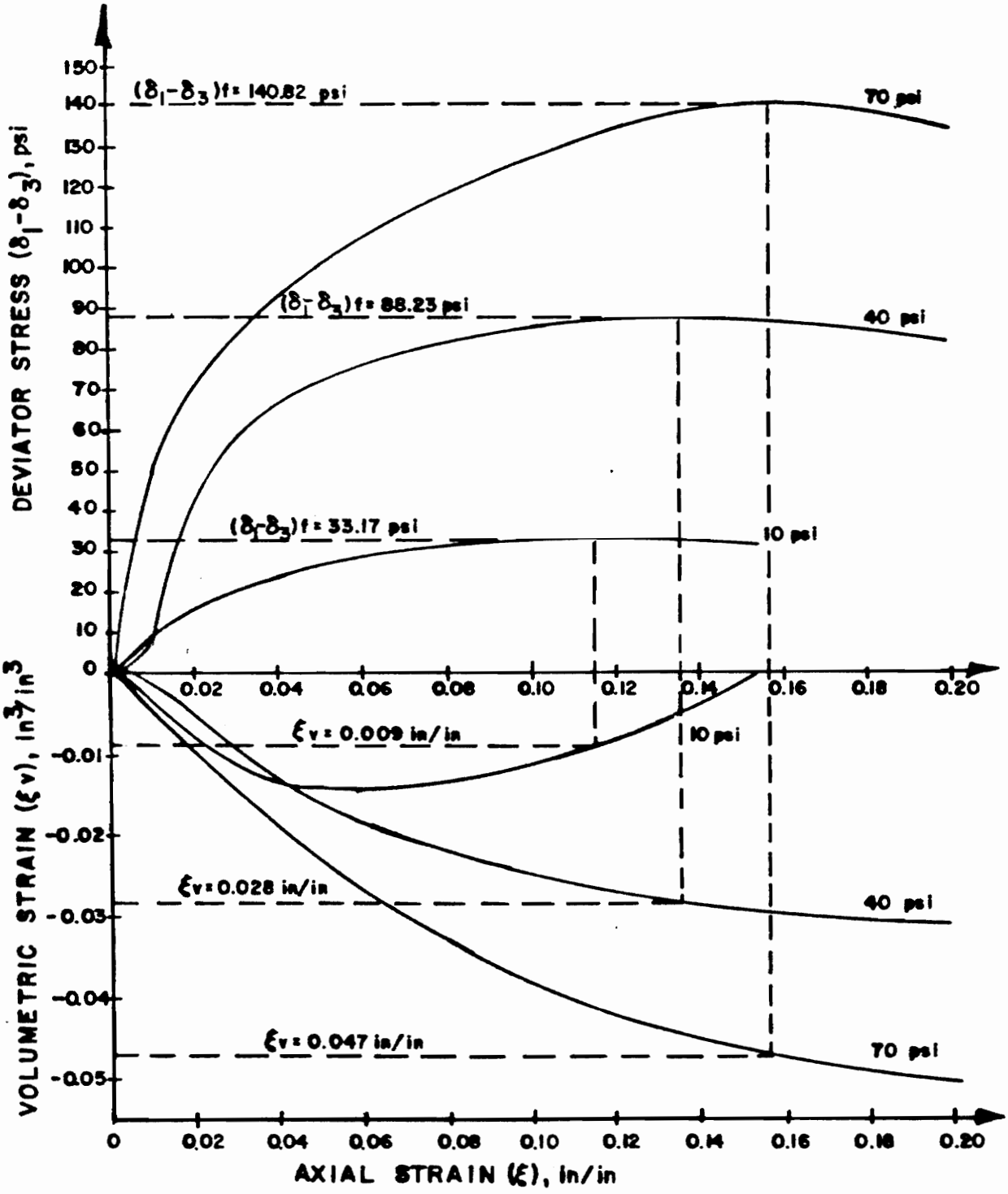

FIGURE C-1 CD-TRIAXIAL TEST CURVES
LOWER YORKTOWN FORMATION
(DEPTH 64.5'-67.0')

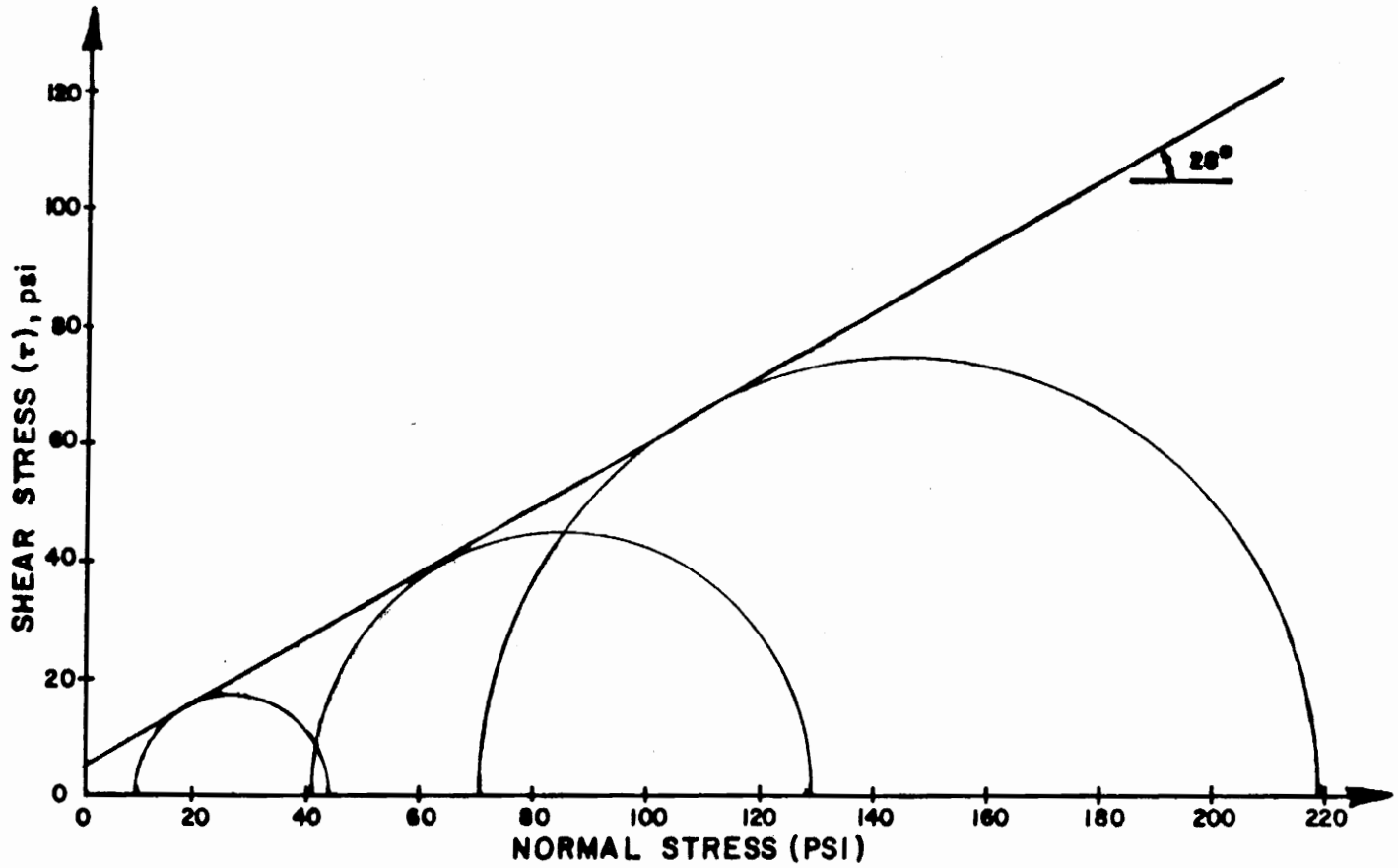

FIGURE C-2 CD-TRIAXIAL FAILURE CURVES
LOWER YORKTOWN FORMATION
(DEPTH 64.5'-67.0')

Soil: Stratum C2

Data for Deviatoric Modulus Parameters								Data for Bulk Modulus Parameters		
		70 % Stress Level			95 % Stress Level					
σ_3 ①	$(\sigma_1-\sigma_3)_f$ ②	$(\sigma_1-\sigma_3)$ ③	ε_a ④	$\frac{\varepsilon_a}{(\sigma_1-\sigma_3)}$ ⑤	$(\sigma_1-\sigma_3)$ ⑥	ε_a ⑦	$\frac{\varepsilon_a}{(\sigma_1-\sigma_3)}$ ⑧	$(\sigma_1-\sigma_3)_b$ ⑨	ε_v ⑩	$\frac{(\sigma_1-\sigma_3)_b}{\varepsilon_v}$ ⑪
10	33.17	23.22	0.038	1.64E-3	31.51	0.081	2.57E-3	23.22	0.013	595.4
40	88.23	61.76	0.034	5.59E-4	83.82	0.091	1.09E-3	61.76	0.011	1871.5
70	140.82	98.57	0.048	4.87E-4	133.78	0.117	8.75E-4	98.57	0.023	1460.3

P_a = 14.5 psi

$\frac{\sigma_3}{P_a}$ ⑫	$\frac{1}{(\sigma_1-\sigma_3)_{ult}}$ ⑬	R_f ⑭	$\frac{E_i}{P_a}$ ⑮	$\frac{B}{P_a}$ ⑯
0.680	2.16E-2	0.71	56.08	41.1
2.721	9.40E-3	0.83	113.40	129.1
4.762	5.62E-3	0.79	139.14	100.7

$$\frac{1}{(\sigma_1-\sigma_3)_{ult}} = \frac{⑧-⑤}{⑦-④} \qquad R_f = ⑫ \times ⑬$$

Average R_f = 0.78

$$\frac{E_i}{P_a} = \frac{2.0}{⑤ + ⑧ \cdot ⑬ \times [④ + ⑦]} \cdot \frac{1}{P_a}$$

$$\frac{B}{P_a} = \frac{⑪}{P_a}$$

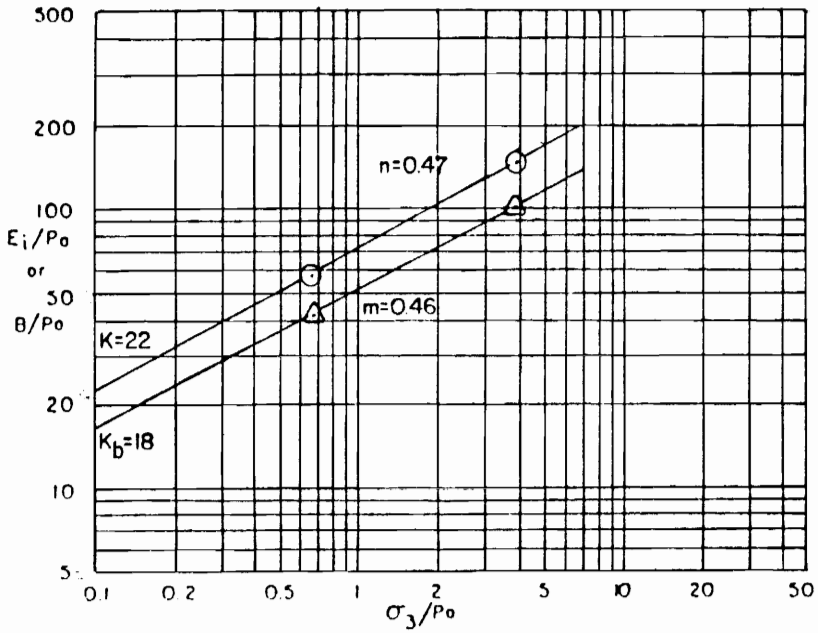

FIGURE C-3 DETERMINATION OF HYPERBOLIC PARAMETERS FROM CD - TRIAXIAL TEST

APPENDIX D

Results of Soil-Concrete Interface Tests

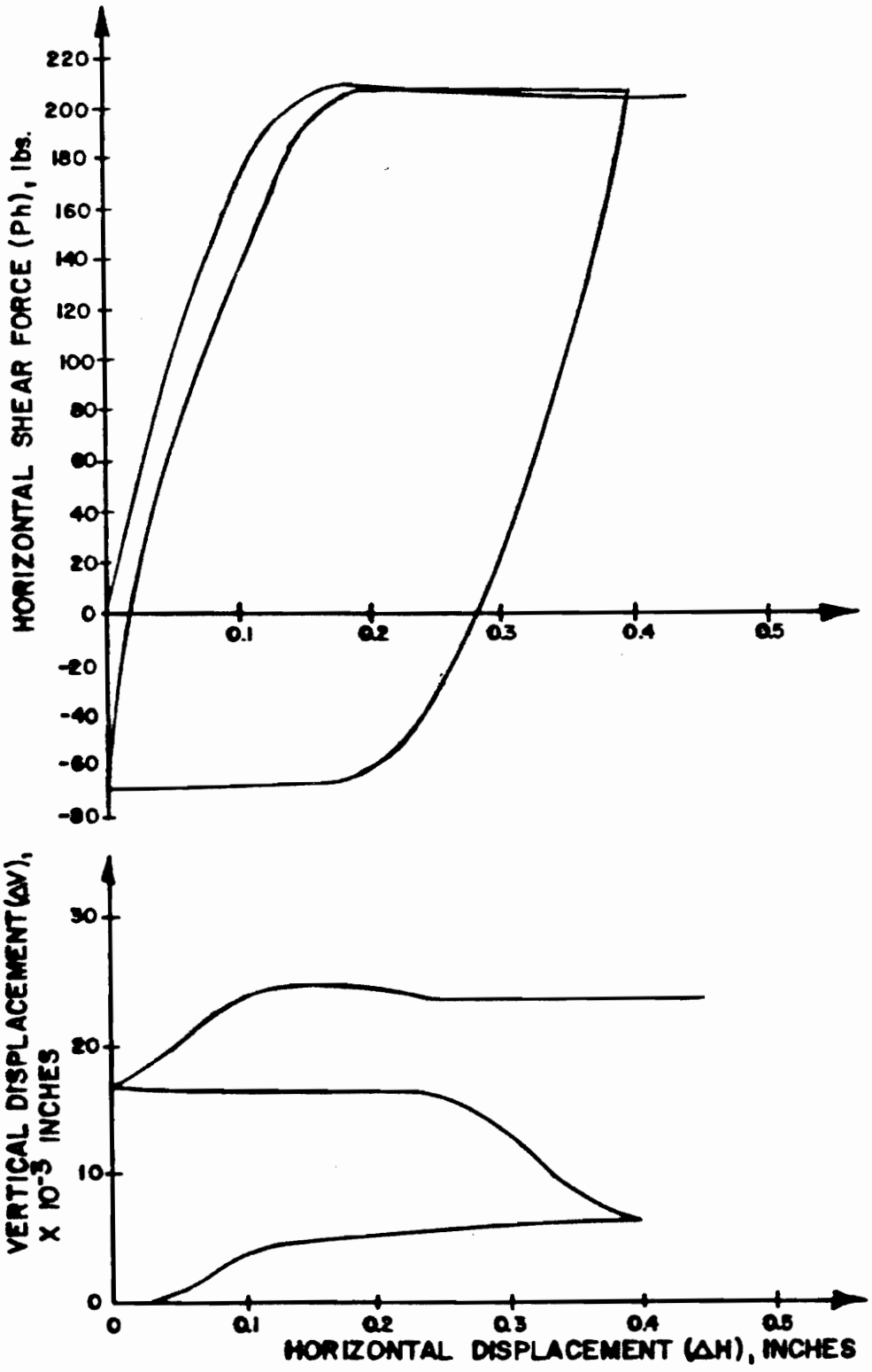

FIGURE D-1 SOIL-CONCRETE INTERFACE TEST SMOOTH SURFACE, δ_n = 0.986 tsf

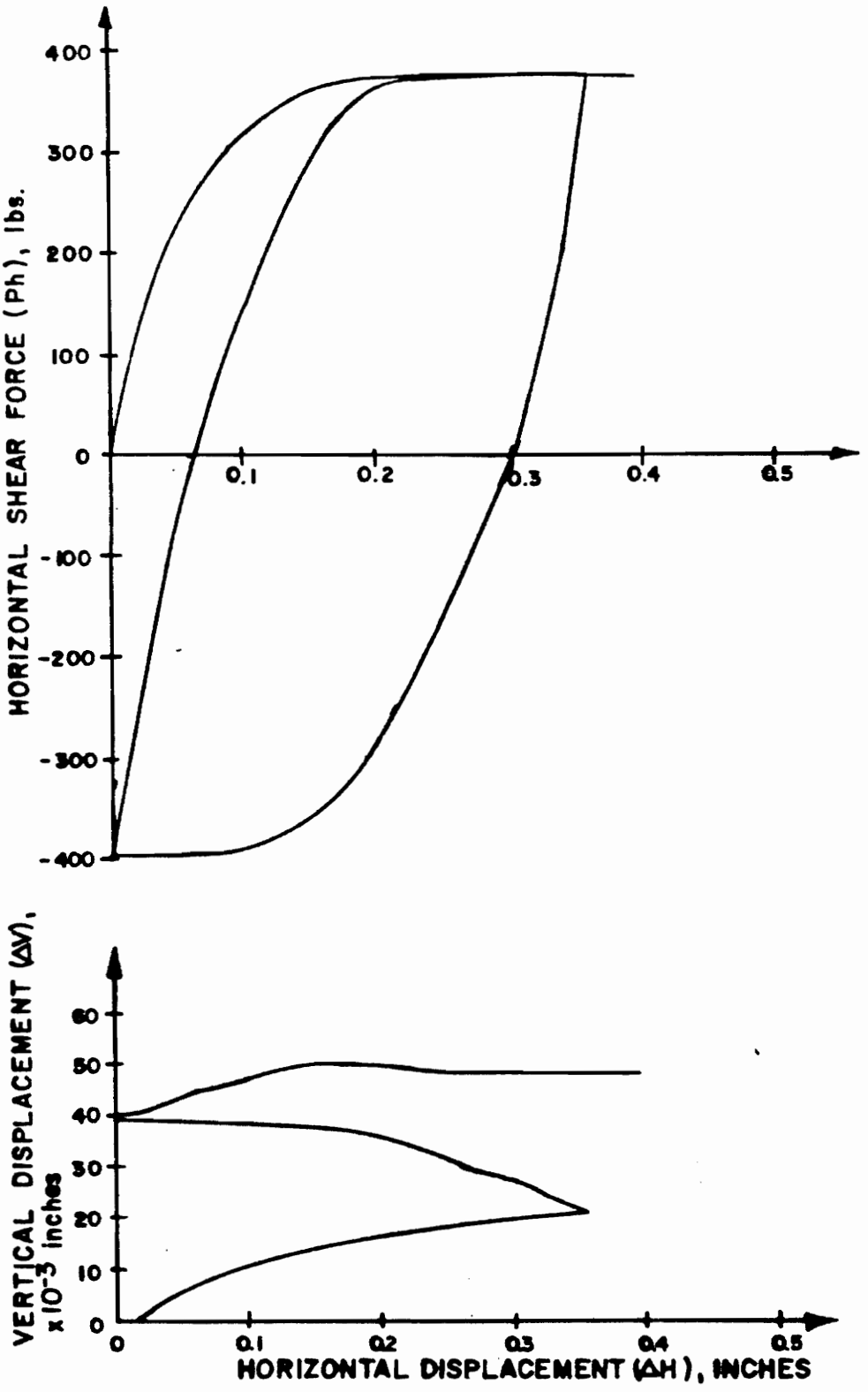

FIGURE D-2 SOIL-CONCRETE INTERFACE TEST SMOOTH SURFACE, δ_n = 2.73 tsf

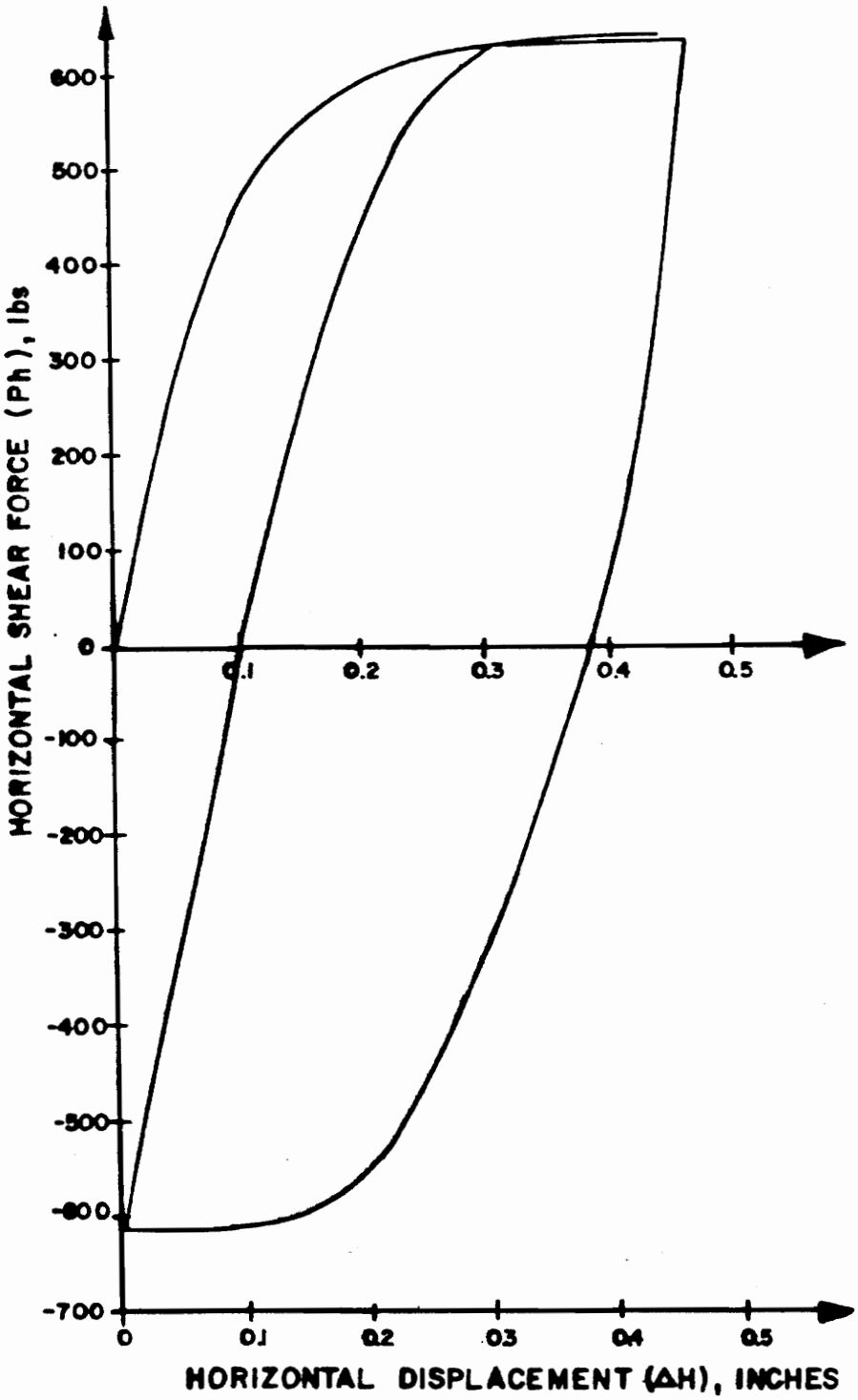

FIGURE D-3 SOIL-CONCRETE INTERFACE TEST, SMOOTH SURFACE, δ_n = 4.481 tsf

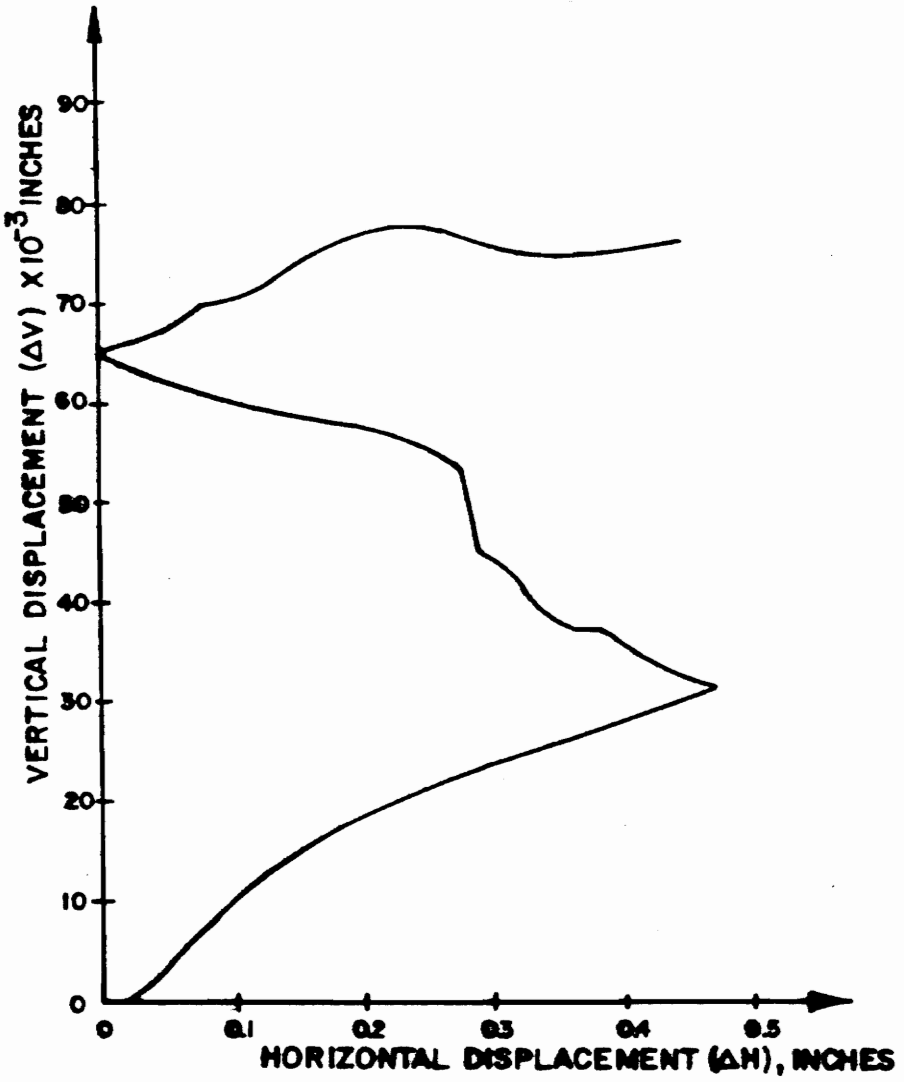

FIGURE D-4 SOIL-CONCRETE INTERFACE TEST, SMOOTH SURFACE, δ_n = 4.481 tsf

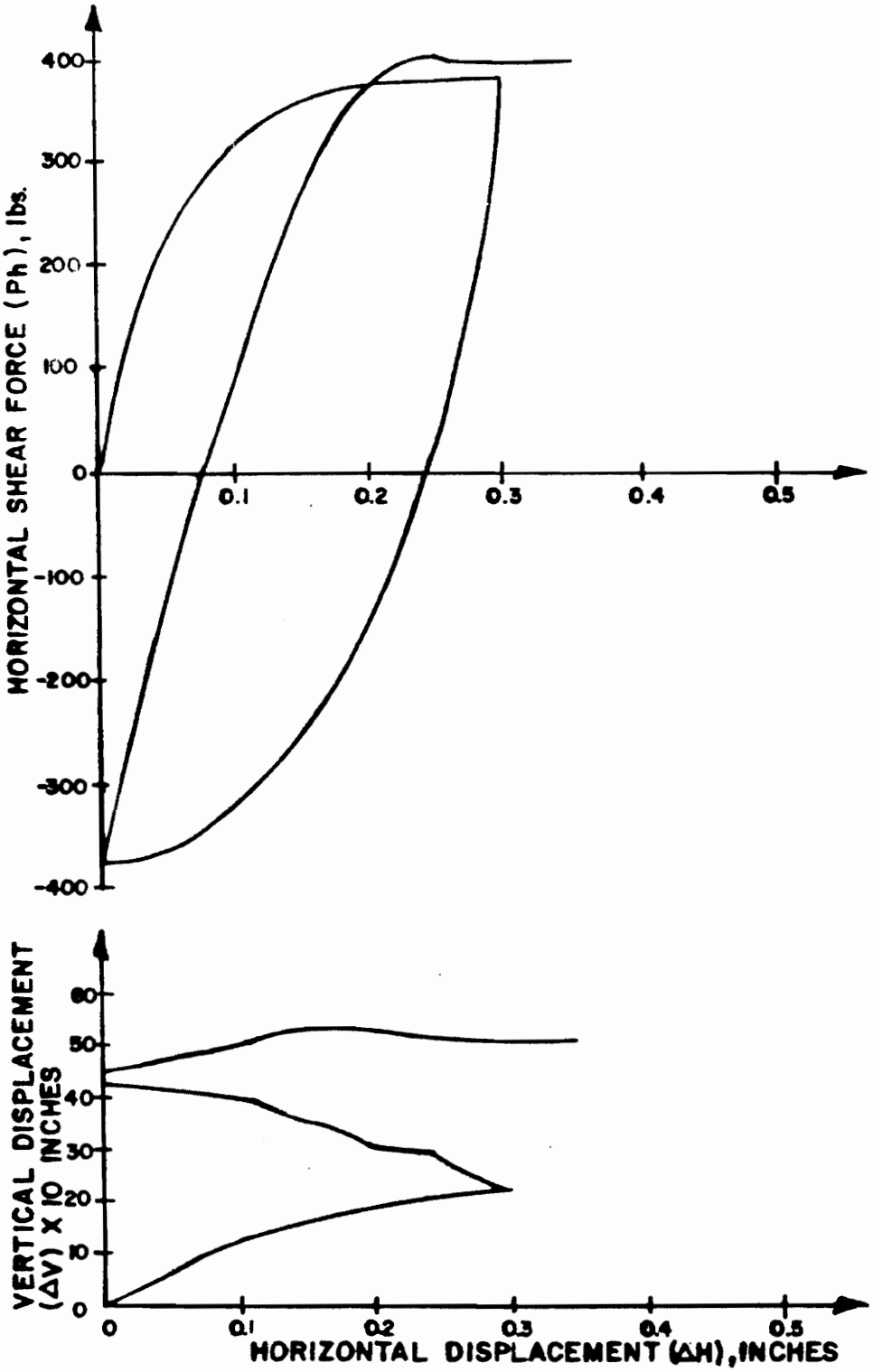

FIGURE D-5 SOIL-CONCRETE INTERFACE TEST, ROUGH SURFACE, δ_n = 2.73 tsf

Soil: Stratum Cl

		70 % Stress Level			95 % Stress Level					
①	②	③	④	⑤	⑥	⑦	⑧	⑨	⑩	⑪
13.69	13.15	9.21	0.082	8.91E-3	12.49	0.14	1.12E-2	0.932	3.97E-2	0.52
37.92	24.04	16.83	0.068	4.04E-3	22.84	0.16	7.01E-3	2.579	2.75E-2	0.66
62.24	40.22	28.15	0.100	3.55E-3	38.21	0.23	6.12E-3	4.230	1.92E-2	0.77

⑫
5942
7975
9974

Pa = 14.7 psi

γ_w = 62.4 psf

$$\frac{1}{\tau_{ult}} = \frac{⑧ - ⑤}{⑦ - ④}$$

$$R_f = ② \times ⑩$$

average R_f = 0.65

$$\frac{Ks}{\gamma_w} = \frac{2.0}{⑤ + ③ - ⑩ \times (④ + ⑦)} \cdot \frac{1}{\gamma_w}$$

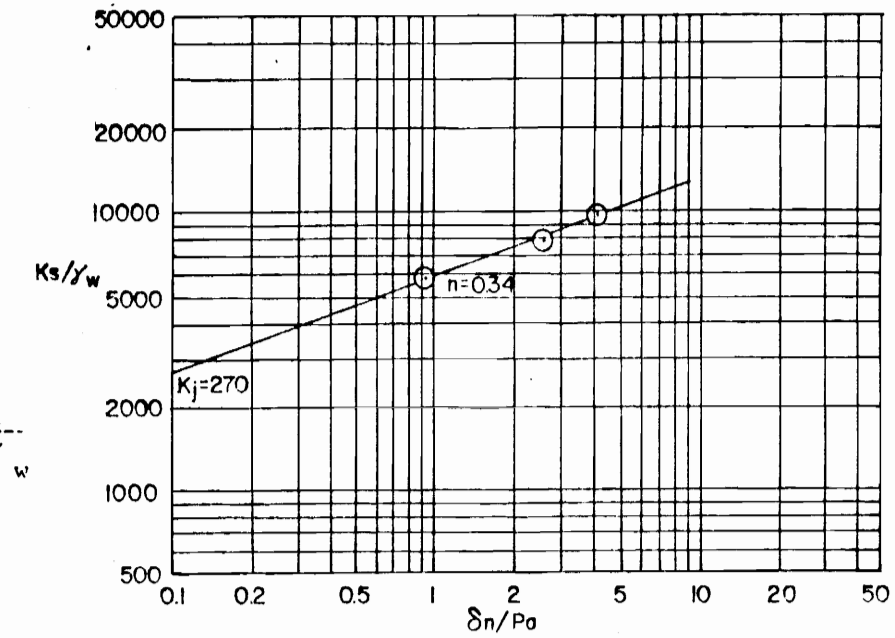

FIGURE D-6 DETERMINATION OF HYPERBOLIC PARAMETERS FROM SOIL / CONCRETE INTERFACE TEST

VITA

John Christos Daoulas was born on March 19, 1958 in Würzburg, Germany to parents that were serving in the U.S. Army. He was graduated in 1976 from Mount Vernon High School in Alexandria, Virginia. In June, 1982, he received a Bachelor of Science Degree in Civil Engineering from Virginia Polytechnic Institute and State University. Upon graduation, he was employed as a Staff Engineer by Schnabel Engineering Associates, P.C. in Richmond, Virginia. He entered the Virginia Polytechnic Institute Graduate School in September, 1983 to pursue studies toward a Master of Science Degree in Civil Engineering. In September, 1984, Mr. Daoulas returned to Schnabel Engineering where he currently serves as Senior Project Manager and Branch Manager for Soil Laboratory Services. Mr. Daoulas was licensed as a Professional Engineer by the Commonwealth of Virginia in April, 1987.